Faculteit Farmaceutische, Biomedische en Diergeneeskundige Wetenschappen
Departement Biomedische Wetenschappen

Heterotetrameric channels of Kv2 and 'silent' Kv subunits: stoichiometry and physiological function

Fysiologische en stoichiometrische analyse van heterotetramere kanalen gevormd door Kv2 en 'stille' Kv subeenheden

Proefschrift voorgelegd tot het behalen van de graad van doctor in de Wetenschappen: Biochemie en Biotechnologie aan de Universiteit Antwerpen te verdedigen door

Glenn REGNIER

Promotoren: Prof. Dr. Dirk J. Snyders
Dr. Elke Bocksteins

Antwerpen, 2016

Members of the jury

Doctoral Committee:

Prof. Dr. P. De Jonghe	(chairman)
Prof. Dr. M. Giugliano	(member)
Prof. Dr. D.J. Snyders	(supervisor)
Dr. E. Bocksteins	(supervisor)

External jury members

Prof. Dr. J. Vriens	(KU Leuven, Belgium)
Prof. Dr. N. Schmitt	(University of Copenhagen, Denmark)

Table of contents

List of abbreviations

4-AP	4-aminopyridine
A	area
AChR	acetylcholine receptor
AMIGO	amphoterin-induced gene and open reading frame
ANOVA	analysis of variance
ATCC	American type culture collection
ATP	adenosine triphosphate
BAPTA	1,2-bis(o-aminophenoxy)ethane-*N,N,N',N'*-tetraacetic acid
BC	inner S6 bundle crossing
Bp	base pairs
BSA	bovine serum albumin
C	capacitance in Farad (F)
cAMP	cyclic adenosine monophosphate
cDNA	copy DNA
C_m	membrane capacitance
COOH-	C- or carboxy terminus
d	diameter
DMEM	Dulbecco's modified Eagle's medium
DNA	deoxyribonucleic acid
dNTP	deoxynucleoside triphosphate
DRG	dorsal root ganglion
DSM	detrusor smooth muscle
E	potential in volt (V)
ε	dielectric constant
ε_o	permittivity constant (8.84×10^{-12} F m^{-1})
ECL	electrochemoluminescence
EDTA	ethylene diamine tetraacetic acid
EGTA	ethylene glycol tetraacetic acid
E_m	membrane potential
ER	endoplasmic reticulum
E_x	Nernst equilibrium potential for ion X

F	Faraday constant (9.65×10^4 C mol^{-1})
FC	fractional contribution
FRET	Förster resonance energy transfer
G	conductance in Siemens (S)
γ	single channel conductance
∆G	Gibbs free energy
G3PDH	glyceraldehyde 3-phosphate dehydrogenase
GABA	γ-amino butyric acid
H&E	haematoxylin and eosin
HEK	human embryonic kidney
HEPES	(4-(2-hydroxyethyl)-1-piperazineethanesulfonic acid
I	current in ampere (A)
I_A	transient outward current
I_{DR}	delayed rectifier current
IgG	immunoglobulin G
I_K	whole-cell K^+ current
I_M	M current
IVF-TALP	*in vitro* fertilization tyrode's albumin lactate pyruvate
I_x	macroscopic current of ion X
k	slope factor (in Boltzmann curve)
K_{2P}	two pore K^+
K_{Ca}	Ca^{2+}-activated K^+
KChAP	K^+ channel associated protein
K_{ir}	inward-rectifying K^+
Kv	voltage-gated K^+
KvS	silent Kv
LDS	lithium dodecyl sulfate
Ltk^-	Mouse fibroblast cell line (ATCC CCL1.3)
MAPK	mitogen-activated protein kinase
MEM	modified Eagle's medium
mRNA	messenger RNA
NH_2-	N- or amino terminus
OAT	oligoasthenoteratozoospermia

P	pore loop
PASMC	pulmonary artery smooth muscle cell
PBS	phosphate buffered saline
PCR	polymerase chain reaction
P_o	probability that the channel protein is in its open conformation
PRC	proximal restriction and clustering
PVDF	polyvinylidene difluoride
P_X	permeability of the membrane for ion X
Q	electrical charge in coulomb (C)
R	electrical resistance in ohm (Ω)
R	universal gas constant (8.31 J mol^{-1} K^{-1})
R_{access}	resistance over the patch pipette access towards the cell
RDV	relative densitometric value
R_m	membrane resistance
RMCA	rat medial cerebral artery
RNA	ribonucleic acid
RT-PCR	reverse transcription PCR
S1-S6	membrane-spanning segments of the Kv channel
ScTx	stromatoxin
SE	standard error
SEM	standard error of mean
SNARE	soluble NSF attachment receptor
SNP	single nucleotide polymorphism
SUMO	small ubiquitin-like modifier
T	absolute temperature in Kelvin (K)
T1	tetramerization domain
TEA	tetraethylammonium
TREK-1	TWIK-1 related K^+ channel
TRP	transient receptor potential
V	voltage
$V_{1/2}$	midpoint (in Boltzmann curve)
VSMC	vascular smooth muscle cell
WT	wild-type

$[X]_i$	intracellular concentration of ion X
$[X]_o$	extracellular concentration of ion X
z	valence

Chapter 1

General Introduction

1. The plasma membrane

1.1 Electrochemical properties underlying excitability

Eukaryotic cells are surrounded by a plasma membrane which consists of a double layer (bilayer) of phosphoplipids each comprising two hydrophobic fatty acid 'tails' and a hydrophilic 'head' joined together by a glycerol molecule. The 'head' groups, which consist of a phosphate that is often modified by small organic molecules, are oriented towards the aqueous environments, whereas the fatty acid 'tails' of adjacent layers are facing each other. As a result, the plasma membrane forms a hydrophobic barrier impermeable to polar and charged molecules and thus separates the intracellular from the extracellular environment (Fig. 1). In this way, they are both able to maintain a different ionic composition, which is an important requisite for several physiological processes including excitability.

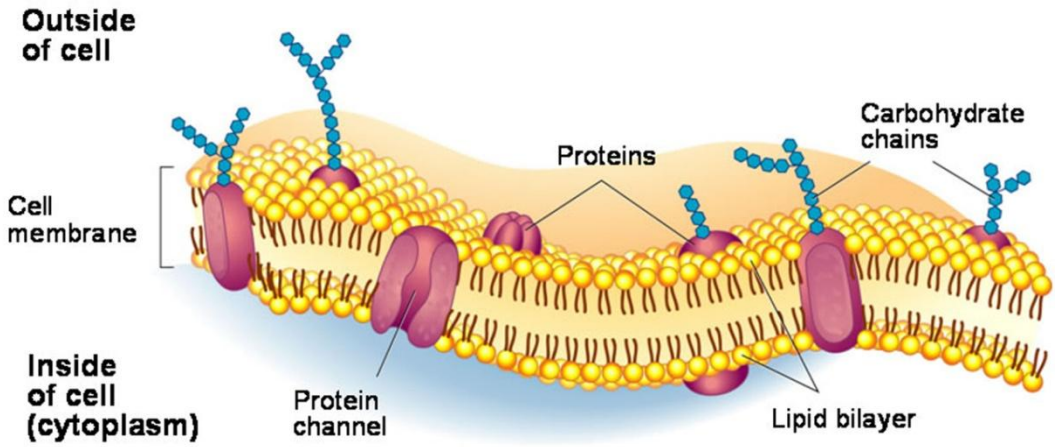

Figure 1: The plasma membrane. The cell membrane is a bilayer of phospholipids with their 'head' groups pointing towards the in- or outside of the cell and their fatty acid 'tails' orienting towards the hydrophobic centre. Transmembrane proteins such as ion channels are embedded in the lipid bilayer in order to facilitate the transport of charged and polar molecules across the plasma membrane (3).

Since the plasma membrane forms a thin insulating layer between two conducting solutions, it behaves as an electrical capacitor. Hence, it can maintain a separation of charges (Q) across its width, which creates a voltage (V)

difference between the conductors. The capability of the capacitor to maintain this charge separation is characterized by its capacitance, defined by the formula:

$$C = \frac{Q}{V} \quad (1)$$

The capacitance of the lipid bilayer can be calculated from its surface (A), its dielectric constant (ε), the permittivity constant (ε_0), and its diameter (d) with the formula:

$$\boldsymbol{C} = \frac{\boldsymbol{A\varepsilon\varepsilon_0}}{\boldsymbol{d}} \quad (\mathbf{2})$$

Ion channels embedded in the membrane (Fig. 1) create ionic permeability pathways with a certain electrical conductance. The reciprocal of conductance is resistance which is measured in Ohm (Ω) and is defined by Ohm's law:

$$\boldsymbol{R} = \frac{\boldsymbol{V}}{\boldsymbol{I}} \quad (\mathbf{3})$$

which says that the resistance (R) of a conductor is proportional to the voltage difference (V) across the conductor and inversely proportional to the current (I) that flows through it. As a result, the plasma membrane can be represented as a parallel RC circuit (Fig. 2). Therefore, a charge displacement across the membrane will cause a change in membrane potential that follows an exponential time course, which is represented by the formula:

$$\boldsymbol{E(t)} = \boldsymbol{E_0}\ \mathbf{exp}\left(-\frac{\boldsymbol{t}}{\boldsymbol{R_m C_m}}\right) \quad (\mathbf{4})$$

in which *E(t)* represents the course of the membrane potential over time, E_0 the starting potential, *t* the time, R_m the membrane resistance, and C_m the membrane capacitance (48).

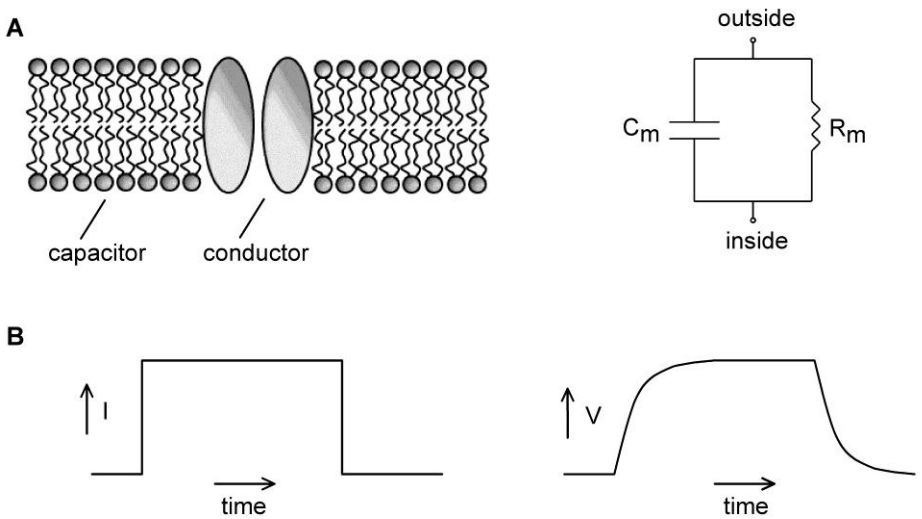

Figure 2: Electrical properties of the plasma membrane. (A) Schematic representation of the electrical components of the lipid bilayer (left) which can be represented as a parallel *RC* circuit (right). (B) Time dependent voltage change (right) in a parallel *RC* circuit caused by a charge displacement (left).

Active transport of ions over the plasma membrane gives rise to an asymmetric ion distribution resulting in a chemical gradient between the intra- and extracellular compartment. Because each system has the predisposition to move towards equilibrium, this chemical gradient drives ions to diffuse from a high to a low concentration. The Gibbs free energy that would hereby be released can be calculated from the formula:

$$\Delta G = RTln\left(\frac{[X]_o}{[X]_i}\right) \quad (5)$$

in which ΔG represents the Gibbs free energy, R the gas constant, T the absolute temperature, and $[X]_o$ and $[X]_i$ the extra- and intracellular concentration of ion X, respectively.

The diffusion of ions causes a net charge displacement across the plasma membrane which results in an electrical gradient. The change in Gibbs free energy resulting from this accumulation of charge at both sides of the lipid bilayer can be calculated as follows:

$$\Delta G = zFE \quad (6)$$

in which z represents the valence of ion X, F the Faraday constant, and E the potential. As a result, the diffusion of ions across the membrane is determined by both the chemical and electrical gradient of that ion, called electrochemical gradient. When both gradients counterbalance each other, there is no net movement of ions across the plasma membrane. The voltage at which a specific ion reaches this equilibrium is called the equilibrium potential of that ion (E_x), which can be calculated with the Nernst equation:

$$E_x = \frac{RT}{zF} ln\left(\frac{[X]_o}{[X]_i}\right) \quad (7)$$

Multiple ions are present in mammalian cells. Therefore, the membrane potential is dependent on the relative permeability of each ion as postulated in the Goldman-Hodgkin-Katz voltage equation (38; 50). If Na^+, K^+, and Cl^- are the permeant ions, this equation is:

$$Em = \frac{RT}{zF} ln\left(\frac{P_K[K]_o + P_{Na}[Na]_o + P_{Cl}[Cl]_i}{P_K[K]_i + P_{Na}[Na]_i + P_{Cl}[Cl]_o}\right) \quad (8)$$

in which *Em* represents the membrane potential and P_X the permeability of the membrane for the respective ion. At rest, the cell membrane is predominantly permeable to K^+ ions. Consequently, the resting potential of mammalian cells approaches the Nernst potential of K^+ which is approximately -85 mV.

1.2 Transmembrane ion transport

The plasma membrane forms an energy barrier which is so high that ions cannot pass through it. Therefore, low resistance pathways are needed to facilitate the transport of ions across the membrane. For this purpose, the bilayer contains integral membrane proteins which can be divided into transporters and channels. Transporters support, depending on whether the ions move down or against their electrochemical gradient, either facilitated diffusion or active transport (Fig. 3A). Most enzymes that perform active transport are ATPases which directly use the metabolic energy released from ATP hydrolysis to transport molecules against their electrochemical gradient. An ATPase universal to eukaryotic cells is the Na^+/K^+ ATPase which maintains a high K^+ and a low Na^+ concentration inside the cell by catalyzing the transport of two K^+ ions into and three Na^+ ions out of the cell. Different types of transporters can be distinguished: uniporters, symporters, and antiporters (Fig. 3B). Uniporters transport one molecule passively down its electrochemical gradient whereas symporters and antiporters use the chemical gradient of one molecule to co-transport another one against its chemical gradient. The difference between symporters and antiporters lies in the direction of the co-transport: symporters involve the movement of ions

in the same direction while in the case of antiporters, ions move in opposite direction (3).

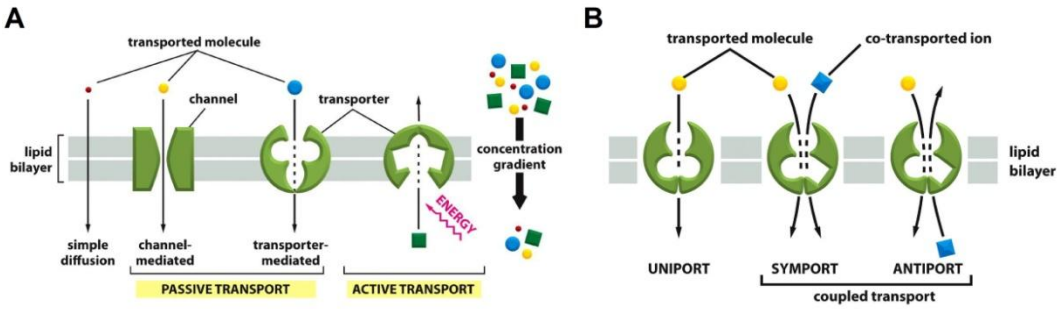

Figure 3: Ion transport across the plasma membrane. (A) Ion transport across the lipid bilayer is facilitated by either channels or transporters. Ion transport through channels does not require energy, whereas transporters can both facilitate passive and energy requiring active transport. (B) Three different types of transporter-mediated transport can be distinguished: uniport, symport, and antiport (3).

Channels, on the other hand, are ion selective pores through which ions flow passively down their electrochemical gradient (Fig. 3A). Ion transport through channels is actively controlled by a channel gate which opens and closes in response to various stimuli. These include mechanical stress (mechanosensitive ion channels, e.g. TWIK-1 related K^+ channel (TREK-1)), ligand binding (ligand-gated ion channels, e.g. Acetylcholine receptor (AChR)), and changes in membrane potential (voltage-gated ion channels, e.g. Kv) (3). The flow of ions through a channel generates an ionic current which is proportional to the driving force (difference between the membrane potential and the Nernst potential), and the open probability and conductance of the channel. The macroscopic current is the sum of the currents of multiple ion channels and is calculated as follows:

$$\boldsymbol{I_X = N\gamma P_O(E - E_x)} \qquad (\mathbf{9})$$

where I_x is the macroscopic current of ion X, N the number of ion channels, γ the

intrinsic conductance of the ion channel, P_o the probability that the pore is open, E the membrane potential, and E_x the Nernst potential for ion X.

2. Measuring ionic currents with the patch clamp technique

The voltage clamp technique is a method used to study ionic currents through cell membranes and was developed in the 1940s by Hodgkin and Huxley (49). In their pioneering work, they inserted two electrodes inside the lumen of a giant squid axon and connected these to an electrical circuit which allowed them to both control the membrane potential and record ionic currents. This technique was further refined to the patch clamp method which allows the measurement of ionic currents from smaller cells including the native currents from mammalian neurons and the currents from cells transiently transfected with channel cDNA (44).

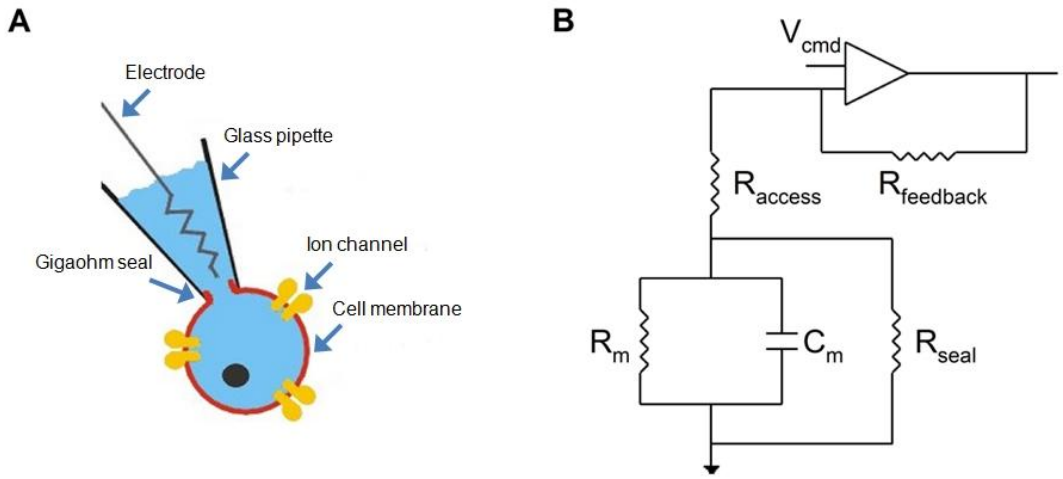

Figure 4: The whole-cell patch clamp technique. (A) Cartoon of the whole-cell mode achieved by forming a gigaohm seal between the pipette opening and the cell membrane followed by rupturing the membrane patch inside the pipette tip. (B) Schematic representation of the electrical circuit in the whole-cell single electrode voltage clamp mode. The access resistance is series connected to the *RC* circuit of the cell membrane which can result in a significant voltage error. The seal resistance is in parallel to the *RC* circuit, thus a gigaohm seal resistance is required to avoid leak that interferes with the current recordings.

The whole-cell patch clamp technique uses a single glass pipette with a very fine tip opening of 1-2 µm to form a high resistance seal (gigaohm seal) between the circular rim of the pipette tip and the cell membrane. Subsequently, a low resistance pathway between the inside of the cell and the pipette can be achieved by only rupturing the piece of sealed membrane (patch) (Fig. 4A). To perform experiments in this whole-cell configuration, cells are placed in a recording chamber which is filled with a saline solution that mimics the extracellular environment, whereas the patch pipette is filled with an equivalent of the intracellular solution of the cell. After patch rupture, the solution inside the pipette starts to diffuse and equilibrates with the interior of the cell after which ionic current recordings can be made through the patch pipette with an electrical voltage clamp circuit. This consists of a negative feedback amplifier that is connected to two electrodes of which the first one is in contact with the solution of the recording chamber and serves as a reference electrode, whereas the second one is in contact with the pipette solution. This establishes an electrical circuit across the membrane in which the amplifier controls the membrane potential and allows the recording of the hereby evoked ionic currents. In order to control the membrane potential, the amplifier determines the difference between the command voltage and the voltage measured over the cell membrane and subsequently injects a current into the cell to minimize this difference. Because the deviation from the command voltage is a result of the evoked ionic current, this injected current is equal and opposite to the ionic current.

The small opening of the patch pipette creates a resistance over the pipette access towards the cell (R_{access}) in series with the membrane resistance (R_m) representing the ion channels inside the membrane. Because the patch electrode is used simultaneously for voltage recording and current passing, R_{access} produces a voltage drop over the patch electrode which, in case of large currents, results in a voltage error that interferes with the recordings (Fig. 4B). This can be circumvented by a series resistance compensation circuitry in the amplifier. However, this compensation is limited so that it cannot be used for very large currents. In this case, the two-electrode voltage clamp technique should be

considered since it uses two separate patch electrodes for voltage recording and current passing, respectively.

3. Voltage-gated potassium channels

Potassium channels form the largest and most heterogeneous group among the ion channels which is illustrated by the approximately 80 known loci in the mammalian genome. Based on structure and function, four different families of potassium channel subunits can be distinguished: inward-rectifying (K_{ir}), two-pore (K_{2P}), Ca^{2+}-activated (K_{ca}), and voltage-gated (Kv) potassium channels (42). The Kv channels form the largest family of more than 40 mammalian genes and are subdivided into twelve subfamilies (Kv1-Kv12) based on sequence homology. In addition, these subfamilies can be classified into three large groups according to their phylogenetic relations: *Shaker*-related (Kv1-Kv6 and Kv8-Kv9), KCNQ (Kv7) and *Eag*-like (Kv10-Kv12) channels (43). The remainder of this chapter will discuss the structure and function of the *Shaker*-related Kv channels in more detail as several members of this group are at the center of the present study.

3.1 Kv channel structure

Kv channels consist of four α-subunits that are arranged symmetrically around an aqueous pore (Fig. 5). Each α-subunit contains six transmembrane segments (S1-S6), a pore loop (P) which is located between S5 and S6, and a cytoplasmic amino (NH_2- or N-) and carboxy (COOH- or C-) terminus. The S1-S4 segments form the voltage sensing component of the channel and surround the potassium selective pore which is formed by the S5-P-S6 segments. The N-terminus contains the T1 domain which is involved in the facilitation of channel assembly (115).

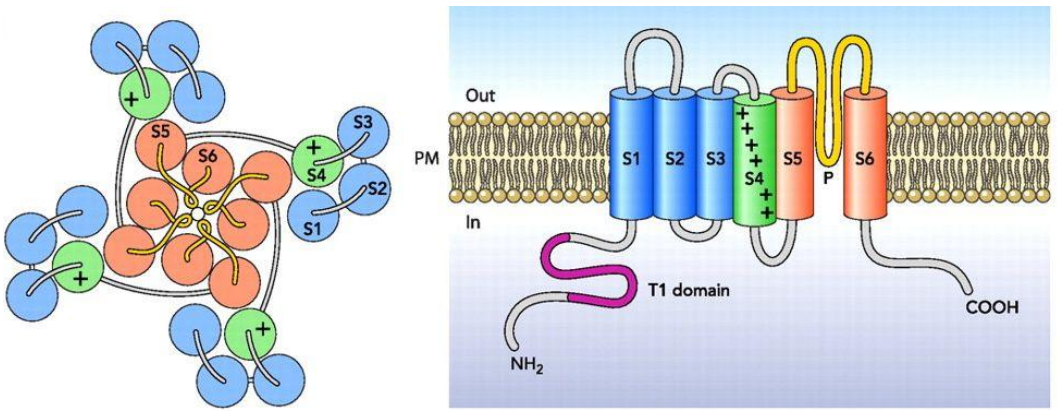

Figure 5: General structure of a voltage-gated potassium (Kv) channel. Side view (right) of an α-subunit consisting of six transmembrane segments (S1-S6) and a cytoplasmic N- and C-terminus. The T1 domain is located on the N-terminus and is responsible for facilitating the subfamily specific tetramerization. Four α-subunits assemble into a Kv channel (top view, left) in which the S5-P-S6 regions line the ion conducting pore, whereas the S1-S4 segments form the voltage sensing domain. The S4 segment contains several positively charged residues and is therefore considered to be the voltage sensor of the Kv channel (15).

3.1.1 The pore

The main function of the Kv channel pore is to create a low resistance pathway that selectively passes K^+ ions across the plasma membrane at a very high rate. The molecular basis of this K^+ conduction and selectivity was elucidated by the 3D crystal structure of the bacterial K^+ channel KcsA (31) (Fig. 6A-B). The α-subunits of this channel each consist of two transmembrane segments (TM1 and TM2) which demonstrate a high sequence similarity to the S5-P-S6 regions of Kv channels. Both helices cross the membrane at an angle of ~25 degrees creating a structure reminiscent of an inverted tepee in which the outer helices face the lipid membrane and the inner helices face the central pore.

The entryways of the pore attract cations due to the presence of negatively charged amino acid side chains, resulting in a high local concentration of K^+ ions. From the intracellular side, the pore creates a 18 Å long tunnel that

opens into a 10 Å wide cavity near the center of the membrane through which K^+ ions can move in their hydrated form (Fig. 6C). Here, the cavity creates a polarisable environment for the K^+ ions, which lowers the energy barrier they face when crossing the plasma membrane. Furthermore, the carboxyl ends of the P helices are oriented towards the central cavity creating a negative electrostatic potential which adds to the stability of K^+ at this location (31).

The central cavity is separated from the extracellular environment by the selectivity filter which forms a narrow tunnel through which only dehydrated K^+ ions can move (Fig. 6D). The inside of this tunnel is lined by oxygen atoms of the peptide backbone belonging to the amino acids that form the molecular signature sequence for K^+ selectivity (i.e., TVGYGD) (31; 47). These oxygen atoms enable the coordination of a dehydrated K^+ ion, thus serving as a water substitute to compensate for the energetic cost of dehydration. Furthermore, the Tyr side chains of the above sequence point away from the pore to form specific interactions with Trp residues of the pore helix, hereby forming a massive sheet of aromatic amino acids. This determines the width of the selectivity filter in such a way that large ions including K^+ (1.33 Å) and Rb^+ (1.48 Å) are ideally coordinated by the oxygen atoms, while small ions like Na^+ (0.95 Å) are not.

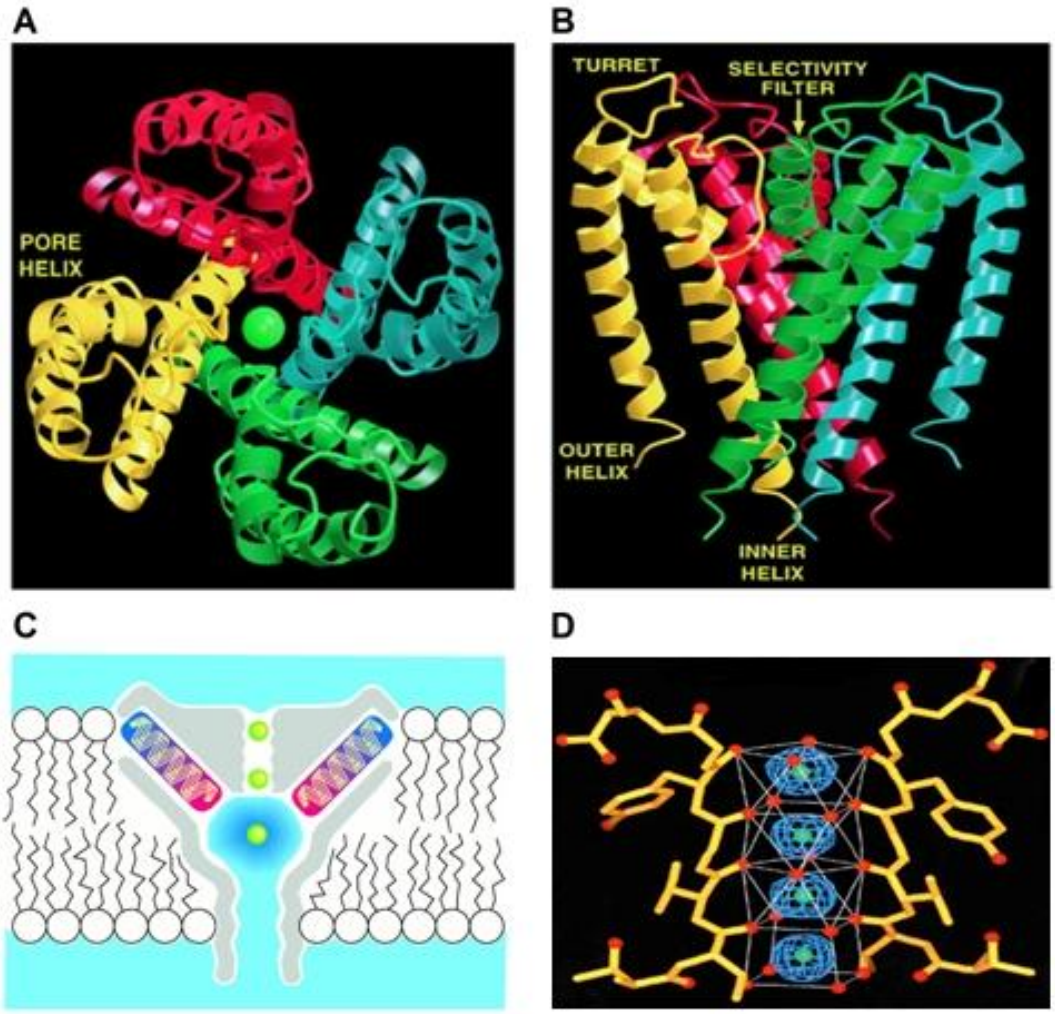

Figure 6: Structure of the KcsA channel pore. Top view (A) and side view (B) of the crystal structure of the bacterial K^+ channel KcsA. The KcsA channel consists of four α-subunits each comprising two transmembrane segments which have a high sequence similarity to the pore region of Kv channels. (C) Cartoon of the K^+ channel pore. K^+ ions (green) are stabilized near the center of the membrane by the aqueous environment of a 10 Å wide cavity and by the carboxyl ends of the pore helices (red). From here, K^+ ions move to the extracellular environment by going through the selectivity filter which can hold two ions at a time (31). (D) Detailed structure of the selectivity filter. The oxygen atoms of the carbonyl backbone provide four potential K^+ binding sites of which only two are occupied under physiological conditions (90).

3.1.2 The voltage sensor and gate

The first eukaryotic Kv channel to be crystallized was that of the mammalian Kv1.2 channel (78) (Fig. 7). The pore domain of Kv1.2 is very similar to that of KcsA which indicates that the structural basis of K^+ conduction and selectivity can be extrapolated to Kv channels. Furthermore, the crystal structure of Kv1.2 shows that the S1-S4 segments form an independent voltage sensitive domain that is latched around the pore of an adjacent subunit. In this domain, S4 is considered to be the major component for voltage sensing since it contains several regularly spaced Arg or Lys residues. Upon membrane depolarization these positively charged residues will move outwardly which gives rise to a gating current (6). Recordings of this current revealed that each voltage sensing domain moves 3 to 3.5 elementary charges which are mainly carried by Arg residues near the extracellular side of the membrane (2; 113). The positively charged residues of the S4 segment are oriented so that they are not exposed to the hydrocarbon region of the membrane. Instead, they are stabilized by facing water-filled crevices that penetrate the core of the voltage sensing domain (60) and by interacting with negatively charged residues of both the S1-S3 side chains and the lipid phosphate groups (80).

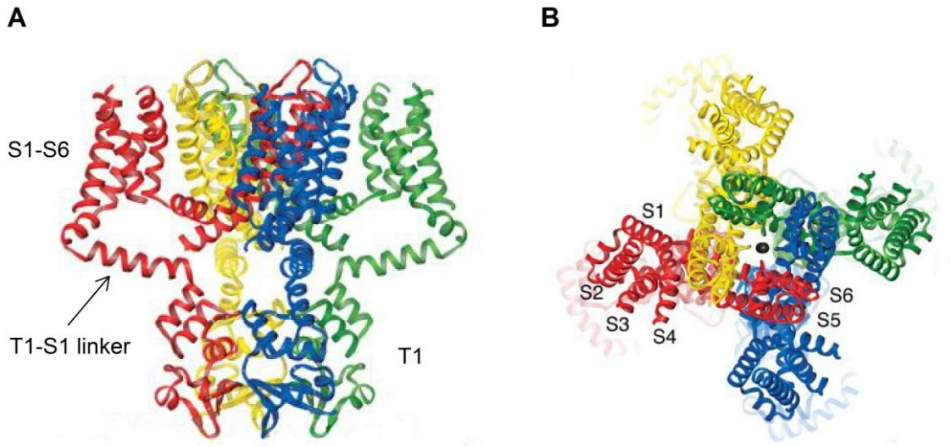

Figure 7: Crystal structure of the Kv1.2 channel. (A) Side view of the four α-subunits each represented by a different colour. The four T1 domains assemble into a symmetrical structure that is attached to the transmembrane core as a hanging gondola by T1-S1 linkers. (B) Top view of the Kv1.2 channel which highlights that the voltage sensing domain (S1-S4) is latched around the pore domain (S5-S6) of an adjacent subunit (78).

At the resting potential, the pore of Kv channels is sealed off by an intracellular gate (bundle crossing (BC) gate) located near the bundle crossing at the C-terminal end of S6 (S6c), where the side chains of nonpolar amino acids form a hydrophobic barrier impossible for K^+ ions to pass (30) (Fig. 8). The bottom part of S6 is bent in regard to the remainder of the S6 helix due to the presence of a highly conserved PXP motif, which creates a flexible hinge that allows motions of the post-hinge S6 segments required for gate opening (72). The motion of the voltage sensor is translated into opening or closing of the BC gate through an electromechanical coupling formed by the interaction between the S4-S5 linker and S6c (79). Consequently, depolarization of the membrane will cause S4 to move from a rested to an activated state thereby moving the post-hinge S6 segment. After all four voltage sensing domains have moved to the activated state, a final concerted step opens the K^+ permeation pathway (29).

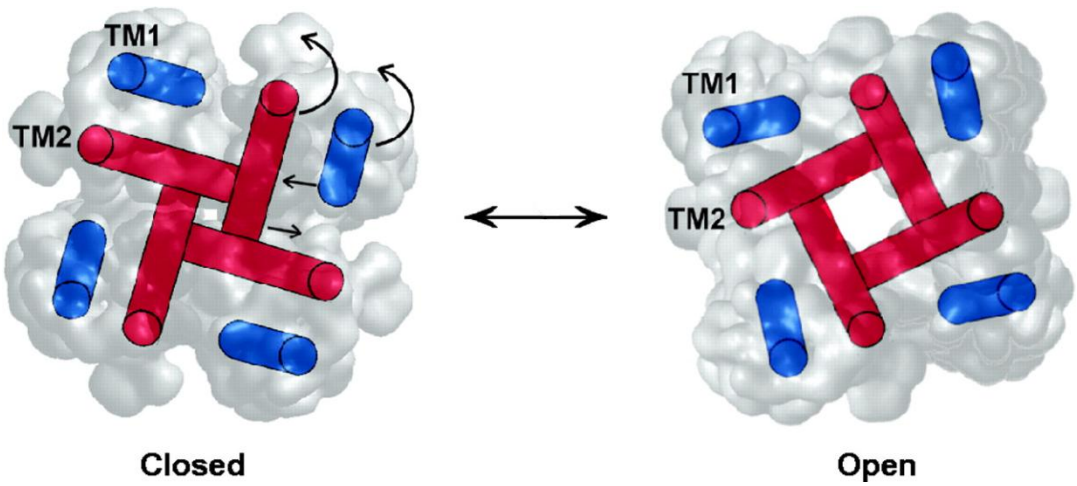

Figure 8: Conformations of the bundle crossing (BC) gate. Schematic representation of the conformational changes that occur during gate opening of the KcsA channel. In the closed conformation (left), the BC gate forms a hydrophobic constriction that dilates upon opening of the channel (right) (102).

3.1.3 The T1 domain

The N-terminus of *Shaker*-related Kv channels contains the tetramerization domain T1. The T1 domains of four α-subunits assemble into a symmetrical structure that is attached to the transmembrane core of the protein as a cytoplasmic 'hanging gondola' by T1-S1 linkers (67) (Fig. 7). These linkers create space between the transmembrane and intracellular regions thereby forming four side portals that serve as diffusion pathways between the cytoplasm and the pore. In addition, the T1-S1 linkers possess several negatively charged residues which results in an electrostatic potential that attracts K^+ ions to the pore entryway (78).

Crystal structures of the T1 domain revealed that the structure of the T1 domain is very similar among the different Kv subfamilies since they all show a common four-layered structure in which layer 4 faces the membrane embedded side of the channel (7) (Fig. 9). However, the structure of the T1 domain of the Kv1 subfamily differs slightly compared to that of other subfamilies since it does not contain a C3H1 motif. This motif is well conserved in the other subfamilies and consists of one His and three Cys residues that coordinate a Zn^{2+} ion at the interface of layer 3 and 4 (7). Although the structural scaffold is very similar for the different T1 tetramers, they all must display differential amino acid side chain rearrangements to allow specific intersubunit interactions since each T1 domain can only associate with that of other subfamily members. As a result, it is a key determinant for channel assembly because it facilitates the tetramerization of compatible subunits while preventing the assembly of incompatible subunits into a functional channel (76; 115; 116; 132).

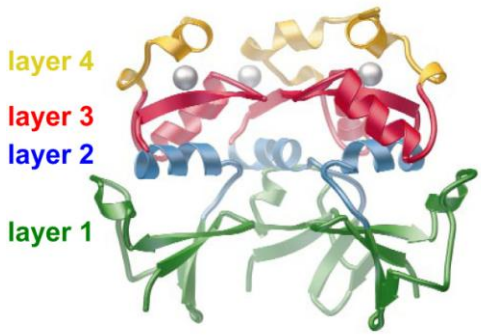

Figure 9: Structure of the T1 domain. Crystal structure of the T1 domain from the Kv3 subfamily. The subunit in the front is not shown for clarity. Layer 4 is situated near the transmembrane core, whereas layer 1 faces the cytoplasm. Each T1 monomer contains one Zn^{2+} ion, positioned between layer 3 and 4, and shown as a gray circle (7).

3.2 Kv channel diversity

3.2.1 Molecular diversity

Kv channels form a remarkably diverse group, much more than would be expected based on the number of genes encoding for Kv α-subunits. This diversity arises from several factors (43).

1) *Heterotetramerization.* Within each subfamily, subunits can assemble into heterotetramers which have different properties compared to homotetramers. Furthermore, the Kv2.1 and Kv2.2 subunits are also able to heterotetramerize with all members of the Kv5, Kv6, Kv8, and Kv9 subfamilies thereby modulating the properties of the Kv2 channels (15).

2) *Accessory proteins.* Kv channels frequently form large channel complexes by associating with accessory proteins. These often modify the properties of the channel, although they are also involved in other mechanisms such as membrane localization and channel trafficking.

3) *Alternative mRNA splicing*. Most Kv channel genes contain multiple exons. These can be alternatively spliced resulting in several isoforms of the same Kv coding gene which further adds to the functional diversity of Kv channels.

4) *Post-translational modifications.* Kv channels can be modulated by post-translational modifications including phosphorylation, SUMOylation and ubiquitinylation. In this way, the cell can dynamically modify channel function in response to environmental stimuli through signalling pathways.

3.2.2 Electrophysiological diversity

The molecular diversity of Kv channels gives rise to a wide range of Kv currents that all differ in their electrophysiological properties including the threshold of activation, the channel conduction, and the activation (opening) and deactivation (closing) kinetics. However, functional channels can be classified into two major groups: A-type channels and delayed rectifiers. The main difference between these groups derives from the rate and degree of inactivation (48). Generally, inactivation is a conformational state of the channel in which ions are not able to permeate the pore even if the activation gate is open, but the molecular mechanisms underlying this nonconductive state vary, resulting in the distinction of several inactivation types (70) (Fig. 10).

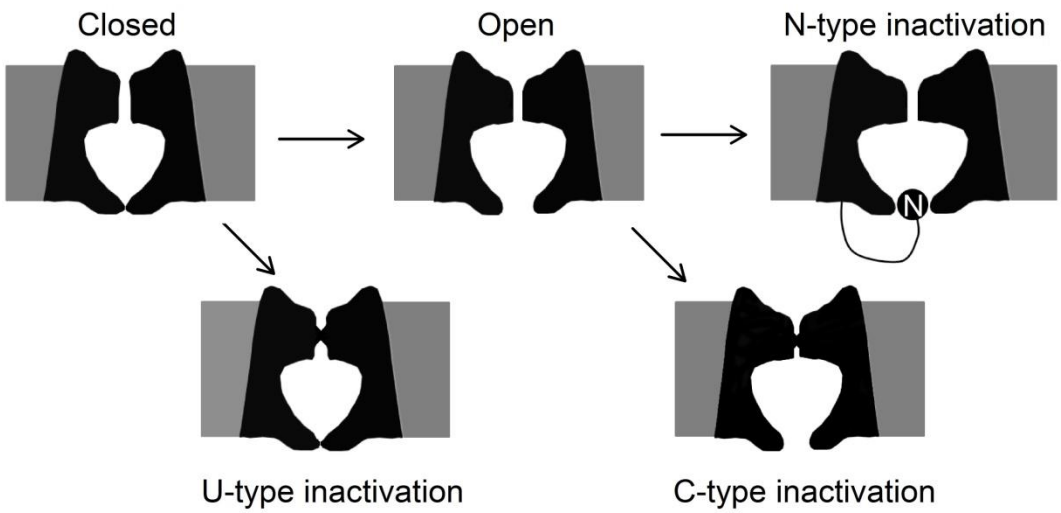

Figure 10: Schematic overview of the different inactivation types. The gray structures show the plasma membrane in which the Kv channels (black) are embedded. The white space within the Kv channel represents the main elements of the channel pore. When the Kv channel goes from the closed to the open state, the BC gate opens while the selectivity filter remains in its native conformation. During N-type inactivation, no ion flux is possible due to the occlusion of the inner pore by the N-terminal ball peptide. In the case of C-type and U-type inactivation, the pore cannot conduct ions due to a constriction of the selectivity filter.

A-type Kv channels activate very fast followed by a fast and complete inactivation. This type of inactivation is designated N-type inactivation due to the involvement of the cytoplasmic N-terminus and is frequently described as the

'ball-and-chain' mechanism (52; 136). It involves a stretch of approximately ten N-terminal hydrophobic amino acids (the ball) which interact with hydrophobic residues that line the inner pore, thereby forming a plug that occludes the K^+ permeation pathway from the intracellular side (51) (Fig. 10). This implies that the pore has to be open which is consistent with the observation that N-type inactivation only takes place after opening of the channel. The stretch of hydrophobic amino acids is followed by a series of positively charged residues (the chain) which promotes entry of the inactivation domain to the inner mouth of the channel pore by interacting with the acidic residues of the T1-S1 linkers (41). This 'ball-and-chain' signature is also carried by some auxiliary β-subunits which allows them to confer N-type inactivation to delayed rectifiers by associating with these channels (1; 91).

Delayed rectifiers, on the other hand, inactivate incompletely and very slowly, usually with time constants in the range of seconds (53). This type of inactivation has been thought to involve conformational changes in the outer part of the channel pore resulting in a constriction of the selectivity filter, which was confirmed by a series of crystal structures showing several conformations of the KcsA channel (23). Two types of slow inactivation can be discriminated depending on whether the channel preferentially inactivates in the open state (C-type) (52) or partially activated state (U-type) (65; 66) (Fig. 10). U-type inactivation is very prominent in Kv2.1 channels and differs from C-type inactivation by two main features. First, the voltage dependence of inactivation is U-shaped with maximum inactivation at the midpoint of activation and less inactivation at stronger depolarizations. Second, it exhibits excessive cumulative inactivation since repetitive pulsing produces more inactivation than a sustained depolarization. Due to the dissimilarities between C-type and U-type inactivation, it is suggested that the molecular mechanisms underlying these two types of inactivation are different (19; 69). However, the structural basis for these differences remains to be determined.

4. The Kv2 subfamily

The Kv2 subfamily consists of 2 members (i.e., Kv2.1 and Kv2.2) that were cloned from mammalian brain reflecting their high expression in central neurons (34; 59). In heterologous expression systems, Kv2.1 and Kv2.2 form both homo- and heterotetrameric channels that have similar biophysical properties (8). However, they are not likely to form heterotetramers *in vivo* since in cortical and hippocampal neurons, the subcellular distribution of both subunits do not overlap (58); Kv2.2 channels are uniformly distributed throughout the soma and dendrites, whereas Kv2.1 channels are specifically localized in large somatodendritic clusters that contain a large number of nonconductive channels (94). This clustered expression pattern of Kv2.1 is due to the presence of a unique C-terminal cytoplasmic domain that acts as a proximal restriction and clustering (PRC) signal (77; 112).

In mammalian neurons, Kv2.1 channels are mainly involved in the regulation of the neuronal firing frequency by affecting the duration of afterhyperpolarization (33; 126). However, they are expressed in a wide range of excitable and non-excitable cells, where they contribute to various processes even in their nonconductive form. For example, nonconductive Kv2.1 channels regulate the exocytosis of insulin in human pancreatic β-cells through interaction with the soluble NSF attachment receptor protein (SNARE) syntaxin 1A (26). In order to exert this manifold of functions, the Kv2.1 channel is modified through several mechanisms including post-translational modifications, association with auxiliary β-subunits, and heterotetramerization with modulatory α-subunits of the Kv5, Kv6, Kv8, and Kv9 subfamilies. In addition, a splice variant of Kv2.2 that heterotetramerizes with Kv2.1 was recently found in cortical pyramidal neurons which adds further to the functional diversity of Kv2.1 channel complexes (63).

4.1 Post-translational modifications

The Kv2.1 protein contains very large cytoplasmic regions comprising almost 75% of this α-subunit. Especially the C-terminus is very long (~50% of the protein) which makes it a convenient target for post-translational modifications. Interestingly, the cytoplasmic regions of Kv2.1 contain more than 100 candidate phosphate acceptor residues of which 60 are predicted as consensus phosphorylation sites, suggesting that phosphorylation can be a major form of post-translational modification for Kv2.1 (88). Indeed, it was demonstrated that in its native form, Kv2.1 is constitutively phosphorylated since treating the native protein with alkaline phosphatase caused a large reduction in its molecular weight (119).

Neurons are able to regulate their excitability by dynamic modulation of the Kv2.1 phosphorylation state. During increased excitatory input, the induced cytoplasmic Ca^{2+} release leads to a rapid dephosphorylation of Kv2.1 mediated by the Ca^{2+}/calmodulin-sensitive phosphatase calcineurin, resulting in lateral dispersion of the channel clusters and a lowered activation threshold (86; 87). As such, the Kv2.1 channel is able to limit the firing frequency during the early phases of hyperexcitable assaults, thereby providing neuroprotection. Notably, this homeostatic control mechanism only involves 16 calcineurin-sensitive residues of which 7 are involved in the regulation of voltage-dependent gating (98).

Kv2.1 phosphorylation is also involved in regulating the induction of neuronal apoptosis (97). Neuronal apoptosis is accompanied by an enhanced K^+ efflux which enables the activation of nucleases and proteases necessary to complete this process (135). In rat hippocampal and cortical neurons, this cellular loss of K^+ is facilitated by an increased Kv2.1 channel insertion in the plasma membrane which is mediated by the dual phosphorylation of the S800 and Y124 residues (83; 106; 107). The phosphorylation of these residues is respectively induced by an increased p38 MAPK and Src kinase activity which in turn is the consequence of a cytoplasmic Ca^{2+} and Zn^+ release. Interestingly, a stimulus-

induced elevation of the $[Ca^{2+}]_i$ can ensure neuroprotection through calcineurin-dependent dephosphorylation, while sustained signalling by that same stimulus can lead to p38 MAPK-dependent plasma membrane insertion of Kv2.1 causing neuronal apoptosis (118). Consequently, depending on which Kv2.1 phosphorylation sites are modulated, Kv2.1 channels can affect both neuronal survival and death.

Kv2.1 channels are also modified by small ubiquitin-like modifier (SUMO) proteins which are attached to specific lysine residues through enzyme-mediated conjugation (25; 103). This post-translational modification of Kv2.1 also affects neuronal excitability since it lowers the Kv2.1 current density. In human pancreatic β-cells, SUMOylation inhibits Kv2.1 currents by accelerating channel inactivation and preventing recovery from inactivation, which results in enhanced insulin secretion (25). In contrast, SUMOylation of Kv2.1 channels in rat hippocampal neurons, suppresses Kv2.1 function by shifting the voltage dependence of activation towards more depolarized potentials (103). However, the degree of current suppression exceeds the inhibition predicted by the G-V relationship. It has been suggested that this may account for the large number of nonconducting Kv2.1 channels found in the somatodendritic clusters of hippocampal neurons (103).

4.2 Auxiliary β-subunits

Kv2.1 subunits are able to form channel complexes with several auxiliary β-subunits. These include subunits such as KChAP that act as a chaperone to increase Kv2.1 membrane expression (71) and subunits that affect the biophysical properties and current density of the Kv2.1 channels including AMIGO (101) and KCNE1-5 (27; 84). Recently, it was demonstrated that KCNE1-5 subunits modulated Kv2.1/Kv6.4 heterotetramers differently compared to Kv2.1 homotetramers (27). This shows that α-modulatory and β-modulatory subunits can simultaneously associate with Kv2.1 into a tripartite complex which may be important for fine-tuning the cell-specific properties of Kv2.1 channel complexes.

4.3 Silent Kv subunits

Members of the Kv5, Kv6, Kv8, and Kv9 subfamilies are modulatory α-subunits of the Kv2 channels. They are designated electrically silent Kv (KvS) subunits since they fail to form functional homotetramers despite possessing all the hallmarks of a functional Kv subunit. Until now ten different KvS subunits have been identified (15) (Table 1). A lot of research has been done to elucidate the molecular mechanisms that underlie the silent character of these subunits and their specific heterotetramerization with Kv2. Furthermore, their contribution to various physiological and pathophysiological processes has been demonstrated in recent years.

Table 1: Overview of the silent Kv subunits. Gene names of each subunit are also given.

Gene name	Silent Kv subunit
KCNF1	Kv5.1
KCNG1	Kv6.1
KCNG2	Kv6.2
KCNG3	Kv6.3
KCNG4	Kv6.4
KCNV1	Kv8.1
KCNV2	Kv8.2
KCNS1	Kv9.1
KCNS2	Kv9.2
KCNS3	Kv9.3

4.3.1 Electrically silent behavior

Immunofluorescence and confocal microscopy of GFP-tagged KvS subunits have shown that KvS subunits remain trapped in the endoplasmic reticulum (ER) instead of being trafficked to the plasma membrane (95; 108; 109; 117) (Fig. 11). It was suggested that this may be due to the presence of an ER retention signal or due to the lack of an ER export signal. However, no ER retention signal has yet been reported for these subunits (15) and, moreover, fusing the Kv6.4 subunit with an ER export signal that greatly enhances the surface expression of Kv1.2 channels (i.e., FCYENE) (82), did not relieve the ER

retention (96). This indicates that the electrically silent behaviour is caused by other parts of the KvS subunits. This was investigated specifically for the Kv6.4 subunit by determining the functionality of several chimeras in which the individual transmembrane segments of Kv6.4 were introduced in a Kv2.1 background (96). Replacing all segments one by one yielded functional channels except for the S6 segment. Interestingly, S6 lacks the second proline of the highly conserved PXP motif. Furthermore, this second proline is absent in all KvS subunits which hints at a general structural difference between functional and silent Kv subunits responsible for the electrically silent behaviour. Unfortunately, restoring the second proline of the PXP motif in the above mentioned non-functional chimera did not restore the functionality of the channel (96).

Various yeast-two-hybrid and Förster resonance energy transfer (FRET) experiments have consistently failed to detect any interaction between KvS subunits using either their N-termini or the full length proteins (62; 85; 95; 104; 122; 138). This indicates that KvS subunits are unable to form homotetramers even in the ER which could explain their silent behavior since four pore domains are necessary to form a K^+ permeation pathway. The lack of interaction between KvS subunits could solely be due to their incompatible N-termini. However, substituting the T1 domain of a KvS subunit with that of a functional channel like Kv2.1, did not relieve the ER retention indicating that other domains are also responsible for the absence of KvS intersubunit interaction (56; 96; 122). It has been suggested that these domains include the S1, S4, and S5 segments given that interactions between these transmembrane regions are important for the functionality of Kv2.1 homotetramers (13). This hypothesis was supported by the observation that simultaneously incorporating the S1 and S5 segments of Kv6.4 in a Kv2.1 background abolished channel functionality which could be restored only by the back mutation of a few residues (13).

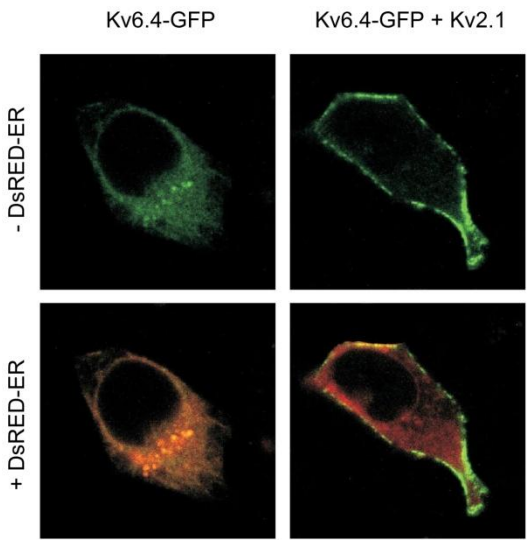

Figure 11: Silent Kv subunits remain trapped in the endoplasmic reticulum (ER). Expression of the GFP-tagged silent Kv subunit Kv6.4 (left) overlaps with the ER marker DsRed-ER, indicating that the KvS subunits are retained in the ER. Co-expression of GFP-tagged Kv6.4 with Kv2.1 (right) results in clear membrane staining. This shows that Kv2.1 relieves the ER retention of Kv6.4 suggesting the formation of heterotetrameric Kv2.1/Kv6.4 channels (95).

4.3.2 Specific Kv2/KvS heterotetramerization

The ER retention of KvS subunits is relieved upon heterotetramerization with members of the Kv2 subfamily (15) (Fig. 11). Like within the Kv1-Kv4 subfamilies, the T1 domain plays an essential role in the association between Kv2 and KvS subunits. So far, two molecular determinants have been identified that mediate the specific interaction between the Kv2.1 and KvS T1 domains. All Kv2 and KvS subunits contain a highly conserved negatively charged CDD amino acid sequence in their N-termini which is absent in the other subfamilies. It was demonstrated that mutating these residues to positively charged ones abolished the interaction between Kv2.1 and Kv6.4 subunits suggesting that these residues are part of an electrostatic network mediating the Kv2/KvS T1-T1 interaction (10). A second molecular determinant is situated in the Zn^{2+} coordinating C3H1 motif as it was observed that mutating the His residue of this motif in the Kv2.1 channel disrupted the interaction with Kv6.3 and Kv6.4 subunits without affecting the interaction with Kv2.1 (85).

In addition to T1-T1 interactions between the Kv2 and KvS subfamilies, yeast-two-hybrid experiments also demonstrated interactions between the N-termini of Kv6.3, Kv6.4, and Kv8.2 and the N-terminus of Kv3.1 (95; 117).

However, these subunits do not form functional heterotetramers at the plasma membrane which suggests that molecular determinants other than the T1 domain are involved as well in the formation of functional Kv2/KvS heterotetramers. Recently, it was found that the Kv2.1/Kv6.4 assembly required the interaction of the Kv6.4 C-terminus with the Kv2.1 N-terminus (12). The intracellular trafficking and voltage-dependent gating of Kv2.1 homotetramers are also regulated by the interaction between the cytoplasmic N- and C-terminus and, moreover, this interaction is governed by a small motif containing the CDD amino acid sequence (89). Interestingly, replacing the Asp residues by positively charged residues of this motif in the Kv2.1 T1 domain prevents the interaction with the Kv6.4 C-terminus (12), suggesting that both the Kv2.1 and Kv6.4 C-terminus interact similarly with the Kv2.1 N-terminus.

The subunit stoichiometry of Kv2/KvS heterotetramers has already been studied for Kv2.1/Kv9.3 channels. From FRET experiments, it was concluded that these heterotetramers assemble with a 3:1 stoichiometry consisting of one Kv9.3 and three Kv2.1 subunits (62). This differs from the other subfamilies in which the assembly presumably occurs as a dimerization of dimers resulting in heterotetramers with a 2:2 stoichiometry (127).

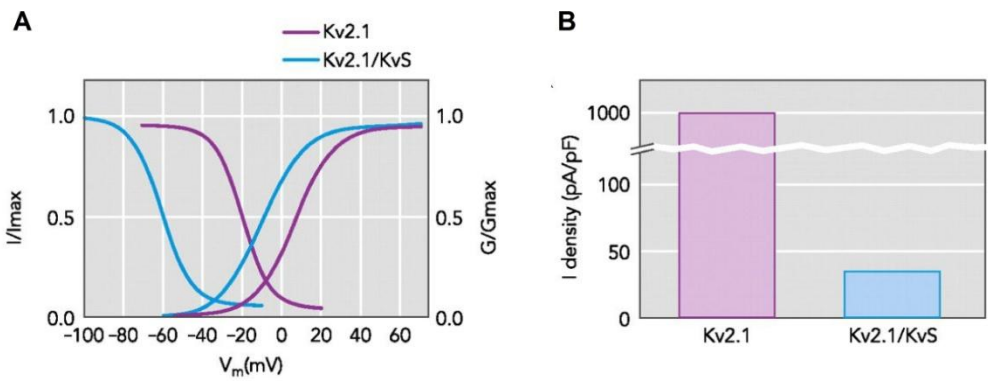

Figure 12: Modulatory behavior of the silent Kv subunits. Schematic overview of the most profound modulatory effects of the KvS subunits on the biophysical properties of the Kv2 channel. Upon heterotetramerization, KvS subunits cause a shift in the voltage dependence of activation and/or inactivation (A). Furthermore, they influence the Kv2 current density (B) (15).

4.3.3 Modulation of the Kv2 properties

Upon heterotetramerization, KvS subunits modulate the biophysical properties of the Kv2 channels. The modulating effects of each KvS subunit are distinct and include shifts in the voltage dependence of activation and/or inactivation, changes in the activation, deactivation and/or inactivation kinetics, and an altered current density (15) (Fig. 12). It has become clear that the molecular determinants underlying these modulating properties may differ among the different KvS subunits. For example, the mechanisms involved in the modulatory effects of the Kv6.1 and Kv6.4 subunits may differ completely, although both subunits cause a large and comparable hyperpolarized shift in the voltage dependence of inactivation. The Kv6.1 subunit possesses a calmodulin-binding domain which may promote the Ca^{2+}/calcineurin-mediated dephosphorylation of Kv2.1 channels resulting in a hyperpolarized shift in the voltage dependence of activation and inactivation (68; 109). In contrast, it was demonstrated that, compared to Kv2.1, the voltage dependence of the Kv6.4 voltage sensor movement shifted into hyperpolarized direction which is in accordance with the shift in the voltage dependence of inactivation (11). Regardless to the underlying mechanisms, KvS-mediated modulation of the Kv2 channels provides each cell type with an additional tool to fine-tune the Kv2 channel properties according to the cell-specific requirements.

4.3.4 Physiological function

Kv2.1 is ubiquitously expressed, while KvS subunits display a more confined expression pattern suggesting that several Kv2/KvS heterotetramers have distinct tissue-specific functions (Fig. 13). This hypothesis is strengthened by the identification of a growing number of physiological processes in which Kv2/KvS heterotetramers are involved and the association between KvS gene mutations and several diseases. Several cell-specific functions have been proposed for KvS subunits (for review see (9)) of which some are described below.

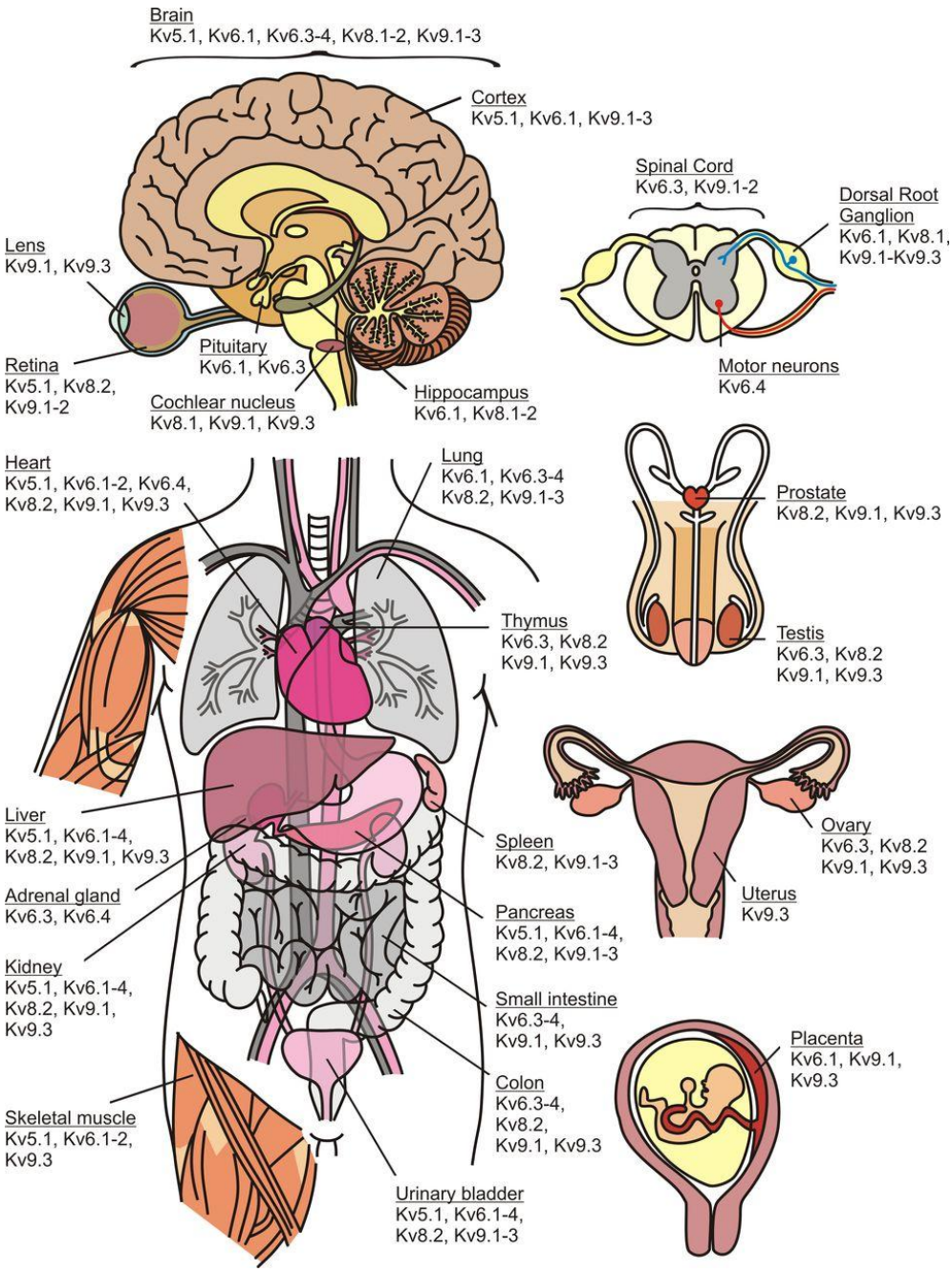

Figure 13: Tissue expression of the silent Kv subunits. Each represented tissue expresses a subset of the KvS subfamily, whereas Kv2.1 is present in all of these tissues (9).

1) Neurons

In the central nervous system, numerous neurons express Kv2.1 channels in their soma and proximal dendrites, where they contribute to the regulation of the firing pattern evoked by synaptic inputs and stimuli (33; 40). Given the wide range of specific neuronal phenotypes, it may be suggested that KvS subunits play a role in shaping these phenotypic identities by modulating the Kv2.1 channel properties. Indeed, it has been demonstrated that several KvS subunits are specifically expressed in certain regions of the brain where they may contribute to the whole-cell K^+ currents (I_K) (17; 20; 32; 35; 37; 61; 129). For example, Kv2.1/Kv8.1 heterotetramers may underlie the slow I_K current of rat hippocampal CA3 pyramidal neurons since Kv8.1 mRNA is expressed in the hippocampus (129) and the properties of this slow I_K current resemble those of heterologously expressed Kv2.1/Kv8.1 channels (81; 108). A role for Kv8.1 in rat hippocampal neurons has been supported further by the observed correlation between Kv8.1 mRNA abundance in the dentate gyrus and the induction of abnormal high-frequency stimulation in the epileptogenic regions of subjects suffering from temporal lobe epilepsy (129). Next to Kv8.1, other KvS subunits are proposed to be involved in epilepsy as well. It was demonstrated, for instance, that polymorphisms in the *KCNV2* gene influenced the severity of seizures in an epileptic mouse model (61). Therefore, Kv8.2 presumably contributes to epilepsy susceptibility which was supported by the identification of two nonsynonymous *KCNV2* single nucleotide polymorphisms (SNPs) associated with human epilepsy (61).

Other diseases involving the central nervous system, including schizophrenia and migraine, are also associated with KvS subunits underscoring their involvement in normal brain function. It was demonstrated that in parvalbumin-containing neurons of the human prefrontal cortex, the Kv9.3 mRNA abundance was lower in schizophrenic subjects compared to controls (36). This suggests that Kv9.3 may play an essential role in the development of schizophrenia, especially since previous work had already indicated that alterations in the activity of parvalbumin-containing γ-amino butyric acid (GABA)

neurons contributed to the development of this disease (39). Migraine has also been linked to proteins involved in ion transport. Recently, a L360P mutation was found in the *KCNG4* gene of migraine patients that was not present in healthy subjects (73), indicating that Kv6.4 may be involved in the onset of migraine.

Photoreceptors of the eye are a specialized type of neurons in which the absorption of photons triggers changes in the membrane potential. Amphibian photoreceptors express a Kv current that sets the dark resting potential and causes hyperpolarizing overshoots in response to illumination (5). The biophysical properties of this current are very similar to those observed after co-expression of Kv2.1 and Kv8.2 in mammalian cell lines (24), suggesting that Kv2.1/Kv8.2 heterotetramers are a major component of the Kv current in these neurons. This has been substantiated by the large spectrum of well characterized human *KCNV2* mutations that cause the retinal disorder 'cone dystrophy with supernormal rod electroretinogram', including mutations that abolish the association of Kv2.1 and Kv8.2 subunits (120; 130) as well as pore mutations that prevent K^+ conduction through Kv2.1/Kv8.2 channels (120). This indicates that normal photoreceptor function requisites the presence of functional Kv2.1/Kv8.2 heterotetramers.

In the peripheral nervous system, several studies have indicated that KvS subunits are involved in regulating the neuronal properties of both sensory and motor neurons. The expression of Kv6.4 was found in a subset of late-gestation chick motor neurons, where it promoted a fast motor neuron biophysical signature characterized by an increased firing threshold and firing frequency, and a shortened duration of the firing periods compared to slow motor neurons (93). The onset of Kv6.4 expression was regulated by the presence of Notch ligand delta-like homologue 1 (Dlk1), which was exclusively expressed in fast motor neurons (93). In small mouse dorsal root ganglion (DRG) neurons, heterotetrameric Kv2/KvS channels also underlie the major component of the whole-cell delayed rectifier K^+ current which was demonstrated by using Kv2-specific channel blockers (i.e., stromatoxin-1 (ScTx) and Kv2.1 antibodies) (14). DRGs contain the cell bodies of sensory neurons of which a subset is involved in

nociception. Interestingly, it was demonstrated that downregulation of Kv9.1 in these neurons, caused a reduction of the mechanical pain threshold in rats (125). This suggests that *KCNS1* may be a putative pain gene, which has been augmented by the identification of two *KCNS1* SNPs associated with pain in humans (22).

2) Cardiac myocytes

Several KvS subunits are expressed in rodent heart tissue (9). Atrial and ventricular myocytes of these animals express both a non-inactivating steady state current and a TEA-sensitive rapidly activating, slowly inactivating current to which Kv2.1 contributes (16; 131). The amplitude of the latter current can differ markedly between individual myocytes which cannot be explained by the varying abundance of Kv2.1 mRNA in these cells (114). This may suggest that KvS subunits fine-tune the cardiac currents in different regions of the heart, although this needs to be investigated further.

3) Smooth muscle cells

Vascular smooth muscle cells (VSMCs) regulate the dilatation and constriction of blood vessels in order to redistribute the blood to the places where it is needed. It has been demonstrated that in several tissues, Kv2.1 and Kv9.3 are substantially expressed in VSMCs where they presumably form Kv2.1/Kv9.3 heterotetramers that contribute to the delayed rectifier K^+ current (92; 99; 137). This suggests that Kv2.1/Kv9.3 channels are involved in the regulation of the blood vessel diameter, which has been supported by several studies. VSMCs regulate the basal vascular tone through the myogenic response. During this response, VSMCs react to stretching of the muscle by opening mechanosensitive channels which causes the membrane to depolarize leading to the contraction of VSMCs (28). Kv2.1/Kv9.3 heterotetramers may be involved in the feedback regulation of this response by contributing to the resting potential and/or the repolarization phase of the VSMCs. This hypothesis has been supported by the observation that Kv2.1 and Kv9.3 subunits are colocalized in the myocytes of rat

medial cerebral arteries (RMCAs) and that inhibition of the Kv2-mediated current in RMCAs causes vasoconstriction (137).

The blood vessel diameter can be influenced by environmental factors such as hypoxia. In lung tissue, hypoxic pulmonary vasoconstriction provides a mechanism to divert the blood flow away from poorly ventilated alveoli (128) and contributes to pulmonary hypertension in, for example, patients with chronic obstructive lung diseases (4). Hypoxia-induced vasoconstriction of small resistance pulmonary artery smooth muscle cells (PASMCs) is caused by inhibition of oxygen-sensitive Kv channels which leads to depolarization of the PASMCs. In response, L-type voltage-gated Ca^{2+} channels open, resulting in vasoconstriction due to the increased cytosolic [Ca^{2+}] (128). It has been suggested that Kv2.1/Kv9.3 heterotetramers are involved in this mechanism as Kv2.1 and Kv9.3 mRNA is abundantly found in rat PASMCs and the biophysical properties of the I_K of rat PASMCs are very similar to those of heterologously expressed Kv2.1/Kv9.3 channels (99; 100). In addition, it was demonstrated that in heterologous expression systems, Kv2.1/Kv9.3 heterotetramers were reversely inhibited by hypoxia suggesting that the Kv2.1/Kv9.3 channels are at least part of the oxygen-sensitive K^+ channel repertoire of rat PASMCs (57). Furthermore, airway responsiveness, which is one of the major clinical symptoms of asthma, has been associated with the *KCNS3* gene by linkage analysis (46; 133). This indicates that Kv9.3 is indeed involved in regulating the airway smooth muscle tone and activity as airway hyperresponsiveness is related to this physiological pathway.

In human fetoplacental arteries, Kv2.1/Kv9.3 heterotetramers may also contribute to hypoxia-induced vasoconstriction which is an important factor in the development of intrauterine growth restriction pregnancies (45). In this pathological condition, babies inside the womb do not grow at the expected rate due to fetal malnutrition caused by hypoperfusion of the placenta (64). A role for Kv9.3 in hypoxia-induced vasoconstriction of fetoplacental arteries has been substantiated by the observed difference in Kv9.3 gene expression between

placental homogenates of normal and intrauterine growth restriction pregnancies (21).

Several KvS subunits have been detected in detrusor smooth muscles (DSMs) of the urinary bladder which express Kv currents that are very similar to the currents seen when Kv2 and KvS subunits are co-expressed in heterologous expression systems (124). The expression of KvS subunits in DSMs seems to be species dependent as in mouse DSMs the presence of Kv5.1, Kv6.1, Kv6.2, and Kv6.4 mRNA was demonstrated (9), whereas in rat and human DSMs only Kv9.3 mRNA was detected so far (18; 54). Regardless of the specific subset of KvS subunits in DSMs, inhibiting the Kv2-containing current of rodent DSMs induced contraction of the urinary bladder suggesting that Kv2/KvS heterotetramers contribute to the regulation of urinary bladder contractility (18; 55).

4) Non-excitable cells

In several non-excitable tissues, the mRNA of different KvS subunits has been detected (9). Although information about the function of KvS subunits in these non-excitable tissues is more sparse than in excitable tissues, there have been some indications on how KvS subunits are involved in non-excitable physiological processes. In lung tissue, for example, Kv9.3 mRNA has been detected in the apical membrane of rat alveolar epithelial cells where they may be involved in basal K^+ secretion (75). The abundance of Kv9.3 mRNA in these cells is correlated to lung function, consolidated by the detection of several SNPs in the *KCNS3* gene that are associated with increased values of forced expiratory volume in the first second, an important parameter to assess lung function (105).

The expression of Kv9.3 has been detected in several human cancer cells including colon carcinoma cells, lung adenocarcinoma cells, and uterine cancer cell lines, where they seem to be involved in regulating cell proliferation (74; 123). This was suggested, for instance, due to the observation that transient knockdown of Kv9.3 expression in human colon and lung carcinoma cells caused cell cycle arrest in the G_0/G_1 phase resulting in a decrease of cancer cell viability (74). Furthermore, Kv9.3 may be involved in the regulation of stem cell

differentiation since Kv9.3 mRNA was detected in high abundance in human neuronal and mesenchymal stem cells, whereas the Kv9.3 mRNA level was much lower in the cells derived from these stem cell types (110; 134). For example, differentiation of mesenchymal stem cells into adipocytes was accompanied by a decrease of Kv9.3 mRNA levels and an increase of Kv2.1 mRNA levels (134).

In human testis tissue, Kv2.1 and the silent Kv subunits Kv6.3, Kv8.1, Kv9.1, and Kv9.3 are expressed (95; 111; 117). Furthermore, Kv9.3 has also been detected in rat testis tissue (99). However, like in a lot of other non-excitable tissues, the influence these KvS subunits have on tissue function remains to be resolved.

5. Aims of the present study

Although no compounds are known yet that selectively target specific Kv2/KvS heterotetramers, it was recently demonstrated that drugs can modulate Kv2.1/Kv6.4 heterotetramers differently than Kv2.1 homotetramers and other Kv2.1/KvS heterotetramers (121). This creates the possibility that Kv2/KvS channels could be specifically pharmacologically targeted in order to modulate the physiological processes regulated by these heterotetramers. Due to their diverse role in various physiological and pathophysiological processes, KvS subunits may therefore be desirable pharmacological targets for the development of novel treatments. However, a lot of questions about the physiology of KvS subunits are to be resolved in order to consider them as therapeutic targets.

In this study, we intended to tackle some of these questions via three specific aims:

1) Determination of the functional Kv2.1/Kv6.4 stoichiometric configurations

It has been demonstrated that the pharmacological characteristics of heteromeric Kv channel complexes can be affected by the stoichiometric and positional arrangements of the involved subunits. Therefore, in order to design drugs that target Kv2/KvS channels, it is important to know the possible stoichiometric configurations of these channels. By determining the functionality of several concatemeric constructs we investigated this specifically for the Kv2.1/Kv6.4 heterotetramers.

2) Determination of the contribution of Kv2-containing channel complexes during the postnatal development of DRG neurons

Postnatal maturation of different neuronal cell types involves developmental changes in different Kv currents including those mediated by Kv2-containing channels. Because Kv2 homotetramers and Kv2/KvS heterotetramers carry the major component of the delayed rectifier K^+ current in DRG neurons, we

examined whether the expression of Kv2 and KvS subunits in these neurons is influenced by postnatal age by combining electrophysiological and semiquantitative RT-PCR experiments.

3) Characterization of the involvement of Kv6.4 in testicular physiology

Although several KvS subunits are expressed in rat and human testis tissue (95; 99; 111; 117), it is unclear how they are involved in the physiological processes taking place in the testis. The creation of a knock-out mouse model in which the *Kcng4* gene was deleted, revealed that male *Kcng4*-null mice are sterile, suggesting a potential role for Kv6.4 in testicular physiology. Therefore, we compared the semen and testicular morphology of wild-type and *Kcng4*-null male mice in order to gain insight in the involvement of Kv6.4 in male fertility.

References

1. **Accili EA, Kiehn J, Yang Q, Wang ZG, Brown AM and Wible BA**. Separable Kv-beta subunit domains alter expression and gating of potassium channels. J Biol Chem 272: 25824-25831, 1997.
2. **Aggarwal SK and MacKinnon R**. Contribution of the S4 segment to gating charge in the Shaker K^+ channel. Neuron 16: 1169-1177, 1996.
3. **Alberts B, Johnson A, Lewis J, Raff M, Roberts K and Walter P**. Molecular biology of the cell. New york and London: Garland Science, 2002.
4. **Barnes PJ and Liu SF**. Regulation of pulmonary vascular tone. Pharmacol Rev 47: 87-131, 1995.
5. **Beech DJ and Barnes S**. Characterization of a voltage-gated K^+ channel that accelerates the rod response to dim light. Neuron 3: 573-581, 1989.
6. **Bezanilla F**. How membrane proteins sense voltage. Nat Rev Mol Cell Biol 9: 323-332, 2008.
7. **Bixby KA, Nanao MH, Shen NV, Kreusch A, Bellamy H, Pfaffinger PJ and Choe S**. Zn^{2+}-binding and molecular determinants of tetramerization in voltage-gated K^+ channels. Nat Struct Biol 6: 38-43, 1999.
8. **Blaine JT and Ribera AB**. Heteromultimeric potassium channels formed by members of the Kv2 subfamily. J Neurosci 18: 9585-9593, 1998.
9. **Bocksteins E**. Kv5, Kv6, Kv8, and Kv9 subunits: No simple silent bystanders. J Gen Physiol 2016.
10. **Bocksteins E, Labro AJ, Mayeur E, Bruyns T, Timmermans JP, Adriaensen D and Snyders DJ**. Conserved negative charges in the N-terminal tetramerization domain mediate efficient assembly of Kv2.1 and Kv2.1/Kv6.4 channels. J Biol Chem 284: 31625-31634, 2009.
11. **Bocksteins E, Labro AJ, Snyders DJ and Mohapatra DP**. The electrically silent Kv6.4 subunit confers hyperpolarized gating charge movement in Kv2.1/Kv6.4 heterotetrameric channels. PLoS ONE 7: e37143, 2012.

12. **Bocksteins E, Mayeur E, van Tilborg A, Regnier G, Timmermans JP and Snyders DJ**. The subfamily-specific interaction between Kv2.1 and Kv6.4 subunits is determined by interactions between the N- and C-termini. PLoS ONE 9: 1-7, 2014.
13. **Bocksteins E, Ottschytsch N, Timmermans JP, Labro AJ and Snyders DJ**. Functional interactions between residues in the S1, S4, and S5 domains of Kv2.1. Eur Biophys J 40: 783-793, 2011.
14. **Bocksteins E, Raes AL, Van de Vijver G, Bruyns T, Van Bogaert PP and Snyders DJ**. Kv2.1 and silent Kv subunits underlie the delayed rectifier K^+ current in cultured small mouse DRG neurons. Am J Physiol Cell Physiol 296: C1271-C1278, 2009.
15. **Bocksteins E and Snyders DJ**. Electrically silent Kv subunits: their molecular and functional characteristics. Physiology (Bethesda) 27: 73-84, 2012.
16. **Bou-Abboud E, Li H and Nerbonne JM**. Molecular diversity of the repolarizing voltage-gated K^+ currents in mouse atrial cells. J Physiol 529 Pt 2: 345-358, 2000.
17. **Castellano A, Chiara MD, Mellstrom B, Molina A, Monje F, Naranjo JR and Lopezbarneo J**. Identification and functional characterization of a K^+ channel alpha-subunit with regulatory properties specific to brain. J Neurosci 17: 4652-4661, 1997.
18. **Chen M, Kellett WF and Petkov GV**. Voltage-gated K^+ channels sensitive to stromatoxin-1 regulate myogenic and neurogenic contractions of rat urinary bladder smooth muscle. Am J Physiol Regul Integr Comp Physiol 299: R177-R184, 2010.
19. **Cheng YM, Azer J, Niven CM, Mafi P, Allard CR, Qi J, Thouta S and Claydon TW**. Molecular determinants of U-type inactivation in Kv2.1 channels. Biophys J 101: 651-661, 2011.
20. **Cioli C, Abdi H, Beaton D, Burnod Y and Mesmoudi S**. Differences in human cortical gene expression match the temporal properties of large-scale functional networks. PLoS ONE 9: e115913, 2014.

21. **Corcoran J, Lacey H, Baker PN and Wareing M**. Altered potassium channel expression in the human placental vasculature of pregnancies complicated by fetal growth restriction. Hypertens Pregnancy 27: 75-86, 2008.
22. **Costigan M, Belfer I, Griffin RS, Dai F, Barrett LB, Coppola G, Wu T, Kiselycznyk C, Poddar M, Lu Y, Diatchenko L, Smith S, Cobos EJ, Zaykin D, Allchorne A, Gershon E, Livneh J, Shen PH, Nikolajsen L, Karppinen J, Mannikko M, Kelempisioti A, Goldman D, Maixner W, Geschwind DH, Max MB, Seltzer Z and Woolf CJ**. Multiple chronic pain states are associated with a common amino acid-changing allele in *KCNS1*. Brain 133: 2519-2527, 2010.
23. **Cuello LG, Jogini V, Cortes DM and Perozo E**. Structural mechanism of C-type inactivation in K^+ channels. Nature 466: 203-208, 2010.
24. **Czirjak G, Toth ZE and Enyedi P**. Characterization of the heteromeric potassium channel formed by Kv2.1 and the retinal subunit Kv8.2 in *Xenopus* oocytes. J Neurophysiol 98: 1213-1222, 2007.
25. **Dai XQ, Kolic J, Marchi P, Sipione S and MacDonald PE**. SUMOylation regulates Kv2.1 and modulates pancreatic beta-cell excitability. J Cell Sci 122: 775-779, 2009.
26. **Dai XQ, Manning Fox JE, Chikvashvili D, Casimir M, Plummer G, Hajmrle C, Spigelman AF, Kin T, Singer-Lahat D, Kang Y, Shapiro AM, Gaisano HY, Lotan I and MacDonald PE**. The voltage-dependent potassium channel subunit Kv2.1 regulates insulin secretion from rodent and human islets independently of its electrical function. Diabetologia 55: 1709-1720, 2012.
27. **David JP, Stas JI, Schmitt N and Bocksteins E**. Auxiliary KCNE subunits modulate both homotetrameric Kv2.1 and heterotetrameric Kv2.1/Kv6.4 channels. Sci Rep 5: 12813, 2015.
28. **Davis MJ and Hill MA**. Signaling mechanisms underlying the vascular myogenic response. Physiol Rev 79: 387-423, 1999.

29. **del Camino D, Kanevsky M and Yellen G**. Status of the Intracellular Gate in the Activated-not-open State of *Shaker* K^+ Channels. J Gen Physiol 126: 419-428, 2005.
30. **del Camino D and Yellen G**. Tight steric closure at the intracellular activation gate of a voltage-gated K^+ channel. Neuron 32: 649-656, 2001.
31. **Doyle DA, Cabral JM, Pfuetzner RA, Kuo A, Gulbis JM, Cohen SL, Chait BT and MacKinnon R**. The structure of the potassium channel: molecular basis of K^+ conduction and selectivity. Science 280: 69-77, 1998.
32. **Drewe JA, Verma S, Frech G and Joho RH**. Distinct spatial and temporal expression patterns of K^+ channel mRNAs from different subfamilies. J Neurosci 12: 538-548, 1992.
33. **Du J, Haak LL, Phillips TE, Russell JT and McBain CJ**. Frequency-dependent regulation of rat hippocampal somato-dendritic excitability by the K^+ channel subunit Kv2.1. J Physiol Lond 522: 19-31, 2000.
34. **Frech GC, VanDongen AM, Schuster G, Brown AM and Joho RH**. A novel potassium channel with delayed rectifier properties isolated from rat brain by expression cloning. Nature 340: 642-645, 1989.
35. **Friedland DR, Eernisse R and Popper P**. Potassium channel gene expression in the rat cochlear nucleus. Hear Res 228: 31-43, 2007.
36. **Georgiev D, Arion D, Enwright JF, Kikuchi M, Minabe Y, Corradi JP, Lewis DA and Hashimoto T**. Lower gene expression for KCNS3 potassium channel subunit in parvalbumin-containing neurons in the prefrontal cortex in schizophrenia. Am J Psychiatry 171: 62-71, 2014.
37. **Georgiev D, Gonzalez-Burgos G, Kikuchi M, Minabe Y, Lewis DA and Hashimoto T**. Selective expression of KCNS3 potassium channel alpha-subunit in parvalbumin-containing GABA neurons in the human prefrontal cortex. PLoS ONE 7: e43904, 2012.
38. **Goldman DE**. Potential, impedance and rectification in membranes. J Gen Physiol 27: 37-60, 1943.

39. **Gonzalez-Burgos G, Hashimoto T and Lewis DA**. Alterations of cortical GABA neurons and network oscillations in schizophrenia. Curr Psychiatry Rep 12: 335-344, 2010.
40. **Guan D, Armstrong WE and Foehring RC**. Kv2 channels regulate firing rate in pyramidal neurons from rat sensorimotor cortex. J Physiol 591: 4807-4825, 2013.
41. **Gulbis JM, Zhou M, Mann S and MacKinnon R**. Structure of the cytoplasmic beta subunit-T1 assembly of voltage-dependent K^+ channels. Science 289: 123-127, 2000.
42. **Gutman GA, Chandy KG, Adelman JP, Aiyar J, Bayliss DA, Clapham DE, Covarriubias M, Desir GV, Furuichi K, Ganetzky B, Garcia ML, Grissmer S, Jan LY, Karschin A, Kim D, Kuperschmidt S, Kurachi Y, Lazdunski M, Lesage F, Lester HA, McKinnon D, Nichols CG, O'Kelly I, Robbins J, Robertson GA, Rudy B, Sanguinetti M, Seino S, Stuehmer W, Tamkun MM, Vandenberg CA, Wei A, Wulff H and Wymore RS**. International Union of Pharmacology. XLI. Compendium of voltage-gated ion channels: potassium channels. Pharmacol Rev 55: 583-586, 2003.
43. **Gutman GA, Chandy KG, Grissmer S, Lazdunski M, McKinnon D, Pardo LA, Robertson GA, Rudy B, Sanguinetti MC, Stuhmer W and Wang X**. International Union of Pharmacology. LIII. Nomenclature and molecular relationships of voltage-gated potassium channels. Pharmacol Rev 57: 473-508, 2005.
44. **Hamill OP, Marty A, Neher E, Sakmann B and Sigworth FJ**. Improved patch clamp techniques for high-resolution current recording from cells and cell-free membrane patches. Pflugers Archiv - European Journal of Physiology 391: 85-100, 1981.
45. **Hampl V and Jakoubek V**. Regulation of fetoplacental vascular bed by hypoxia. Physiol Res 58 Suppl 2: S87-S93, 2009.

46. **Hao K, Niu T, Xu X, Fang Z and Xu X**. Single nucleotide polymorphisms of the *KCNS3* gene are significantly associated with airway hyperresponsiveness. Hum Genet 116: 378-383, 2005.
47. **Heginbotham L, Lu Z, Abramson T and MacKinnon R**. Mutations in the K^+ channel signature sequence. Biophys J 66: 1061-1067, 1994.
48. **Hille B**. Ion channels of excitable membranes. Sunderland, Mass: Sinauer, 2001.
49. **Hodgkin AL, Huxley AF and Katz B**. Measurement of current-voltage relations in the membrane of the giant axon of Loligo. J Physiol 116: 424-448, 1952.
50. **Hodgkin AL and Katz B**. The effect of sodium ions on the electrical activity of the giant axon of the squid. J Physiol (Lond) 108: 37-77, 1949.
51. **Hoshi T, Zagotta WN and Aldrich RW**. Biophysical and molecular mechanisms of *Shaker* potassium channel inactivation. Science 250: 533-538, 1990.
52. **Hoshi T, Zagotta WN and Aldrich RW**. Two types of inactivation in *Shaker* K^+ channels: effects of alterations in the carboxy-terminal region. Neuron 7: 547-556, 1991.
53. **Hoshi T, Zagotta WN and Aldrich RW**. Two types of inactivation in *Shaker* K^+ channels: effects of alterations in the carboxy-terminal region. Neuron 7: 547-556, 1991.
54. **Hristov KL, Chen M, Afeli SA, Cheng Q, Rovner ES and Petkov GV**. Expression and function of Kv2-containing channels in human urinary bladder smooth muscle. Am J Physiol Cell Physiol 302: C1599-C1608, 2012.
55. **Hristov KL, Chen M, Soder RP, Parajuli SP, Cheng Q, Kellett WF and Petkov GV**. Kv2.1 and electrically silent Kv channel subunits control excitability and contractility of guinea pig detrusor smooth muscle. Am J Physiol Cell Physiol 302: C360-C372, 2012.

56. **Hugnot JP, Salinas M, Lesage F, Guillemare E, de Weille J, Heurteaux C, Mattei MG and Lazdunski M**. Kv8.1, a new neuronal potassium channel subunit with specific inhibitory properties towards *Shab* and *Shaw* channels. EMBO J 15: 3322-3331, 1996.
57. **Hulme JT, Coppock EA, Felipe A, Martens JR and Tamkun MM**. Oxygen sensitivity of cloned voltage-gated K^+ channels expressed in the pulmonary vasculature. Circ Res 85: 489-497, 1999.
58. **Hwang PM, Fotuhi M, Bredt DS, Cunningham AM and Snyder SH**. Contrasting immunohistochemical localizations in rat brain of two novel K^+ channels of the *Shab* subfamily. J Neurosci 13: 1569-1576, 1993.
59. **Hwang PM, Glatt CE, Bredt DS, Yellen G and Snyder SH**. A novel K^+ channel with unique localizations in mammalian brain: molecular cloning and characterization. Neuron 8: 473-481, 1992.
60. **Jogini V and Roux B**. Dynamics of the Kv1.2 voltage-gated K^+ channel in a membrane environment. Biophys J 93: 3070-3082, 2007.
61. **Jorge BS, Campbell CM, Miller AR, Rutter ED, Gurnett CA, Vanoye CG, George AL, Jr. and Kearney JA**. Voltage-gated potassium channel KCNV2 (Kv8.2) contributes to epilepsy susceptibility. Proc Natl Acad Sci U S A 108: 5443-5448, 2011.
62. **Kerschensteiner D, Soto F and Stocker M**. Fluorescence measurements reveal stoichiometry of K^+ channels formed by modulatory and delayed rectifier alpha-subunits. Proc Natl Acad Sci U S A 102: 6160-6165, 2005.
63. **Kihira Y, Hermanstyne TO and Misonou H**. Formation of heteromeric Kv2 channels in mammalian brain neurons. J Biol Chem 285: 15048-15055, 2010.
64. **Kingdom JC and Kaufmann P**. Oxygen and placental villous development: origins of fetal hypoxia. Placenta 18: 613-621, 1997.
65. **Klemic KG, Kirsch GE and Jones SW**. U-type inactivation of Kv3.1 and *Shaker* potassium channels. Biophys J 81: 814-826, 2001.

66. **Klemic KG, Shieh CC, Kirsch GE and Jones SW**. Inactivation of Kv2.1 potassium channels. Biophys J 74: 1779-1789, 1998.
67. **Kobertz WR, Williams C and Miller C**. Hanging gondola structure of the T1 domain in a voltage-gated K^+ channel. Biochem 39: 10347-10352, 2000.
68. **Kramer JW, Post MA, Brown AM and Kirsch GE**. Modulation of potassium channel gating by coexpression of Kv2.1 with regulatory Kv5.1 or Kv6.1 alpha-subunits. Am J Physiol 274: C1501-C1510, 1998.
69. **Kurata HT, Doerksen KW, Eldstrom JR, Rezazadeh S and Fedida D**. Separation of P/C- and U-type inactivation pathways in Kv1.5 potassium channels. J Physiol 568: 31-46, 2005.
70. **Kurata HT and Fedida D**. A structural interpretation of voltage-gated potassium channel inactivation. Prog Biophys Mol Biol 92: 185-208, 2006.
71. **Kuryshev YA, Gudz TI, Brown AM and Wible BA**. KChAP as a chaperone for specific K^+ channels. Am J Physiol Cell Physiol 278: C931-C941, 2000.
72. **Labro AJ, Raes AL, Bellens I, Ottschytsch N and Snyders DJ**. Gating of *Shaker*-type channels requires the flexibility of S6 caused by prolines. J Biol Chem 278: 50724-50731, 2003.
73. **Lafreniere RG and Rouleau GA**. Identification of novel genes involved in migraine. Headache 52 Suppl 2: 107-110, 2012.
74. **Lee JH, Park JW, Byun JK, Kim HK, Ryu PD, Lee SY and Kim DY**. Silencing of voltage-gated potassium channel Kv9.3 inhibits proliferation in human colon and lung carcinoma cells. Oncotarget 6: 8132-8143, 2015.
75. **Lee SY, Maniak PJ, Ingbar DH and O'Grady SM**. Adult alveolar epithelial cells express multiple subtypes of voltage-gated K^+ channels that are located in apical membrane. Am J Physiol Cell Physiol 284: C1614-C1624, 2003.
76. **Lee TE, Philipson LH, Kusnetsov A and Nelson DJ**. Structural determinant for assembly of mammalian K^+ channels. Biophys J 66: 667-673, 1994.

77. **Lim ST, Antonucci DE, Scannevin RH and Trimmer JS**. A novel targeting signal for proximal clustering of the Kv2.1 K^+ channel in hippocampal neurons. Neuron 25: 385-397, 2000.
78. **Long SB, Campbell EB and MacKinnon R**. Crystal structure of a mammalian voltage-dependent *Shaker* family K^+ channel. Science 309: 897-903, 2005.
79. **Long SB, Campbell EB and MacKinnon R**. Voltage sensor of Kv1.2: structural basis of electromechanical coupling. Science 309: 903-908, 2005.
80. **Long SB, Tao X, Campbell EB and MacKinnon R**. Atomic structure of a voltage-dependent K^+ channel in a lipid membrane-like environment. Nature 450: 376-382, 2007.
81. **Luthi A, Gahwiler BH and Gerber U**. A slowly inactivating potassium current in CA3 pyramidal cells of rat hippocampus *in vitro*. J Neurosci 16: 586-594, 1996.
82. **Ma D, Zerangue N, Lin YF, Collins A, Yu M, Jan YN and Jan LY**. Role of ER export signals in controlling surface potassium channel numbers. Science 291: 316-319, 2001.
83. **McCord MC and Aizenman E**. Convergent Ca^{2+} and Zn^{2+} signaling regulates apoptotic Kv2.1 K^+ currents. Proc Natl Acad Sci U S A 110: 13988-13993, 2013.
84. **McCrossan ZA, Roepke TK, Lewis A, Panaghie G and Abbott GW**. Regulation of the Kv2.1 potassium channel by MinK and MiRP1. J Membr Biol 228: 1-14, 2009.
85. **Mederos y Schnitzler M, Rinne S, Skrobek L, Renigunta V, Schlichthorl G, Derst C, Gudermann T, Daut J and Preisig-Muller R**. Mutation of histidine 105 in the T1 domain of the potassium channel Kv2.1 disrupts heteromerization with Kv6.3 and Kv6.4. J Biol Chem 284: 4695-4704, 2009.

86. **Misonou H, Mohapatra DP, Menegola M and Trimmer JS**. Calcium- and metabolic state-dependent modulation of the voltage-dependent Kv2.1 channel regulates neuronal excitability in response to ischemia. J Neurosci 25: 11184-11193, 2005.
87. **Misonou H, Mohapatra DP, Park EW, Leung V, Zhen D, Misonou K, Anderson AE and Trimmer JS**. Regulation of ion channel localization and phosphorylation by neuronal activity. Nat Neurosci 7: 711-718, 2004.
88. **Misonou H, Mohapatra DP and Trimmer JS**. Kv2.1: a voltage-gated K^+ channel critical to dynamic control of neuronal excitability. Neurotoxicology 26: 743-752, 2005.
89. **Mohapatra DP, Siino DF and Trimmer JS**. Interdomain cytoplasmic interactions govern the intracellular trafficking, gating, and modulation of the Kv2.1 channel. J Neurosci 28: 4982-4994, 2008.
90. **Morais-Cabral JH, Zhou Y and MacKinnon R**. Energetic optimization of ion conduction rate by the K^+ selectivity filter. Nature 414: 37-42, 2001.
91. **Morales JM, Castellino RC, Crewe AL, Rasmusson RL and Strauss HC**. A novel beta-subunit increases rate of inactivation of specific voltage-gated potassium channel alpha-subunits. J Biol Chem 270: 6272-6277, 1995.
92. **Moreno-Dominguez A, Cidad P, Miguel-Velado E, Lopez-Lopez JR and Perez-Garcia MT**. *De novo* expression of Kv6.3 contributes to changes in vascular smooth muscle cell excitability in a hypertensive mice strain. J Physiol 587: 625-640, 2009.
93. **Muller D, Cherukuri P, Henningfeld K, Poh CH, Wittler L, Grote P, Schluter O, Schmidt J, Laborda J, Bauer SR, Brownstone RM and Marquardt T**. Dlk1 promotes a fast motor neuron biophysical signature required for peak force execution. Science 343: 1264-1266, 2014.
94. **O'Connell KM, Loftus R and Tamkun MM**. Localization-dependent activity of the Kv2.1 delayed-rectifier K^+ channel. Proc Natl Acad Sci U S A 107: 12351-12356, 2010.

95. **Ottschytsch N, Raes A, Van Hoorick D and Snyders DJ**. Obligatory heterotetramerization of three previously uncharacterized Kv channel alpha-subunits identified in the human genome. Proc Natl Acad Sci U S A 99: 7986-7991, 2002.
96. **Ottschytsch N, Raes AL, Timmermans JP and Snyders DJ**. Domain analysis of Kv6.3, an electrically silent channel. J Physiol 568: 737-747, 2005.
97. **Pal S, Hartnett KA, Nerbonne JM, Levitan ES and Aizenman E**. Mediation of neuronal apoptosis by Kv2.1-encoded potassium channels. J Neurosci 23: 4798-4802, 2003.
98. **Park KS, Mohapatra DP, Misonou H and Trimmer JS**. Graded regulation of the Kv2.1 potassium channel by variable phosphorylation. Science 313: 976-979, 2006.
99. **Patel AJ, Lazdunski M and Honore E**. Kv2.1/Kv9.3, a novel ATP-dependent delayed-rectifier K^+ channel in oxygen-sensitive pulmonary artery myocytes. EMBO J 16: 6615-6625, 1997.
100. **Patel AJ, Lazdunski M and Honore E**. Kv2.1/Kv9.3, an ATP-dependent delayed-rectifier K^+ channel in pulmonary artery myocytes. Ann N Y Acad Sci 868: 438-441, 1999.
101. **Peltola MA, Kuja-Panula J, Lauri SE, Taira T and Rauvala H**. AMIGO is an auxiliary subunit of the Kv2.1 potassium channel. EMBO Rep 12: 1293-1299, 2011.
102. **Perozo E, Cortes DM and Cuello LG**. Structural rearrangements underlying K^+-channel activation gating. Science 285: 73-78, 1999.
103. **Plant LD, Dowdell EJ, Dementieva IS, Marks JD and Goldstein SA**. SUMO modification of cell surface Kv2.1 potassium channels regulates the activity of rat hippocampal neurons. J Gen Physiol 137: 441-454, 2011.
104. **Post MA, Kirsch GE and Brown AM**. Kv2.1 and electrically silent Kv6.1 potassium channel subunits combine and express a novel current. FEBS Lett 399: 177-182, 1996.

105. **Reardon BJ, Hansen JG, Crystal RG, Houston DK, Kritchevsky SB, Harris T, Lohman K, Liu Y, O'Connor GT, Wilk JB, Mezey J, Gao C and Cassano PA**. Vitamin D-responsive *SGPP2* variants associated with lung cell expression and lung function. BMC Med Genet 14: 122, 2013.

106. **Redman PT, Hartnett KA, Aras MA, Levitan ES and Aizenman E**. Regulation of apoptotic potassium currents by coordinated zinc-dependent signalling. J Physiol 587: 4393-4404, 2009.

107. **Redman PT, He K, Hartnett KA, Jefferson BS, Hu L, Rosenberg PA, Levitan ES and Aizenman E**. Apoptotic surge of potassium currents is mediated by p38 phosphorylation of Kv2.1. Proc Natl Acad Sci U S A 104: 3568-3573, 2007.

108. **Salinas M, de Weille J, Guillemare E, Lazdunski M and Hugnot JP**. Modes of regulation of *shab* K^+ channel activity by the Kv8.1 subunit. J Biol Chem 272: 8774-8780, 1997.

109. **Salinas M, Duprat F, Heurteaux C, Hugnot JP and Lazdunski M**. New modulatory alpha-subunits for mammalian *Shab* K^+ channels. J Biol Chem 272: 24371-24379, 1997.

110. **Sandberg CJ, Vik-Mo EO, Behnan J, Helseth E and Langmoen IA**. Transcriptional profiling of adult neural stem-like cells from the human brain. PLoS ONE 9: e114739, 2014.

111. **Sano Y, Mochizuki S, Miyake A, Kitada C, Inamura K, Yokoi H, Nozawa K, Matsushime H and Furuichi K**. Molecular cloning and characterization of Kv6.3, a novel modulatory subunit for voltage-gated K^+ channel Kv2.1. FEBS Lett 512: 230-234, 2002.

112. **Scannevin RH, Murakoshi H, Rhodes KJ and Trimmer JS**. Identification of a cytoplasmic domain important in the polarized expression and clustering of the Kv2.1 K^+ channel. J Cell Biol 135: 1619-1632, 1996.

113. **Schoppa NE, McCormack K, Tanouye MA and Sigworth FJ**. The size of the gating charge in wild type and mutant *Shaker* Potassium channels. Science 255: 1712-1715, 1992.

114. **Schultz JH, Volk T and Ehmke H**. Heterogeneity of Kv2.1 mRNA expression and delayed rectifier current in single isolated myocytes from rat left ventricle. Circ Res 88: 483-490, 2001.
115. **Shen NV, Chen X, Boyer MM and Pfaffinger PJ**. Deletion analysis of K^+ channel assembly. Neuron 11: 67-76, 1993.
116. **Shen NV and Pfaffinger PJ**. Molecular recognition and assembly sequences involved in the subfamily-specific assembly of voltage-gated K^+ channel subunit proteins. Neuron 14: 625-633, 1995.
117. **Shepard AR and Rae JL**. Electrically silent potassium channel subunits from the human lens epithelium. Am J Physiol 277: C412-C424, 1999.
118. **Shepherd AJ, Loo L, Gupte RP, Mickle AD and Mohapatra DP**. Distinct modifications in Kv2.1 channel via chemokine receptor CXCR4 regulate neuronal survival-death dynamics. J Neurosci 32: 17725-17739, 2012.
119. **Shi G, Kleinklaus AK, Marrion NV and Trimmer JS**. Properties of Kv2.1 K^+ channels expressed in transfected mammalian cells. J Biol Chem 269: 23204-23211, 1994.
120. **Smith KE, Wilkie SE, Tebbs-Warner JT, Jarvis BJ, Gallasch L, Stocker M and Hunt DM**. Functional analysis of missense mutations in Kv8.2 causing cone dystrophy with supernormal rod electroretinogram. J Biol Chem 287: 43972-43983, 2012.
121. **Stas JI, Bocksteins E, Labro AJ and Snyders DJ**. Modulation of Closed-State Inactivation in Kv2.1/Kv6.4 Heterotetramers as Mechanism for 4-AP Induced Potentiation. PLoS ONE 10: e0141349, 2015.
122. **Stocker M, Hellwig M and Kerschensteiner D**. Subunit assembly and domain analysis of electrically silent K^+ channel alpha-subunits of the rat Kv9 subfamily. J Neurochem 72: 1725-1734, 1999.
123. **Suzuki T and Takimoto K**. Selective expression of HERG and Kv2 channels influences proliferation of uterine cancer cells. Int J Oncol 25: 153-159, 2004.

124. **Thorneloe KS and Nelson MT**. Properties and molecular basis of the mouse urinary bladder voltage-gated K^+ current. J Physiol 549: 65-74, 2003.

125. **Tsantoulas C, Zhu L, Shaifta Y, Grist J, Ward JP, Raouf R, Michael GJ and McMahon SB**. Sensory neuron downregulation of the Kv9.1 potassium channel subunit mediates neuropathic pain following nerve injury. J Neurosci 32: 17502-17513, 2012.

126. **Tsantoulas C, Zhu L, Yip P, Grist J, Michael GJ and McMahon SB**. Kv2 dysfunction after peripheral axotomy enhances sensory neuron responsiveness to sustained input. Exp Neurol 251: 115-126, 2014.

127. **Tu L and Deutsch C**. Evidence for dimerization of dimers in K^+ channel assembly. Biophys J 76: 2004-2017, 1999.

128. **Weir EK and Archer SL**. The mechanism of acute hypoxic pulmonary vasoconstriction: the tale of two channels. FASEB J 9: 183-189, 1995.

129. **Winden KD, Bragin A, Engel J and Geschwind DH**. Molecular alterations in areas generating fast ripples in an animal model of temporal lobe epilepsy. Neurobiol Dis 78: 35-44, 2015.

130. **Wissinger B, Schaich S, Baumann B, Bonin M, Jagle H, Friedburg C, Varsanyi B, Hoyng CB, Dollfus H, Heckenlively JR, Rosenberg T, Rudolph G, Kellner U, Salati R, Plomp A, De BE, Andrassi-Darida M, Sauer A, Wolf C, Zobor D, Bernd A, Leroy BP, Enyedi P, Cremers FP, Lorenz B, Zrenner E and Kohl S**. Large deletions of the *KCNV2* gene are common in patients with cone dystrophy with supernormal rod response. Hum Mutat 32: 1398-1406, 2011.

131. **Xu H, Barry DM, Li H, Brunet S, Guo W and Nerbonne JM**. Attenuation of the slow component of delayed rectification, action potential prolongation, and triggered activity in mice expressing a dominant-negative Kv2 alpha subunit. Circ Res 85: 623-633, 1999.

132. **Xu J, Yu W, Jan YN, Jan LY and Li M**. Assembly of voltage-gated potassium channels. J Biol Chem 270: 24761-24768, 1995.

133. **Xu X, Fang Z, Wang B, Chen C, Guang W, Jin Y, Yang J, Lewitzky S, Aelony A, Parker A, Meyer J, Weiss ST and Xu X**. A genomewide search for quantitative-trait loci underlying asthma. Am J Hum Genet 69: 1271-1277, 2001.

134. **You MH, Song MS, Lee SK, Ryu PD, Lee SY and Kim DY**. Voltage-gated K^+ channels in adipogenic differentiation of bone marrow-derived human mesenchymal stem cells. Acta Pharmacol Sin 34: 129-136, 2013.

135. **Yu SP, Yeh CH, Sensi SL, Gwag BJ, Canzoniero LM, Farhangrazi ZS, Ying HS, Tian M, Dugan LL and Choi DW**. Mediation of neuronal apoptosis by enhancement of outward potassium current. Science 278: 114-117, 1997.

136. **Zagotta WN, Hoshi T and Aldrich RW**. Restoration of inactivation in mutants of *Shaker* potassium channels by a peptide derived from ShB. Science 250: 568-571, 1990.

137. **Zhong XZ, Abd-Elrahman KS, Liao CH, El-Yazbi AF, Walsh EJ, Walsh MP and Cole WC**. Stromatoxin-sensitive, heteromultimeric Kv2.1/Kv9.3 channels contribute to myogenic control of cerebral arterial diameter. J Physiol 588: 4519-4537, 2010.

138. **Zhu XR, Netzer R, Bohlke K, Liu Q and Pongs O**. Structural and functional characterization of Kv6.2 a new gamma-subunit of voltage-gated potassium channel. Receptors and Channels 6: 337-350, 1999.

Chapter 2

Kv2.1/Kv6.4 heterotetramers are functional in two stoichiometric configurations

Glenn Regnier, Elke Bocksteins, Dirk J. Snyders

Laboratory for Molecular Biophysics, Physiology and Pharmacology, Department of Biomedical Sciences, University of Antwerp, CDE, Universiteitsplein 1, 2610 Antwerpen, Belgium

Manuscript in preparation

Abstract

Members of the voltage-gated K^+ (Kv) subfamilies Kv5, Kv6, Kv8, and Kv9, which are collectively identified as electrically silent (KvS) subunits, selectively modulate the biophysical properties of Kv2 channels by forming heterotetrameric Kv2/KvS channel complexes. Förster resonance energy transfer (FRET) analysis previously demonstrated that Kv2.1/Kv9.3 channels are composed of three Kv2.1 subunits and one Kv9.3 subunit. However, it remains unknown whether Kv2.1/KvS channels can have other stoichiometries. We investigated this specifically for the Kv2.1/Kv6.4 channel by comparing the biophysical properties of different concatemeric constructs to these of the corresponding monomers. Dimers of Kv2.1 and Kv6.4 subunits yielded delayed rectifier currents that had all the characteristics of Kv2.1/Kv6.4 channels, which suggested that these channels are functional with a 2:2 stoichiometry. Electrophysiological analysis of tetrameric constructs revealed that in this stoichiometric configuration, the positional arrangement of the Kv6.4 subunits is crucial. Indeed, we could not detect any functional channels when the Kv6.4 subunits were positioned side by side which confirmed that Kv6.4 subunits have no compatible interaction sites. Additionally, Kv2.1/Kv6.4 tetramers that represented a 3:1 stoichiometry also had the signature properties of a Kv2.1/Kv6.4 channel. Taken together, our data suggest that the stoichiometry can be either 3:1 or 2:2 with the restriction that Kv2.1 and Kv6.4 have to alternate in the channel complex.

Introduction

Voltage-gated K^+ (Kv) channels are integral membrane proteins which regulate the selective transport of K^+ ions across the cell membrane by opening, closing, and/or inactivating in response to changes in membrane voltage (11). A fully assembled Kv channel consists of four α-subunits each comprising six transmembrane segments (S1-S6), a pore loop (P), and a cytoplasmic NH_2- and COOH-terminus (20). The S1-S4 segments form the voltage sensing domain

(VSD) that translates changes in membrane potential into opening or closing of the pore which in turn is composed of the P helices and the S5 and S6 segments (21). The N-terminus contains the T1 domain which is a key determinant in the subfamily-specific assembly of Kv1-Kv4 subunits (18; 31).

In order to tune the native Kv currents to the tissue-specific requirements, each tissue expresses a specific set of α-subunits which are subdivided into several subfamilies based on sequence homology. In the case of the closely *Shaker*-related subunits, eight different subfamilies can be distinguished: Kv1-Kv6 and Kv8-Kv9 (9). Within each of the Kv1-Kv4 subfamilies, subunits cannot only oligomerize into homotetramers, but also into heterotetramers which greatly increases the diversity of Kv channel complexes. On the other hand, members of the Kv5, Kv6, Kv8, and Kv9 subfamilies are unable to form functional channels even though they have the typical topology of a Kv α-subunit and were therefore designated silent Kv (KvS) subunits (for review see (7)). However, they selectively interact with members of the Kv2 subfamily, forming functional Kv2/KvS heterotetramers that possess unique biophysical and pharmacological properties. Generally, they slow the activation and deactivation kinetics, shift the voltage dependence of activation and/or inactivation, and reduce the current density relative to Kv2 homotetramers and are thus considered modulatory α-subunits of the Kv2 subfamily.

The oligomerization of Kv subunits into a functional channel may occur by the sequential addition of monomers to the channel complex, but there is evidence that this preferentially occurs by dimerization of dimers in which the dimeric interaction sites differ from those mediating monomer-monomer interactions (36). Therefore, it is expected that heterotetramers assemble with a 2:2 stoichiometry which has been confirmed in the case of the Kv4 subfamily (12). However, for Kv2.1/Kv9.3 heterotetramers a stoichiometry of three Kv2.1 subunits and one Kv9.3 subunit has been deduced (14). Whether this 3:1 stoichiometry can be generalized to all Kv2/KvS channels has not been tested.

Several studies have shown that the subunit stoichiometry of heteromeric Kv channel complexes can be variable depending on the relative expression of

the involved subunits (15; 16; 25; 34; 39). This could imply that the stoichiometry of Kv2/KvS channels is not fixed at 3:1 and that other configurations yield functional channels as well. To study this we created different Kv2.1/Kv6.4 concatemeric constructs and compared their biophysical properties to those of the corresponding monomeric constructs, an approach that has previously been used successfully to study the stoichiometry and conformational rearrangements of ion channels (19; 26; 30). Our data indicate that Kv2.1/Kv6.4 heterotetramers are functional in both a 3:1 and a 2:2 configuration. Furthermore, functional Kv2.1/Kv6.4 channels with a 2:2 stoichiometry were only observed when the Kv6.4 subunits were not positioned next to each other, which confirmed that Kv6.4 subunits fail to interact with themselves.

Material and methods

Concatemer design

Concatemeric constructs were created by the sequential insertion of the individual subunits into a digested vector whereby adjacent subunits share a unique restriction-enzyme site. Neighbouring subunits were segregated by a linker sequence of 30-36 bp which was tagged to the individual subunits before they were inserted into the concatemer. Human Kv2.1 (GenBank Accession number NM_004975) and Kv6.4 (NM_172347) were both cloned in the mammalian expression vector pEGFP-N1 (Clontech, Mountain View, CA, USA) as described previously (27). Both the appropriate restriction-enzyme sites and the linker sequences were introduced by PCR amplification using the QuickChange Site-directed Mutagenesis kit (Agilent Technologies, Santa Clara, CA, USA) and mutant primers. The presence of the desired modifications and the absence of unwanted mutations were confirmed by DNA sequencing.

Western blot

Concatemeric constructs (10 µg) were transiently transfected into human embryonic kidney 293 (HEK293) cells using the Lipofectamine reagent (ThermoFisher Scientific, Waltham, MA, USA) according to the manufacturer's guidelines. Cells were cultured in modified Eagle's medium (MEM) (ThermoFisher Scientific) supplemented with 10% fetal bovine serum, 1% penicillin/streptomycin, and 1% non-essential amino acids under a 5% CO_2 atmosphere. Transfections were performed in 75 cm² cell culture flasks filled with 13 mL culture medium and 48 hours after transfection, cells were dissociated with trypsin. Lysates were obtained by applying lysis buffer, consisting of phosphate buffered saline (PBS) supplemented with 5 mmol/L EDTA, 1% Triton X-100, and a complete protease inhibitor mixture (Roche Diagnostics, Basel, Switzerland) and were denatured afterwards in NuPAGE LDS sample buffer (ThermoFisher Scientific) for 30 min at 37°C. The samples were separated on a NuPAGE 3-8% Tric-Acetate gel (ThermoFisher Scientific) and then transferred to a polyvinylidene difluoride (PVDF) membrane which was subsequently blocked with 5% non-fat milk powder in PBS. Concatemers were detected by overnight incubation with 1 µg/mL mouse Kv2.1 antibodies (K89/34) (UC Davis/NIH NeuroMab Facility, Davis, CA, USA), followed by incubation with horseradish peroxidase-labeled anti-mouse IgG (GE healthcare, Little Chalfont, UK) and subsequent enhanced chemilluminescence (ECL) detection using the WesternBright Sirius Chemiluminescent Detection kit (Advansta, Menlo Park, CA, USA) according to the manufacturer's guidelines. Western blot experiments were performed on two independent HEK preparations.

Electrophysiology

Ltk^- cells (mouse fibroblasts, ATCC CCL 1.3) were cultured in Dulbecco's modified Eagle's medium (DMEM) (ThermoScientific) supplemented with 10% horse serum and 1% penicillin/streptomycin under a 5% CO_2 atmosphere. Cells were transiently transfected with the appropriate amount of cDNA (as indicated in the figure legends) in combination with 0.5 µg GFP as a transfection marker

using the Lipofectamine2000 reagent (ThermoFisher Scientific) according to the manufacturer's guidelines. Transfections were performed in 60 mm cell culture dishes filled with 5 mL culture medium. Cells transfected with dimeric and tetrameric constructs were incubated at 37°C for 16-24 h and at 25°C for 42-48 h, respectively, before they were dissociated with trypsin and used for electrophysiological analysis.

Whole cell current recordings were obtained at room temperature (20-22°C) with an Axopatch-200B amplifier (Molecular Devices, Sunnyvale, CA, USA) and were digitized using a Digidata-1440A low-noise data acquisition system (Molecular Devices). Command voltages and data storage were controlled with the pClamp10.2 software (Molecular Devices). Patch pipettes were pulled from 1.2 mm borosilicate glass (World Precision Instruments, Sarasota, FL, USA) and heat polished after which the resistance was 1-3 MΩ in the bath solution. The cells were perfused continuously with a bath solution containing (in mmol/L): 145 NaCl, 4 KCl, 1 $MgCl_2$, 1.8 $CaCl_2$, 10 HEPES, and 10 glucose with the pH adjusted to 7.35 with NaOH. The patch pipettes were filled with an intracellular solution containing (in mmol/L): 110 KCl, 5 K_2ATP, 2 $MgCl_2$, 10 HEPES, and 5 K_4BAPTA adjusted to pH 7.2 with KOH. Junction potentials were zeroed with the filled pipette in the bath solution. Cells were excluded from analysis if the voltage error exceeded 5 mV after series resistance compensation.

Pulse protocols and data analysis

Voltage protocols were adjusted based on the biophysical properties of the channels as shown in the figures. The holding potential was -80 mV and the interpulse interval ranged from 15 to 30 sec to prevent channels from accumulating in the inactivated state. The voltage dependence of activation and inactivation was fitted with a Boltzmann equation: $y = 1/\{1+\exp[-(V-V_{1/2})/k]\}$ in which V represents the applied voltage, $V_{1/2}$ the voltage at which 50% of the channels are open or inactivated, and k the slope factor. Time constants of activation and deactivation were determined by fitting the current traces with a single or double exponential function. Results are presented as mean ± SEM.

Results

Kv2.1/Kv6.4 heterotetramers are functional in a 2:2 stoichiometric configuration

In a previous study, Förster resonance energy transfer (FRET) analysis of the Kv2/KvS stoichiometry had revealed a 3:1 configuration for Kv2.1/Kv9.3 channels (i.e., three Kv2.1 subunits and one Kv9.3 subunit) after transient transfection of the corresponding monomers in a 1:2 ratio (14). However, in heterologous expression systems, the ratio between compatible Kv subunits influences the stoichiometry of heterotetrameric channel complexes (15; 16; 25; 34; 39). Therefore, we investigated whether Kv2/KvS heterotetramers can also be functional in a 2:2 configuration, using Kv6.4 as a representative member of the KvS family given its profound modulating effect on the Kv2 channel properties (27). Since Kv channels assemble most likely by the dimerization of dimers (36), we initially created different dimeric constructs for this purpose (i.e., Kv2.1-Kv2.1, Kv2.1-Kv6.4, and Kv6.4-Kv2.1) (fig. 1A) in order to compare their electrophysiological properties with those of channels obtained from the corresponding monomers. To avoid limitations on the conformational flexibility of the covalently linked subunits, we inserted a linker peptide between them (Fig. 1A) which has been proven to be an effective approach to circumvent this potential problem (10; 13; 19; 30). Before the biophysical properties of these dimers were studied, we examined them with Western blot analysis to confirm their expression as a single polypeptide (Fig. 1B): all positive controls and dimeric constructs yielded one major protein band when probed with Kv2.1 antibodies with a molecular mass that approached their estimated weight (i.e., Kv2.1: 96 kDa, Kv2.1-Kv2.1: 192 kDa, Kv2.1-Kv6.4 and Kv6.4-Kv2.1: 155 kDa).

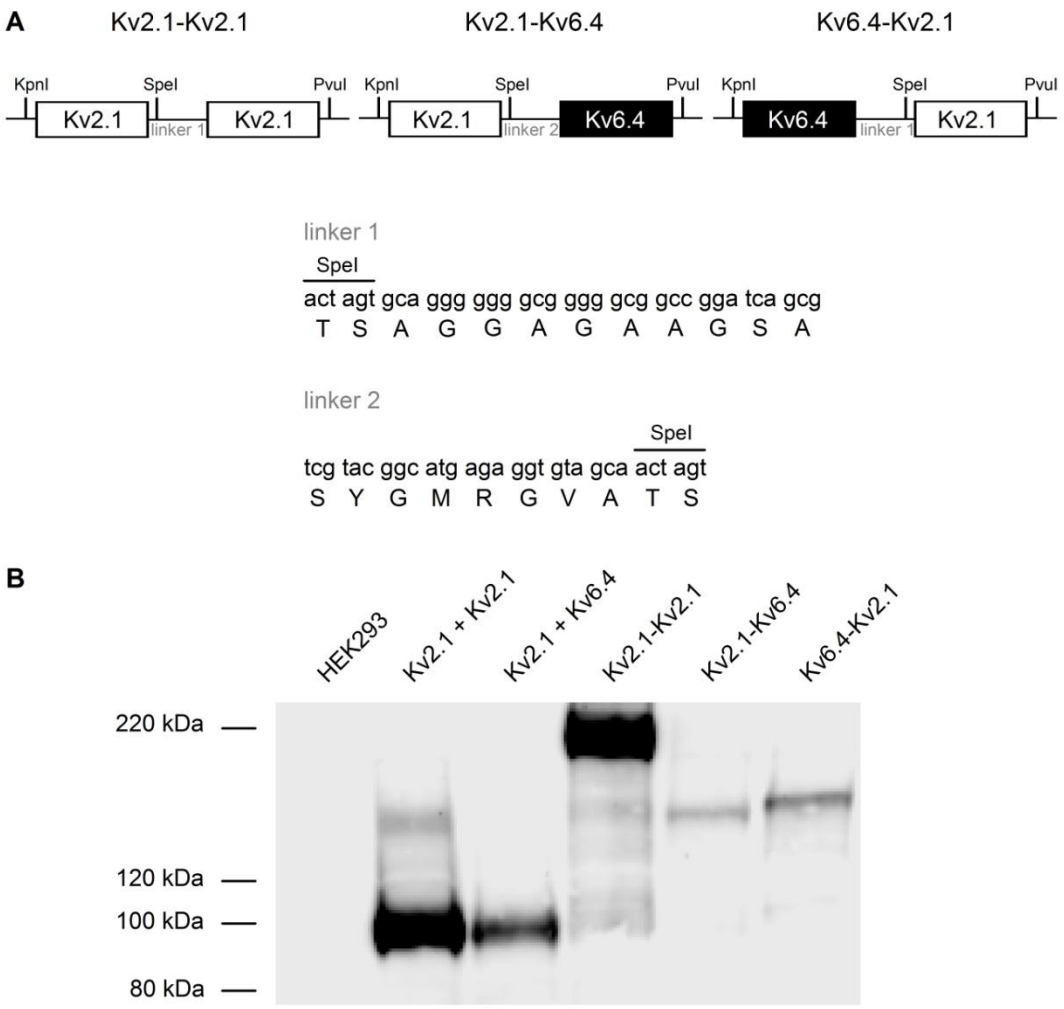

Figure 1: Overview and Western blot analysis of dimeric Kv2.1 and Kv2.1/Kv6.4 constructs. (A) Design of Kv2.1-Kv2.1 (left), Kv2.1-Kv6.4 (middle), and Kv6.4-Kv2.1 (right) dimers. The Kv2.1 and Kv6.4 subunits are shown in white and black, respectively. Neighbouring subunits had a common, unique restriction enzyme (RE) site enabling the linkage of subunits using specific RE digests. Subunits were covalently joined by a peptide linker of which the nucleotide and amino acid sequences are shown below in lower and upper case, respectively. (B) Expression of dimers as a single polypeptide was examined with Western blotting using Kv2.1 antibodies. As a positive control, lysates of HEK293 cells (co-)transfected with Kv2.1 and Kv6.4 or with Kv2.1 alone were used. In all lysates containing the positive controls or the dimers, a single band was noticeable which corresponded to the predicted molecular mass, while no signal was detected in lysates of nontransfected HEK293 cells.

In order to verify the above approach to investigate the functionality of Kv2.1/Kv6.4 channels with a 2:2 stoichiometry, we first compared the biophysical properties of Kv2.1 monomers and Kv2.1 dimers of which typical current recordings are shown in figure 2 (panels A and B). No differences could be observed in the voltage dependence of activation (Fig. 2C and Table 1) and inactivation (Fig. 2D and table 1) or in the time constants of activation and deactivation (Fig. 2E). This indicated that the peptide sequence used to covalently link both Kv2.1 subunits allowed enough conformational flexibility to yield functional channels without affecting their biophysical properties.

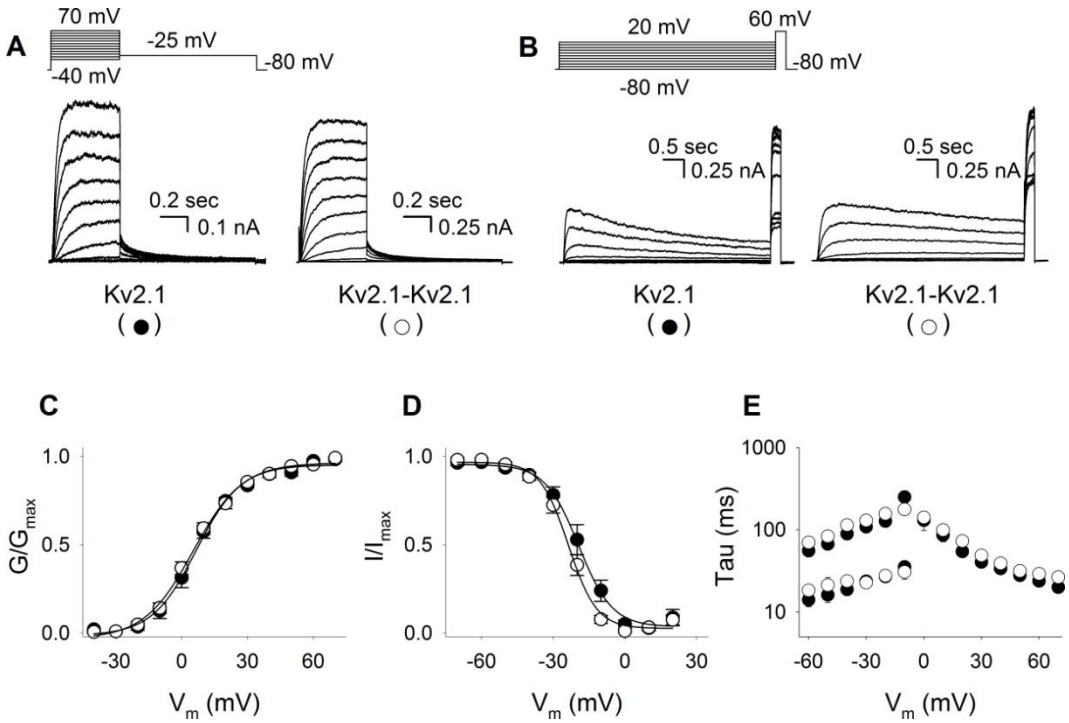

Figure 2: Biophysical properties of Kv2.1 monomers and dimers. Whole cell current recordings of Kv2.1 channels composed of Kv2.1 monomers (●) or Kv2.1 dimers (○) used to determine the activation (A) and inactivation (B) properties. Voltage protocols are shown on top. (C) Voltage dependence of activation derived from plotting the normalized tail current amplitudes at -25 mv as a function of the prepulse potential. (D) Voltage dependence of inactivation obtained from the normalized peak current amplitude at +60 mV in function of the prepulse potential. (E) Time constants of activation and deactivation obtained as described in Material and Methods. Note that the biophysical properties of Kv2.1 dimers were similar to those of Kv2.1 monomers.

Table 1: Biophysical properties of homotetrameric Kv2.1 and heterotetrameric Kv2.1/Kv6.4 channels composed of monomers or dimers

	Activation			Inactivation		
	$V_{1/2}$	k	n	$V_{1/2}$	K	n
Kv2.1	6.1 ± 2.2	9.0 ± 0.4	7	-18.2 ± 2.3	6.4 ± 0.5	7
Kv2.1-Kv2.1	5.6 ± 2.4	10.9 ± 1.5	7	-23.4 ± 2.2	5.6 ± 0.9	7
Kv2.1 + Kv6.4	7.9 ± 0.7	20.2 ± 0.7	3	-59.2 ± 2.5	7.4 ± 1.2	7
Kv2.1-Kv6.4	-4.6 ± 1.0	18.4 ± 0.6	3	-58.4 ± 0.7	7.3 ± 0.3	7
Kv6.4-Kv2.1	2.4 ± 2.7	21.6 ± 2.5	4	-62.5 ± 1.9	7.3 ± 0.2	6

Values are given as mean ± SEM and n the number of cells analysed. The midpoints of activation and inactivation ($V_{1/2}$), represented in mV, and the slope factor (k) were obtained from a single Boltzmann fit.

It has been demonstrated previously that the biophysical properties of dimers containing two different subunits can be affected by the position of these subunits in the dimeric construct (23). Therefore, we designed two different dimeric constructs to investigate the functionality of Kv2.1/Kv6.4 channels in a 2:2 configuration: Kv2.1-Kv6.4 and Kv6.4-Kv2.1. Co-expression of Kv2.1 and Kv6.4 monomers yielded functional Kv2.1/Kv6.4 heterotetramers which possessed biophysical properties that differed from those of Kv2.1 homotetramers and that were comparable with those of earlier reports on co-expression of these subunits (4-6; 8; 27; 28; 33) (Table 1). The most distinct differences compared to Kv2.1 homotetramers included a ~40 mV hyperpolarizing shift in the voltage dependence of inactivation ($V_{1/2}$ = -59.2 ± 2.5 mV, n = 7) and a decreased slope factor of the voltage dependence of activation (k = 20.2 ± 0.7, n = 3). Kv2.1-Kv6.4 and Kv6.4-Kv2.1 dimers produced currents with similar characteristics (Fig. 3A): the voltage dependence of inactivation of these dimers was characterized by a $V_{1/2}$ of -58.4 ± 0.7 mV and -62.5 ± 1.9 mV, respectively, while the slope factor k was 18.4 ± 0.6 and 21.6 ± 2.5 (Fig. 3B and Table 1). Furthermore, the activation and deactivation kinetics of both dimers were comparable to those of the co-

expressed Kv2.1 and Kv6.4 monomers (Fig. 3C). These results suggested that Kv2.1 and Kv6.4 subunits can heterotetramerize into functional channels with a 2:2 stoichiometry in which Kv2.1 and Kv6.4 subunits are arranged alternately.

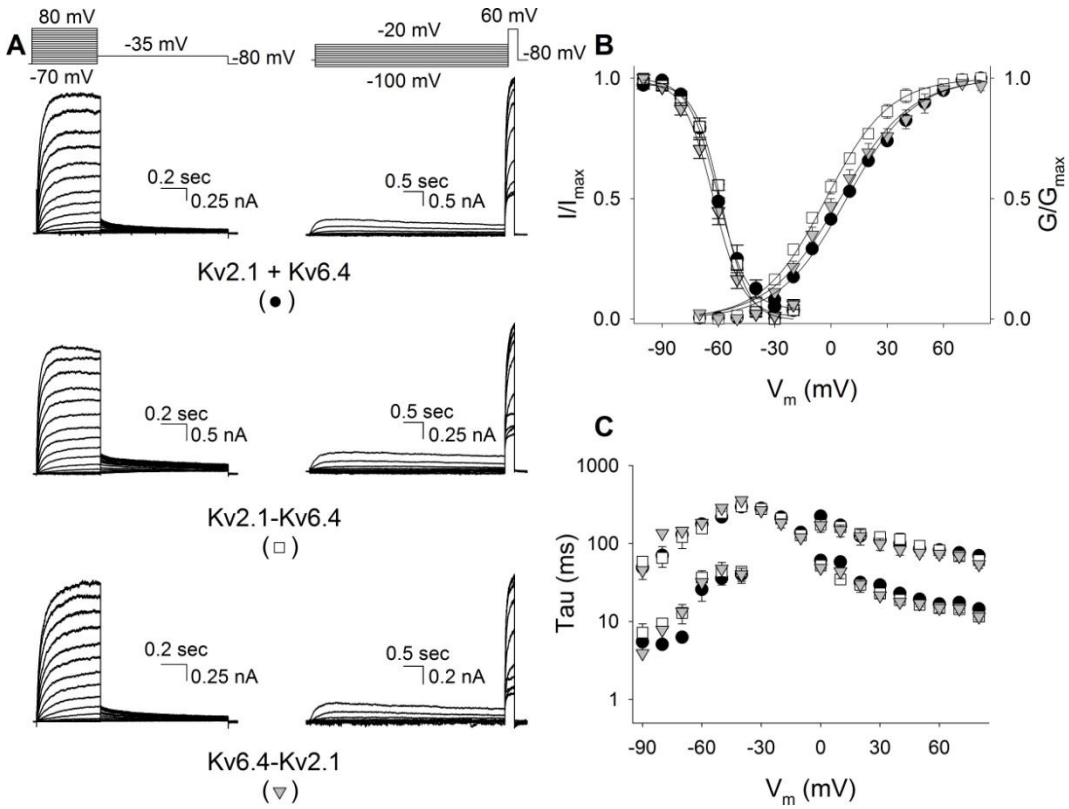

Figure 3: (A) Whole cell current recordings after (co-)transfection of 0.5 µg Kv2.1 and 5 µg Kv6.4 (top) (●), 5 µg Kv2.1-Kv6.4 (middle) (□), and 5 µg Kv6.4-Kv2.1 (top) (▽) used to determine the activation (left) and inactivation (right) properties. Voltage protocols are shown on top. (B) Voltage dependence of activation (right) and inactivation (left). Voltage dependence of activation was derived from plotting the normalized tail current amplitudes at -35 mv as a function of the prepulse potential. Voltage dependence of inactivation was obtained from the normalized peak current amplitude at +60 mV in function of the prepulse potential. (E) Time constants of activation and deactivation obtained as described in Material and Methods. Note that the biophysical properties of the Kv2.1-Kv6.4 and Kv6.4-Kv2.1 dimers were similar to those of the co-expressed Kv2.1 and Kv6.4 monomers.

Kv2.1/Kv6.4 heterotetramers are not functional in a 2:2 configuration when the Kv6.4 subunits are positioned side by side

Although we could demonstrate that Kv2.1/Kv6.4 channels are functional in a 2:2 configuration by using dimeric constructs, we could not test the functionality of different geometrical arrangements with this approach. These include other stoichiometric configurations and in the case of a 2:2 stoichiometry two different spatial configurations; the Kv6.4 subunits can be positioned side by side or can be separated from each other by Kv2.1 subunits which we will refer to as the adjacent and alternating configuration, respectively. To explore these possible configurations of the Kv2.1/Kv6.4 channel, we created following tetrameric constructs (Fig. 4A): Kv2.1 tetramer, Kv2.1-Kv6.4-Kv2.1-Kv6.4, Kv2.1-Kv6.4-Kv6.4-Kv2.1, and Kv2.1-Kv6.4-Kv2.1-Kv2.1. As for the dimeric constructs, neighbouring subunits were covalently coupled with a linker peptide. Using Kv2.1 antibodies, Western blot analysis revealed that all tetrameric constructs were expressed as a single polypeptide with a molecular mass that corresponded with the estimated weight (i.e., Kv2.1 tetramer: 384 kDa, Kv2.1-Kv6.4-Kv2.1-Kv2.1: 347 kDa, Kv2.1-Kv6.4-Kv2.1-Kv6.4 and Kv2.1-Kv6.4-Kv6.4-Kv2.1: 310 kDa) (Fig. 4B).

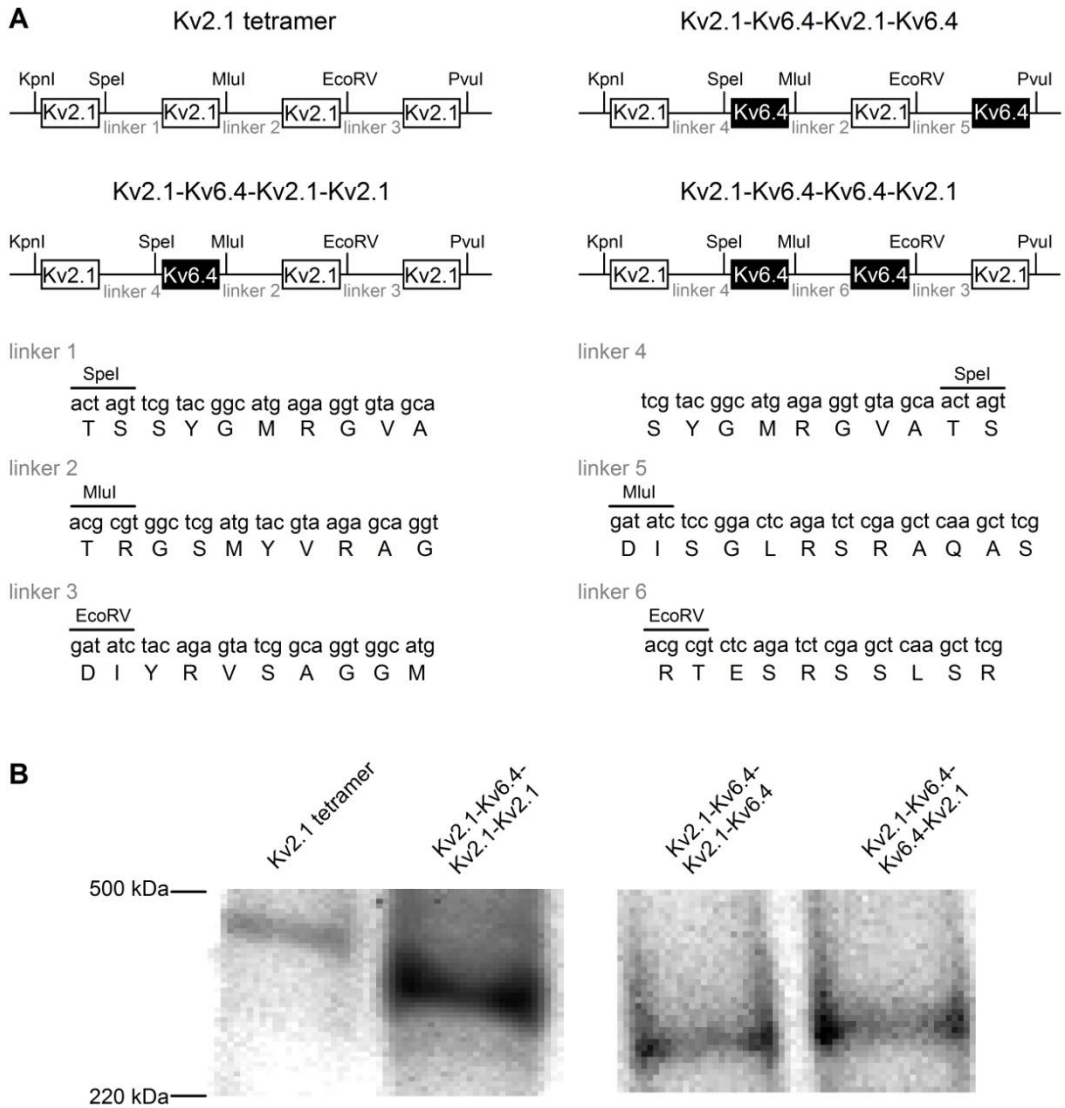

Figure 4: Overview and Western blot analysis of tetrameric constructs. (A) Design of different tetrameric constructs composed of different unique rearrangements of Kv2.1 and Kv6.4 subunits which are shown in white and black, respectively. Neighbouring subunits had a common, unique RE site enabling the linkage of subunits using specific RE digests. Subunits were covalently joined by a peptide linker of which the nucleotide and amino acid sequences are shown below in lower and upper case, respectively. (B) Expression of tetramers as a single polypeptide was examined with Western blotting using Kv2.1 antibodies. In all lysates a single band was detected which corresponded to the predicted molecular mass. The positive and negative controls were the same as in figure 1 and are not included in this figure.

Initially, we investigated whether the functionality of Kv2.1/Kv6.4 channels with a 2:2 stoichiometry is affected by the position of the Kv6.4 subunits. Therefore, the functionality of the tetramers that represented the adjacent (Kv2.1-Kv6.4-Kv6.4-Kv2.1) and alternating (Kv2.1-Kv6.4-Kv2.1-Kv6.4) configurations were assessed and their biophysical properties were, if possible, compared with those of the Kv2.1 tetrameric construct. Overnight incubation at 37°C after transfection of these constructs yielded currents with biophysical properties that did not resemble those of Kv2.1/Kv6.4 heteroteramers (data not shown), which we suspected was due to folding problems. Incubation of the transfected cells at 25°C for 48h seemed to overcome these problems. Under these conditions tetramers representing the alternating configuration produced currents (Fig. 5A) which possessed the typical biophysical signatures of Kv2.1/Kv6.4 heterotetramers: the voltage dependence of inactivation shifted ~40 mV into hyperpolarized direction ($V_{1/2}$ = -62.2 ± 1.7 mV, n = 6) and the slope factor k increased to 21.8 ± 2.5 (n = 4) compared to the Kv2.1 tetramer ($V_{1/2}$ = -21.8 ± 2.5 mV and k = 9.4 ± 0.6) (Fig. 5B-C and Table 2). Moreover, the kinetics of activation and deactivation differed from those of the Kv2.1 tetramer (Fig. 5D), while the current density decreased from 360 ± 76 pA/pF (n = 7) to 160 ± 57 pA/pF (n = 6) at +30 mV for the Kv2.1 tetramer and Kv2.1-Kv6.4-Kv2.1-Kv6.4 (Fig. 5E), respectively, as reported previously (27). In contrast, tetramers representing the adjacent configuration produced no delayed rectifier currents (Fig. 5A) as the current density at + 30 mV was only 9 ± 3 pA/pF (n = 49) (Fig. 5E), which most likely represents background currents. These results indicated that Kv2.1/Kv6.4 heterotetramers are not functional when the Kv6.4 subunits are positioned side by side.

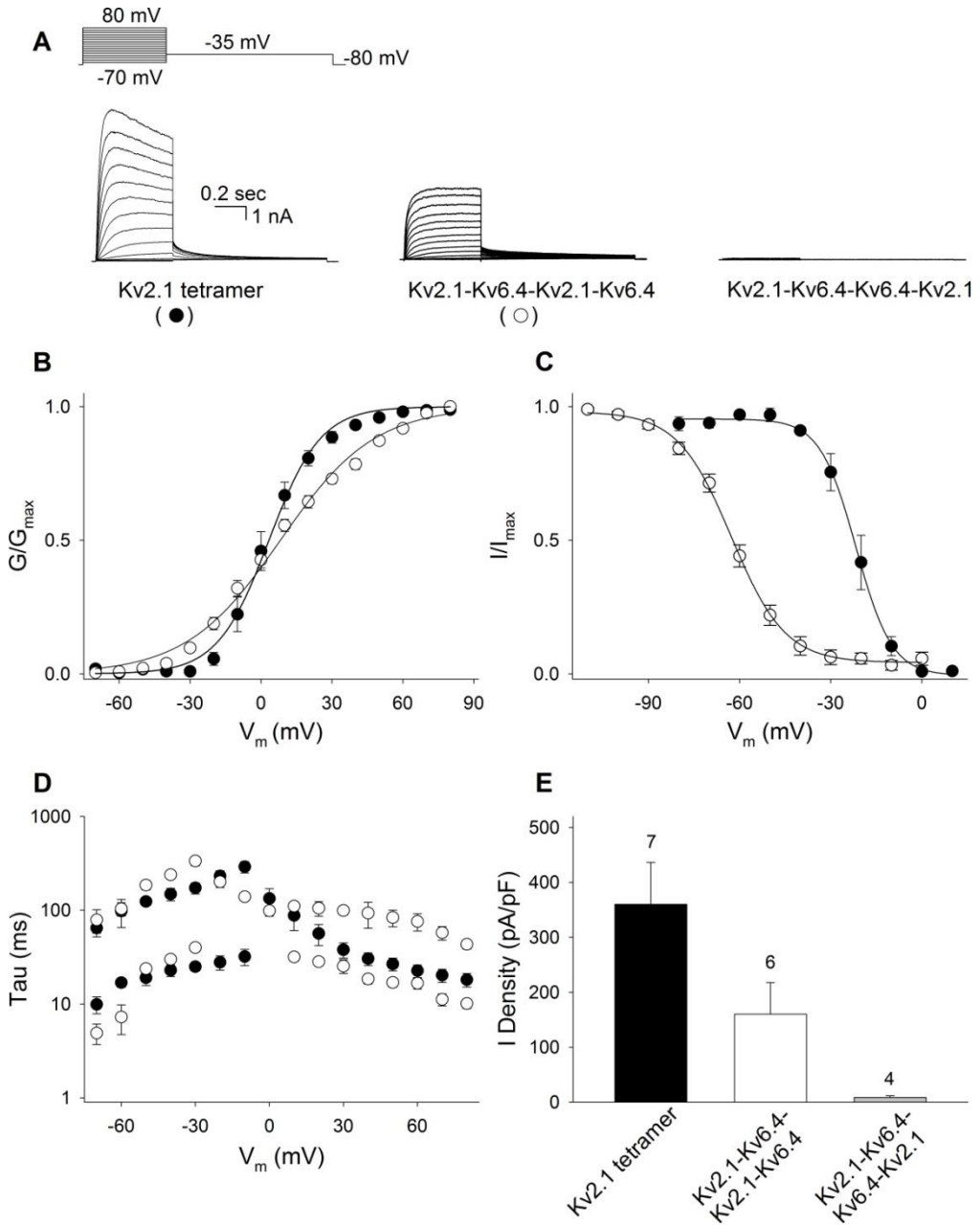

Figure 5: (A) Whole cell current recordings after transfection of 5 µg of Kv2.1 tetramer (left) (●), Kv2.1-Kv6.4-Kv2.1-Kv6.4 (middle) (○), and Kv2.1-Kv6.4-Kv6.4-Kv2.1 (right) elicited by the voltage protocol shown on top. Same scale bars for all recordings. (B) Voltage dependence of activation derived from plotting the normalized tail current amplitudes at -35 mv as a function of the prepulse potential. (C) Voltage dependence of inactivation obtained from the normalized peak current amplitude at +60 mV in function of the prepulse potential. (D) Time constants of activation and deactivation obtained as described in Material and Methods. (E) Current density of tetramers determined at the end of a 500 msec pulse at +30 mV. The numbers above every bar plot indicate the number of cells analysed.

Table 2: **Biophysical properties of Kv2.1 and Kv2.1/Kv6.4 tetramers**

	Kv2.1 tetramer	Kv2.1-Kv6.4-Kv2.1-Kv2.1	Kv2.1-Kv6.4-Kv2.1-Kv6.4
Activation			
$V_{1/2}$	1.8 ± 2.8	1.7 ± 2.9	5.7 ± 3.1
k	9.4 ± 0.6	14.9 ± 1.8	21.9 ± 0.3
n	5	4	5
Inactivation			
$V_{1/2}$	-21.8 ± 2.5	-51.0 ± 5.3	-62.2 ± 1.7
k	5.1 ± 0.4	8.5 ± 0.6	9.3 ± 1.3
n	4	4	6

Values are given as mean ± SEM and n the number of cells analysed. The midpoints of activation and inactivation ($V_{1/2}$), represented in mV, and the slope factor (k) were obtained from a single Boltzmann fit.

Kv2.1/Kv6.4 channels are functional in a 3:1 stoichiometric configuration

In addition to the observed 2:2 stoichiometry, Kv2.1/Kv6.4 channels could be arranged in several other stoichiometric configurations. However, since the above results indicated that Kv6.4 subunits have no compatible interaction sites, it seems very unlikely that functional Kv2.1/Kv6.4 channels containing more than two Kv6.4 subunits can be formed. On the other hand, Kv2.1/Kv6.4 channels containing three Kv2.1 and one Kv6.4 subunit are still expected to be functional, especially since this stoichiometric configuration was demonstrated previously for Kv2.1/Kv9.3 channels (14).

To confirm the functionality of Kv2.1/Kv6.4 channels possessing this 3:1 stoichiometry, we determined the biophysical properties of the Kv2.1-Kv6.4-Kv2.1-Kv2.1 construct of which typical current recordings are shown in figure 6 (panel A) and compared them with those of the Kv2.1 tetramer. The biophysical properties of the Kv2.1-Kv6.4-Kv2.1-Kv2.1 tetramer differed from those of the Kv2.1 tetramer and were similar to those of channels formed by co-expression of

both subunits. More specifically, the voltage dependence of inactivation was shifted into hyperpolarized direction ($V_{1/2}$ = -51.0 ± 5.3 mV, n = 4) (Fig. 5C and Table 2), the slope factor of the activation curve was decreased (k = 14.9 ± 1.8, n = 4) (Fig. 5C and table 2), and the time constants of activation displayed a fast and a slow component (Fig. 5D). These results indicated that Kv2.1/Kv6.4 heterotetramers can produce functional channels in two different stoichiometric configurations.

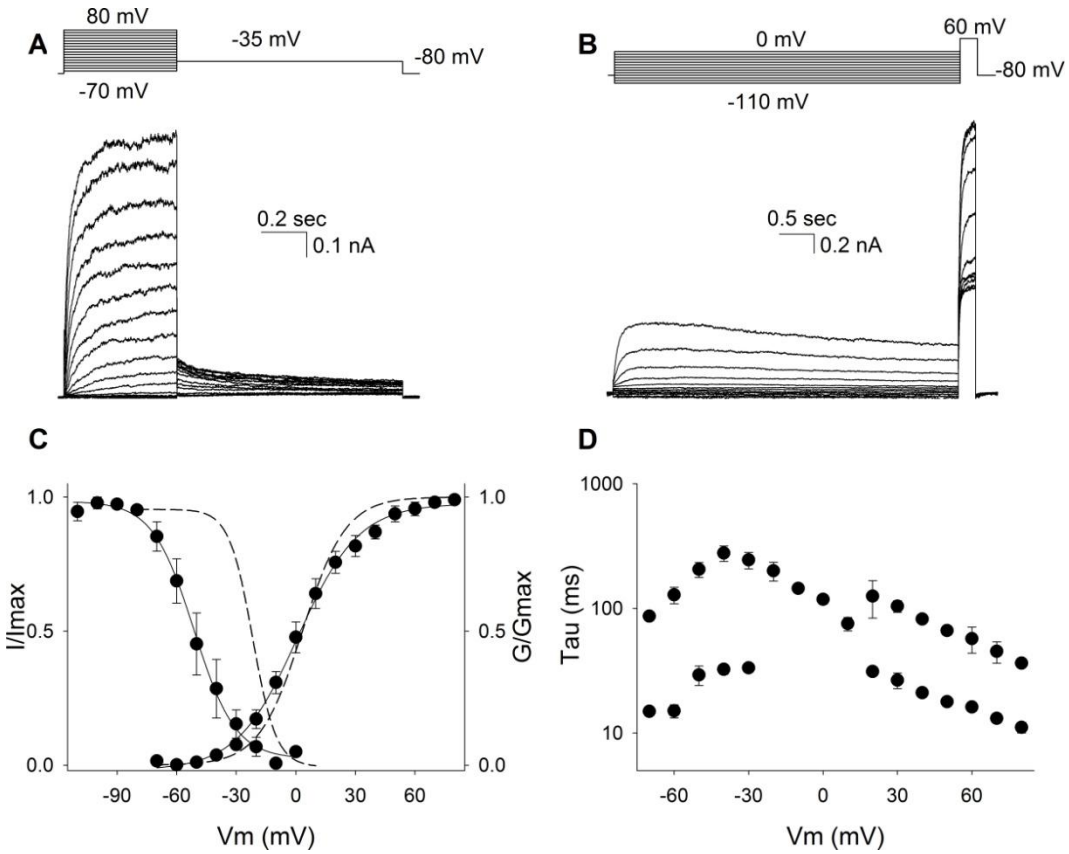

Figure 6: Biophysical properties of Kv2.1-Kv6.4-Kv2.1-Kv2.1. Representative whole cell current recordings of Kv2.1-Kv6.4-Kv2.1-Kv2.1 used to determine the activation (A) and inactivation (B) properties. Voltage protocols are shown on top. (C) Voltage dependence of activation (right) and inactivation (left). Voltage dependence of activation was derived from plotting the normalized tail current amplitudes at -25 mV as a function of the prepulse potential. Voltage dependence of inactivation was obtained from the normalized peak current amplitude at +60 mV in function of the prepulse potential. The Boltzmann curve of the Kv2.1 tetramer is represented as a dashed line. (E) Time constants of activation and deactivation obtained as described in Material and Methods.

Discussion

KvS subunits display, compared to the ubiquitously expressed Kv2 subunits, a restricted expression pattern. Hence the hypothesis that the KvS subunits tune the Kv2 currents in order to meet the tissue-specific requirements which has been confirmed by the involvement of different KvS subunits in several (patho)physiological processes (for review see (3)). This makes them interesting potential therapeutic targets, especially since it was demonstrated that Kv2.1/Kv6.4 channels are modulated differently by 4-aminopyridine (4-AP) compared to Kv2.1 homotetramers and other Kv2/KvS heterotetramers (33). It has been shown that the pharmacological characteristics of heteromeric Kv channel complexes can be affected by the stoichiometric and positional arrangements of the involved subunits (1; 2; 39). Therefore, in order to design drugs that target Kv2/KvS channels, it is important to know the possible stoichiometric configurations of these channels. Consequently, we investigated the potential arrangements of Kv2.1/Kv6.4 channels by determining and comparing the biophysical properties of different dimeric (Fig. 1) and tetrameric (Fig. 4) constructs with these of co-expressed Kv2.1 and Kv6.4 monomers. Previously, it has been deduced that Kv2.1/Kv9.3 heterotetramers consist of three Kv2.1 subunits and one Kv9.3 subunit (14). We demonstrated that Kv2/KvS heterotetramers are presumably functional in multiple stoichiometric configurations: our results showed that Kv2.1/Kv6.4 heterotetramers are functional with a 3:1 stoichiometry (Fig. 6) and a 2:2 stoichiometry provided that the Kv6.4 subunits alternate in the channel complex (Figs. 3 & 5).

The tetramerization of Kv1-Kv4 subunits into a functional Kv channel presumably occurs as a dimerization of dimers and is guided by the N-terminal T1 domain which facilitates the assembly of compatible subunits and prevents the addition of incompatible subunits into the channel tetramer (17; 32; 37; 38). For example, removal of the T1 domain from the incompatible subunits Kv2.1 and Kv1.4 resulted in the co-assembly of these subunits into a functional channel (17). The T1-T1 interactions responsible for the subfamily-specific tetramerization most likely occur while the Kv subunits are still attached to the ribosome (22) and

it is thus expected that these interactions predominate during the formation of dimers in the endoplasmic reticulum (ER). Consequently, since yeast-two hybrid assays and FRET analysis have shown that the T1 domain of KvS subunits interacts with that of Kv2.1 but not with that of themselves (6; 24; 27; 29; 35; 40), it is very unlikely that Kv6.4 dimers can be formed which thus implies that not more than two Kv6.4 subunits can be incorporated into a Kv2.1/Kv6.4 heterotetramer. Our results supported this hypothesis as concatemers in which the Kv6.4 subunits are positioned side by side, were not functional (Fig. 5). In addition, this confirms the observation that full-length KvS subunits fail to interact among themselves (24).

Concatemers have been used successfully to investigate the stoichiometry of Kv channels (19; 26). However, due to the occurrence of T1-T1 interactions while the proteins are still attached to the ribosomes (22), it is possible that multiple concatemers associate with each other extruding some of the covalently-attached subunits from the Kv channel complex. For example, it was observed that using dimeric constructs containing two different Kv subunits the phenotype of the subunit positioned first in the dimer seemed to predominate suggesting that this subunit was more likely to be incorporated into the Kv channel (23). The dimeric constructs used in this study did not seem to encounter this potential problem since the biophysical properties of Kv2.1-Kv6.4 and Kv6.4-Kv2.1 dimers were similar and comparable with those of co-expressed Kv2.1 and Kv6.4 monomers (Fig. 3). On the other hand, transfection of the tetrameric constructs followed by overnight incubation at 37°C yielded currents with biophysical properties that did not match those of Kv2.1/Kv6.4 heterotetramers. This was presumably due to the association of multiple tetramers which could result in the formation of Kv cannels containing various subunit stoichiometries. Incubation of the transfected cells at 25°C for 48h seemed to overcome this problem as under these conditions the biophysical properties of the tetramers were similar to those characteristic for Kv2.1/Kv6.4 heterotetramers (Fig. 5 and 6). Furthermore, the functionality of the tetrameric construct representing a 2:2 stoichiometry was abolished by changing the position of the Kv6.4 subunits from

an alternating to an adjacent configuration (Fig. 5). Together this indicated that under these conditions the stoichiometric and positional arrangements in our tetrameric constructs were well-constrained.

Heterotetrameric Kv channels can assemble with a random subunit stoichiometry and arrangement depending on the ratio between the involved subunits (15; 16; 34; 39). For example, Kv7.2/Kv7.3 heterotetramers display a fixed 2:2 stoichiometry when cells express an equal amount of both subunits, but varying this ratio results in Kv7.2/Kv7.3 heterotetramers with a variable stoichiometry (34). This raises the possibility that cells can modulate Kv currents through changes in subunit expression level. Our present study demonstrated a similar stoichiometric variability for Kv2.1/Kv6.4 channels which suggests that the stoichiometry of other Kv2/KvS heterotetramers can be variable as well. However, we observed that this variability is restricted since only a 3:1 stoichiometry and a 2:2 stoichiometry in which Kv2.1 and Kv6.4 subunits alternate were functional. Yet, it is remarkable that two Kv6.4 subunits can exist within the same channel protein even though it has been consistently shown that KvS subunits fail to interact with themselves. This may suggest the intriguing existence of Kv2/KvS heterotetramers that contain two different KvS subunits which would add molecular and functional variety to the already remarkable diverse group of Kv channel complexes.

Acknowledgements

We thank Evy Mayeur and Gerda Van de Vijver for the excellent technical assistance and Alain Labro for helpful discussions. This work was supported by the section cardiovascular research of the Sheid-van Bogaert foundation, the postdoctoral fellowships FWO−1291913N and FWO-1291916N to EB, and the grants G.0449.11N & G.0443.12N to DJS from the Research Foundation – Flanders (FWO).

References

1. **Al-Sabi A, Kaza SK, Dolly JO and Wang J**. Pharmacological characteristics of Kv1.1- and Kv1.2-containing channels are influenced by the stoichiometry and positioning of their alpha-subunits. Biochem J 454: 101-108, 2013.
2. **Al-Sabi A, Shamotienko O, Dhochartaigh SN, Muniyappa N, Le BM, Shaban H, Wang J, Sack JT and Dolly JO**. Arrangement of Kv1 alpha-subunits dictates sensitivity to tetraethylammonium. J Gen Physiol 136: 273-282, 2010.
3. **Bocksteins E**. Kv5, Kv6, Kv8, and Kv9 subunits: No simple silent bystanders. J Gen Physiol 147(2): 105-125, 2016.
4. **Bocksteins E, Labro AJ, Mayeur E, Bruyns T, Timmermans JP, Adriaensen D and Snyders DJ**. Conserved negative charges in the N-terminal tetramerization domain mediate efficient assembly of Kv2.1 and Kv2.1/Kv6.4 channels. J Biol Chem 284: 31625-31634, 2009.
5. **Bocksteins E, Labro AJ, Snyders DJ and Mohapatra DP**. The electrically silent Kv6.4 subunit confers hyperpolarized gating charge movement in Kv2.1/Kv6.4 heterotetrameric channels. PLoS ONE 7: e37143, 2012.
6. **Bocksteins E, Mayeur E, van Tilborg A, Regnier G, Timmermans JP and Snyders DJ**. The subfamily-specific interaction between Kv2.1 and Kv6.4 subunits is determined by interactions between the N- and C-termini. PLoS ONE 9: 1-7, 2014.
7. **Bocksteins E and Snyders DJ**. Electrically silent Kv subunits: their molecular and functional characteristics. Physiology (Bethesda) 27: 73-84, 2012.
8. **David JP, Stas JI, Schmitt N and Bocksteins E**. Auxiliary KCNE subunits modulate both homotetrameric Kv2.1 and heterotetrameric Kv2.1/Kv6.4 channels. Sci Rep 5: 12813, 2015.

9. **Gutman GA, Chandy KG, Grissmer S, Lazdunski M, McKinnon D, Pardo LA, Robertson GA, Rudy B, Sanguinetti MC, Stuhmer W and Wang X**. International Union of Pharmacology. LIII. Nomenclature and molecular relationships of voltage-gated potassium channels. Pharmacol Rev 57: 473-508, 2005.
10. **Heginbotham L and MacKinnon R**. The aromatic binding site for tetraethylammonium ion on potassium channels. Neuron 8: 483-491, 1992.
11. **Hille B**. Ionic channels of excitable membranes. Sunderland, Mass.: Sinauer Associates, 1991.
12. **Jegla T and Salkoff L**. A novel subunit for *Shal* K^+ channels radically alters activation and inactivation. J Neurosci 17: 32-44, 1997.
13. **Kavanaugh MP, Hurst RS, Yakel J, Varnum MD, Adelman JP and North RA**. Multiple subunits of a voltage-dependent potassium channel contribute to the binding site for tetraethylammonium. Neuron 8: 493-497, 1992.
14. **Kerschensteiner D, Soto F and Stocker M**. Fluorescence measurements reveal stoichiometry of K^+ channels formed by modulatory and delayed rectifier alpha-subunits. Proc Natl Acad Sci U S A 102: 6160-6165, 2005.
15. **Kitazawa M, Kubo Y and Nakajo K**. The Stoichiometry and Biophysical Properties of the Kv4 Potassium Channel Complex with K^+ Channel-interacting Protein (KChIP) Subunits Are Variable, Depending on the Relative Expression Level. J Biol Chem 289: 17597-17609, 2014.
16. **Kitazawa M, Kubo Y and Nakajo K**. Kv4.2 and Accessory Dipeptidyl Peptidase-like Protein 10 (DPP10) Subunit Preferentially Form a 4:2 (Kv4.2:DPP10) Channel Complex. J Biol Chem 290: 22724-22733, 2015.
17. **Lee TE, Philipson LH, Kusnetsov A and Nelson DJ**. Structural determinant for assembly of mammalian K^+ channels. Biophys J 66: 667-673, 1994.
18. **Li M, Jan YN and Jan LY**. Specification of subunit assembly by the hydrophilic amino- terminal domain of the *Shaker* potassium channel. Science 257: 1225-1230, 1992.

19. **Liman ER, Tytgat J and Hess P**. Subunit stoichiometry of a mammalian K^+ channel determined by construction of multimeric cDNAs. Neuron 9: 861-871, 1992.
20. **Long SB, Campbell EB and MacKinnon R**. Crystal structure of a mammalian voltage-dependent *Shaker* family K^+ channel. Science 309: 897-903, 2005.
21. **Long SB, Campbell EB and MacKinnon R**. Voltage sensor of Kv1.2: structural basis of electromechanical coupling. Science 309: 903-908, 2005.
22. **Lu J, Robinson JM, Edwards D and Deutsch C**. T1-T1 interactions occur in ER membranes while nascent Kv peptides are still attached to ribosomes. Biochem 40: 10934-10946, 2001.
23. **McCormack K, Lin L, Iverson LE, Tanouye MA and Sigworth FJ**. Tandem linkage of *Shaker* K^+ channel subunits does not ensure the stoichiometry of expressed channels. Biophys J 63: 1406-1411, 1992.
24. **Mederos y Schnitzler M, Rinne S, Skrobek L, Renigunta V, Schlichthorl G, Derst C, Gudermann T, Daut J and Preisig-Muller R**. Mutation of histidine 105 in the T1 domain of the potassium channel Kv2.1 disrupts heteromerization with Kv6.3 and Kv6.4. J Biol Chem 284: 4695-4704, 2009.
25. **Nakajo K, Ulbrich MH, Kubo Y and Isacoff EY**. Stoichiometry of the KCNQ1-KCNE1 ion channel complex. Proc Natl Acad Sci U S A 107: 18862-18867, 2010.
26. **Naso A, Montisci R, Gambale F and Picco C**. Stoichiometry Studies Reveal Functional Properties of KDC1 in Plant Shaker Potassium Channels. Biophys J 91: 3673-3683, 2006.
27. **Ottschytsch N, Raes A, Van Hoorick D and Snyders DJ**. Obligatory heterotetramerization of three previously uncharacterized Kv channel alpha-subunits identified in the human genome. Proc Natl Acad Sci U S A 99: 7986-7991, 2002.
28. **Ottschytsch N, Raes AL, Timmermans JP and Snyders DJ**. Domain analysis of Kv6.3, an electrically silent channel. J Physiol 568: 737-747, 2005.

29. **Post MA, Kirsch GE and Brown AM**. Kv2.1 and electrically silent Kv6.1 potassium channel subunits combine and express a novel current. FEBS Lett 399: 177-182, 1996.
30. **Shapiro MS and Zagotta WN**. Stoichiometry and arrangement of heteromeric olfactory cyclic nucleotide-gated ion channels. Proc Natl Acad Sci U S A 95: 14546-14551, 1998.
31. **Shen NV, Chen X, Boyer MM and Pfaffinger PJ**. Deletion analysis of K^+ channel assembly. Neuron 11: 67-76, 1993.
32. **Shen NV and Pfaffinger PJ**. Molecular recognition and assembly sequences involved in the subfamily-specific assembly of voltage-gated K^+ channel subunit proteins. Neuron 14: 625-633, 1995.
33. **Stas JI, Bocksteins E, Labro AJ and Snyders DJ**. Modulation of Closed-State Inactivation in Kv2.1/Kv6.4 Heterotetramers as Mechanism for 4-AP Induced Potentiation. PLoS ONE 10: e0141349, 2015.
34. **Stewart AP, Gomez-Posada JC, McGeorge J, Rouhani MJ, Villarroel A, Murrell-Lagnado RD and Edwardson JM**. The Kv7.2/Kv7.3 heterotetramer assembles with a random subunit arrangement. J Biol Chem 287: 11870-11877, 2012.
35. **Stocker M, Hellwig M and Kerschensteiner D**. Subunit assembly and domain analysis of electrically silent K^+ channel alpha-subunits of the rat Kv9 subfamily. J Neurochem 72: 1725-1734, 1999.
36. **Tu L and Deutsch C**. Evidence for dimerization of dimers in K^+ channel assembly. Biophys J 76: 2004-2017, 1999.
37. **Tu LW, Santarelli V, Sheng ZF, Skach W, Pain D and Deutsch C**. Voltage-gated K^+ channels contain multiple intersubunit association sites. J Biol Chem 271: 18904-18911, 1996.
38. **Xu J, Yu W, Jan YN, Jan LY and Li M**. Assembly of voltage-gated potassium channels. J Biol Chem 270: 24761-24768, 1995.

39. **Yu H, Lin Z, Mattmann ME, Zou B, Terrenoire C, Zhang H, Wu M, McManus OB, Kass RS, Lindsley CW, Hopkins CR and Li M**. Dynamic subunit stoichiometry confers a progressive continuum of pharmacological sensitivity by KCNQ potassium channels. Proc Natl Acad Sci U S A 110: 8732-8737, 2013.

40. **Zhu XR, Netzer R, Bohlke K, Liu Q and Pongs O**. Structural and functional characterization of Kv6.2 a new gamma-subunit of voltage-gated potassium channel. Receptors and Channels 6: 337-350, 1999.

Chapter 3

The contribution of Kv2.2-mediated currents decreases during the postnatal development of mouse dorsal root ganglion neurons.

Glenn Regnier[1], Elke Bocksteins[1], Gerda Van de Vijver[2], Dirk J. Snyders[1], Pierre-Paul van Bogaert[2]

Physiol Rep. 2016 March; 4(3):e12731

[1]Laboratory for Molecular Biophysics, Physiology and Pharmacology, Department of Biomedical Sciences, University of Antwerp, CDE, Universiteitsplein 1, 2610 Antwerpen, Belgium
[2]Laboratory for Cardiovascular Research, Institute Born-Bunge, University of Antwerp, CDE, Universitetitsplein 1, 2610 Antwerpen, Belgium

Abstract

Delayed rectifier voltage-gated K^+ (Kv) channels play an important role in the regulation of the electrophysiological properties of neurons. In mouse dorsal root ganglion (DRG) neurons, a large fraction of the delayed rectifier current is carried by both homotetrameric Kv2 channels and heterotetrameric channels consisting of Kv2 and silent Kv (KvS) subunits (i.e., Kv5-Kv6 and Kv8-Kv9). However, little is known about the contribution of Kv2-mediated currents during the postnatal development of DRG neurons. Here, we report that the Stromatoxin-1 (ScTx)-sensitive fraction of the total outward K^+ current (I_K) from mouse DRG neurons gradually decreased (~13%, $P < 0.05$) during the first month of postnatal development. Because ScTx inhibits both Kv2.1- and Kv2.2-mediated currents, this gradual decrease may reflect a decrease in currents containing either subunit. However, the fraction of Kv2.1 antibody-sensitive current that only reflects the Kv2.1-mediated currents remained constant during that same period. These results suggested that the fractional contribution of Kv2.2-mediated currents relative to I_K decreased with postnatal age. Semiquantitative RT-PCR analysis indicated that this decrease can be attributed to developmental changes in Kv2.2 expression as the mRNA levels of the Kv2.2 subunit decreased gradually between 1 and 4 weeks of age. In addition, we observed age-dependent fluctuations in the mRNA levels of the Kv6.3, Kv8.1, Kv9.1 and Kv9.3 subunits. These results support an important role of both Kv2 and KvS subunits in the postnatal maturation of DRG neurons.

Introduction

Neuronal function depends heavily on the spatial and temporal expression of voltage-gated K^+ (Kv) channels which contribute to neuronal excitability by regulating the membrane potential, action potential waveform and firing frequency, transmitter release, and synaptic strength (21). Kv channels are integral transmembrane proteins consisting of four α-subunits that form a central ion conducting pore through which K^+ ions flow according to their electrochemical

gradient. Each α-subunit consists of six transmembrane segments (S1-S6) and a cytoplasmic NH_2- and COOH-terminus (26). Based on sequence homology, eight closely *Shaker*-related subfamilies can be distinguished: Kv1-Kv6 and Kv8-Kv9 (19). All members of the Kv1-Kv4 subfamilies form functional homotetrameric channels and the diversity within these subfamilies is further increased by both the formation of heterotetrameric channels and the interaction with auxiliary β-subunits (38; 50). On the other hand, members of the Kv5, Kv6, Kv8, and Kv9 subfamilies do not form functional channels due to retention in the endoplasmic reticulum (ER) and were therefore designated silent Kv (KvS) subunits (for review see (6)). Co-assembly of these KvS subunits with members of the Kv2 subfamily relieves this ER retention leading to heterotetrameric Kv2/KvS channel complexes with biophysical properties that differ from the homotetrameric Kv2 channels. These differences include shifts in the voltage dependence of activation and inactivation, changes in gating kinetics, and alteration of the current density.

Due to the molecular diversity of Kv channel complexes, it is very challenging to determine the molecular composition of native Kv currents in neurons. In rodent dorsal root ganglion (DRG) neurons, at least three different Kv currents have been distinguished: the M-current (I_M), the transient outward current (I_A), and the delayed rectifier current (I_{DR}) (1; 13; 15). The M-current is a non-inactivating K^+ current generated by channels composed of Kv7.2-Kv7.5 subunits; the major component is carried by heterotetrameric Kv7.2/Kv7.3 channels and homotetrameric Kv7.2 channels (33). I_A is a very fast activating and inactivating current generated by Kv1.4, Kv3.4, Kv4.1, Kv4.2, and/or Kv4.3 subunits. Depending on the subpopulation of DRG neurons, one or several of these subunits contribute to I_A (9; 35; 37; 49). The major component (~60%) of I_{DR} is carried by both homotetrameric Kv2 and heterotetrameric Kv2/KvS channels, although subunits of the Kv1 and Kv3 subfamilies also contribute to I_{DR} (3; 5; 7; 46).

The functional diversity of different neuronal subtypes does not only emanate from the molecular composition of different channel complexes but also

from the variation in expression of K^+ currents during different developmental stages (for review see (39)). In the case of the Kv2 subfamily, changes in spatiotemporal expression and cellular abundance have been demonstrated during the development of different neuronal cell types (2; 16; 18; 27; 40). For example, in rat neocortical pyramidal neurons, the density of Kv2-mediated currents increased with postnatal age (16) while in embryonic *Xenopus* spinal neurons, a Kv2.2-specific upregulation was demonstrated during maturation (18). However, it is not known if the contribution of Kv2-mediated currents to I_K in DRG neurons is influenced by postnatal age. Therefore, we analyzed the Kv2-containing currents and characterized the expression of Kv2 and their modulatory KvS subunits in mouse DRG neurons during the first month of postnatal development.

Material and methods

Animals and cell culture

DRG neurons were obtained from P7 ± 1, P14 ± 1, P21 ± 1, and P28 ± 1 old C57BL/6 male mice. Experiments were conducted in agreement with the European Communities Council Directive on the protection of animals used for experimental and other scientific purposes (2010/63/EU). DRG neurons were isolated as described previously (41). Briefly, DRGs were dissected from the spinal cord and dissociated by consecutive enzymatic treatment with 2 mg/mL collagenase A (Merck Millipore, Billerica, MA, USA) and 1 mg/mL pronase (Merck Millipore). After enzymatic dissociation, DRG neurons were further dissociated using flame-polished Pasteur pipettes of decreasing diameters and plated on glass-bottom dishes coated with poly-D-lysine (MatTek Corp., Ashland, MA, USA). Cells were grown in 50:50 DMEM/TNB medium (ThermoFisher Scientific, Waltham, MA, USA/Merck Millipore) supplemented with 2.5% horse serum (ThermoFisher Scientific), 2.5% fetal bovine serum (ThermoFisher Scientific), 100 U/mL penicillin/streptomycin, 1.25% lipid-protein complex (Merck Millipore), 1 mmol/L L-glutamine, and 0.25 µg/mL nerve growth factor (Sigma-Aldrich, Saint

Louis, MO, USA) and maintained at 37°C in a humidified atmosphere of 5% CO_2. Electrophysiological and RT-PCR analyses were performed 3 days after plating.

Electrophysiology

Whole-cell patch clamp current recordings were performed on DRG neurons (30-60 pF) at room temperature (20-22°C) with an Axoclamp-2A amplifier (Molecular Devices, Sunnyvale, CA, USA) in the two-electrode voltage clamp configuration and were sampled with a TL-1 labmaster (Molecular Devices). Patch pipettes with a resistance of 3-5 MΩ were pulled from 1.7 mm glass capillaries with a Brown Flaming P-87 horizontal pipette puller and heat polished. DRG neurons were superfused continuously with an extracellular solution, containing (in mmol/L): 140 N-methyl D-glucamine, 5 KCl, 1 $MgCl_2$, 1.8 $CaCl_2$, 10 glucose, and 5 HEPES with the pH adjusted to 7.4 with HCl. Pipettes were filled with an intracellular solution, containing (in mmol/L): 140 KCl, 10 HEPES, 5 EGTA, 5 NaCl, 3 MgATP, 1 $MgCl_2$, 1 $CaCl_2$, and 0.1 cAMP with the pH adjusted to 7.4 with KOH. Outward K^+ currents were elicited by 500 msec depolarizing pulses between -60 and +60 mV from a holding potential of -70 mV, followed by a 1 sec pulse at -40 mV. Cell capacitance was obtained from the current evoked by a 30 msec step from -60 to -65 mV.

Stromatoxin-1 (ScTx)-sensitive currents were obtained by subtracting the currents obtained after application of 300 nmol/L ScTx (Alomone Labs, Jerusalem, Israel) (dissolved in the extracellular solution) from the currents obtained before ScTx application. For the anti-Kv2.1 current recordings, patch pipettes were dipped in normal intracellular solution and back filled with the anti-Kv2.1-containing solution obtained by dissolving 10 µg/mL Kv2.1 antibody (Alomone Labs) in the intracellular solution. Steady-state reduction of the total outward K^+ current was reached 15-20 min after patch rupture. The specificity of this reduction (i.e., due to Kv2.1 antibody block and not due to time artifacts) was confirmed previously (5). The anti-Kv2.1-sensitive currents were obtained by subtracting the currents obtained after steady-state Kv2.1 block from the currents obtained immediately after patch rupture.

Reverse transcription-PCR (RT-PCR) analysis

Total RNA was isolated from the DRG cultures as previously described (7). Briefly, RNA was isolated using the TriZol (ThermoFisher Scientific) reagent, samples were treated with deoxyribonuclease I (ThermoFisher Scientific) to exclude genomic DNA contamination and cDNA was obtained using the Superscript III RT-PCR system (ThermoFisher Scientific) according to the manufacturer's guidelines. Expression of the Kv2 and KvS subunits was assessed using gene-specific primers that spanned intron boundaries (except for the intronless Kv5.1) (Table 1). Glyceraldehyde 3-phosphate dehydrogenase (G3PDH) was used as a loading control to perform the semiquantitative RT-PCR analysis. Co-amplification of the target gene and G3PDH was performed in a reaction mixture containing 1x Colorless GoTaq Flexi buffer, 3 mmol/L $MgCl_2$, 0.4 mmol/L dNTP mix, 2.5 U GoTaq G2 Flexi DNA Polymerase (Progema, Madison, WI, USA), and 0.5 µmol/L of each forward and reverse primer. The cDNA samples were amplified for 35 cycles, separated on a 1% agarose gel, and stained with SYBR Safe gel stain (ThermoFisher Scientific) for densitometric analysis. For each PCR analysis, one positive control (reaction that contains the target subunit cDNA) and two negative controls (reaction without cDNA or without reverse transcriptase) were performed. We ensured that the amplification of each gene was still within the exponential phase of the PCR reaction after 35 cycles by comparing the densitometric values with these obtained after 33 and 37 cycles of amplification. Gels were scanned with the LumiImager system using the LumiAnalyst software (Roche Diagnostics, Basel, Switzerland) and the data were analyzed using the ImageJ software (National Institutes of Health, Bethesda. MD, USA). Each PCR product was sequenced to exclude nonspecific amplification.

Table 1: List of primer pairs used in semiquantitative RT-PCR experiments

	Primer pair sequence
G3PDH	5'-ACGGGAAGCTCACTGGCATG-3'
	5'-GGGAGTTGCTGTTGAAGTCG-3'
K_v2.1	5'-TCGACAACACGTGCTGTGCT-3'
	5'-GGCCAACTTCAGGATGCGC-3'
K_v2.2	5'-TTGATAACACCTGCTGCCCG-3'
	5'-TGGCGAGTTTCAGTATCCTGA-3'
K_v5.1	5'-CTGGTGGGCTATCATCACCA-3'
	5'-CGGGTCCTATGATGCTTCTC-3'
K_v6.1	5'-GTCCGTTCTGTTTGTCACCG-3'
	5'-GGATCAGCACCCGTTCTTGT-3'
K_v6.2	5'-GGCTCTTCGCCTACGTCTC-3'
	5'-CATCACGCGTGCTGTCCTC-3'
K_v6.3	5'-GTGGTGTTCGTGATCGTGTC-3'
	5'-CTTGAGAGTCAAGCCCAGTG-3'
K_v6.4	5'-GCCAGGAGTTCTTCTTCGAC-3'
	5'-CATCAGGAGACCAAACTCTC-3'
K_v8.1	5'-TCTGCGCATGCTGAAACTGG-3'
	5'-AGTACTTGCTCTCTCCCTGC-3'
K_v8.2	5'-CTTCCGAATCCTCAAGCTGG-3'
	5'-GTTGACCTTTCCTCGTTCCC-3'
K_v9.1	5'-AGGTAGTGCAAGTGTTCCGC-3'
	5'-AAGTCCTCAAACTCGCGCTG-3'
K_v9.2	5'-TTCTCAAGCTGGCCAGACAC-3'
	5'-TGACCGAAGGGACCTCTTTC-3'
K_v9.3	5'-TGTAGGGCTTCGGTCTCTTG-3'
	5'-AGTACGGTAGCTCATGGCAC-3'

Data analysis

Densitometric analysis of the bands obtained after electrophoresis was done using the ImageJ software. The signal intensity of the target band was normalized to the intensity of the G3PDH signal which was represented as relative densitometric value (RDV).

All values are presented as mean ± SEM. Statistical analyses were performed using one-way ANOVA followed by Tukey's test in case a significant difference was present among the test groups. Trend analysis of age-dependent changes was performed using linear regression and represented by the regression coefficient ± SE. *P*-values < 0.05 were considered to be significant.

Results

The fractional contribution of the ScTx-sensitive current gradually decreases during postnatal development while that of the Kv2.1 antibody-sensitive current remains unchanged.

To study potential changes in the Kv2-mediated currents during the postnatal development of mouse DRG neurons, we determined the fractional contribution of the ScTx-sensitive and anti-Kv2.1-sensitive currents relative to the total outward K^+ current (I_K) in these neurons obtained from mice at different postnatal ages. We used this dual approach to determine the fractional contribution of the Kv2.1- and Kv2.2-mediated currents relative to I_K in developing DRG neurons since ScTx inhibits both Kv2.1- and Kv2.2-containing channels (11) whereas Kv2.1 antibodies only block Kv2.1-containing channels (5; 17; 31). It has previously been demonstrated that the ScTx-induced Kv2 inhibition is less efficient at higher potentials (> 0 mV) (11) and that the fractional contribution of Kv2-mediated currents relative to the whole-cell outward K^+ current is higher after 500 msec (7). Therefore, we determined the fractional contribution of the ScTx- and anti-Kv2.1-sensitive currents relative to I_K in the DRG neurons of different developmental stages by normalizing their current density to the total outward K^+ current density at the end of a 500 msec depolarizing pulse to 0 mV. The ScTx- and anti-Kv2.1-sensitive currents were obtained as described in Material and Methods, and the current density was determined by dividing the recorded current amplitude at 0 mV after 500 msec by the cell capacitance. For the different development stages, we isolated DRG neurons from P7 ± 1, P14 ± 1, P21 ± 1, and P28 ± 1 mice that were considered as 1, 2, 3, and 4 weeks old mice, respectively. Only DRG neurons with a cell capacitance in the 30-60 pF range were selected for analysis; as a result, the mean whole-cell capacitance of the analyzed DRG neurons did not change significantly during postnatal development (Fig. 1A). However, the current density of the outward K^+ current rose gradually (regression coefficient = 30 ± 9 pA/pF/week, $P < 0.05$) with age

reaching significance ($P < 0.05$) between 1 week (270 ± 15 pA/pF) and 4 weeks (370 ± 23 pA/pF) (Fig. 1B-C).

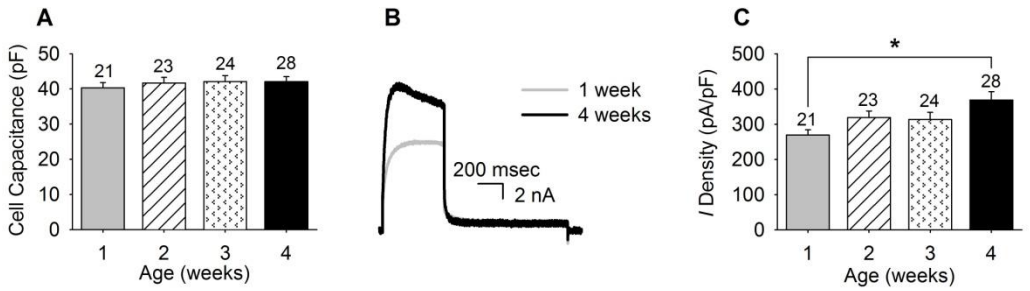

Figure 1: Postnatal development of the whole cell outward K^+ current in mouse dorsal root ganglion (DRG) neurons. (A) Average cell capacitance of the recorded DRG neurons obtained from 1, 2, 3, and 4 weeks old mice. The numbers above each bar indicate the number of recorded cells. (B) Representative current recordings of the whole cell outward K^+ current in DRG neurons obtained from 1 week (gray) and 4 weeks (black) old mice elicited by a 500 msec depolarizing pulse to 0 mV from a holding potential of -70 mV. (C) Postnatal development of the whole cell outward K^+ current density at the end of a 500 msec pulse at 0 mV. The current density at 4 weeks was significantly higher than the current density at 1 week, indicated with an asterisk ($P < 0.05$). The numbers above each bar indicate the number of cells analyzed.

Typical current recordings of DRG neurons obtained from 1 and 4 weeks old mice before and after application of 300 nmol/L ScTx are shown in Figure 2A. Extracellular application of 300 nmol/L ScTx reduced I_K significantly as previously described (7). The absolute current density of the ScTx-sensitive current did not change in DRG neurons of the different age groups (regression coefficient: 0.26 ± 6.39 pA/pF/week, $P = 0.97$) (Fig. 2B): the ScTx-sensitive current density was 143 ± 15, 144 ± 13, 136 ± 10, and 146 ± 17 pA/pF in DRG neurons of 1, 2, 3, and 4 weeks old mice, respectively. However, the total outward K^+ current density rose significantly (Fig. 1C) and therefore the fractional contribution of the ScTx-sensitive current relative to I_K (FC_{ScTx}) decreased gradually (regression coefficient = -0.044 ± 0.012 FC_{ScTx}/week, $P < 0.05$) with age reaching significance ($P < 0.05$) at 4 weeks, compared to 1 and 2 weeks old mice (Fig. 2C): ScTx inhibited 52 ± 4% and 49 ± 3% of the outward K^+ current at week 1 and week 2 respectively, while only inhibiting 39 ± 3% at week 4. These results demonstrated that the fractional contribution of Kv2-containing channels relative to I_K in DRG neurons

decreased during postnatal development, but these data did not discriminate between Kv2.1- and Kv2.2-containing channels. Therefore, we determined the fraction of anti-Kv2.1-sensitive currents.

Representative current recordings of the anti-Kv2.1-sensitive currents obtained from 1 and 4 weeks old mice are shown in Figure 3A. Intracellular diffusion of Kv2.1 antibodies reduced I_K significantly as previously described (5). The current density of the anti-Kv2.1-sensitive current rose (regression coefficient: 7.7 ± 5.1 pA/pF/week, P = 0.14), although not significantly, from 70 ± 9 pA/pF at 1 week to 95 ± 14 pA/pF at 4 weeks (Fig. 3B). However, the fractional contribution of the anti-Kv2.1-sensitive current relative to I_K remained similar in DRG neurons obtained from the different age groups (Fig. 3C): the Kv2.1 antibody blocked 27 ± 3%, 26 ± 3%, 28 ± 3%, and 28 ± 3% of the total outward K^+ current of the DRG neurons from 1, 2, 3, and 4 weeks old mice, respectively. These results together indicated that the fractional contribution of Kv2.1-mediated currents relative to I_K remained similar, whereas the fractional contribution of Kv2.2-mediated currents relative to I_K decreased with postnatal age.

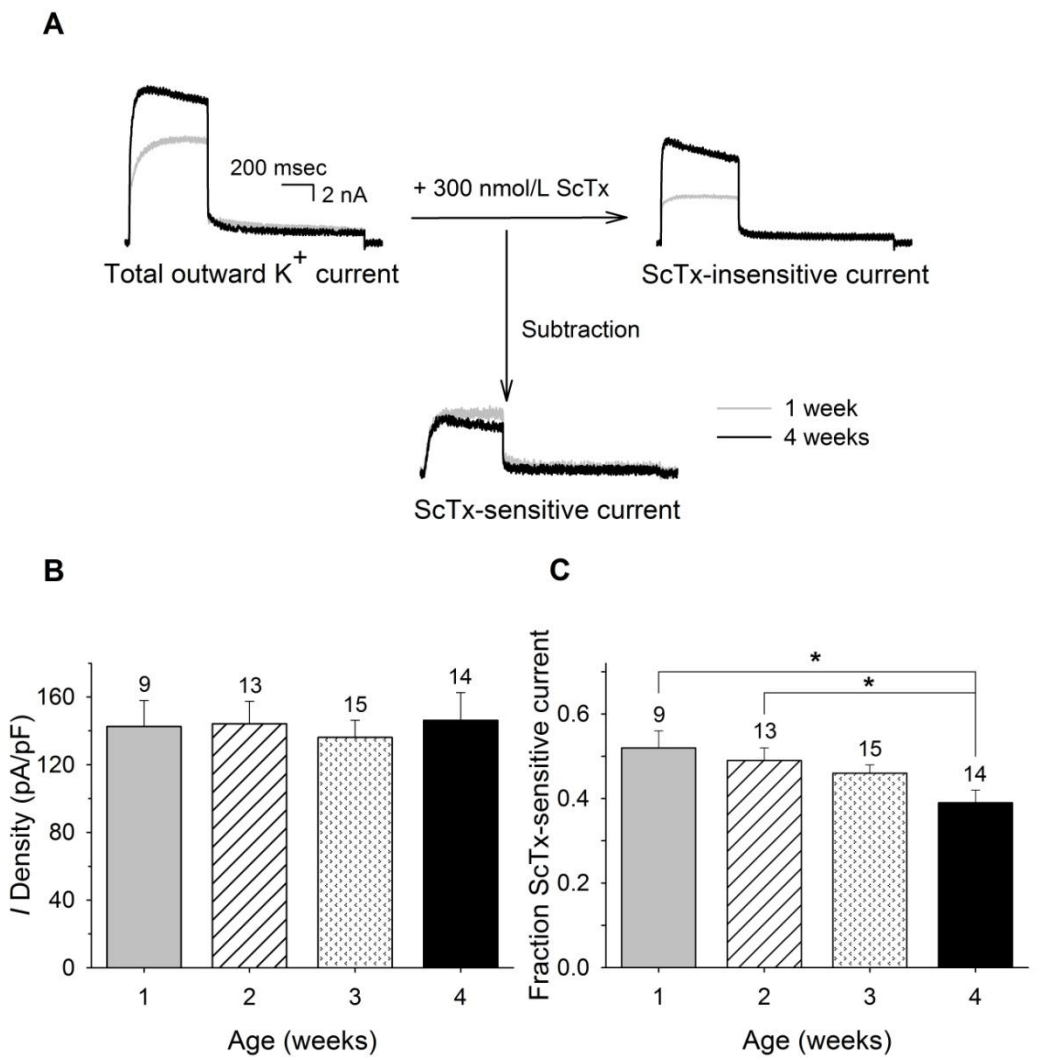

Figure 2: Postnatal development of the ScTx-sensitive current in dorsal root ganglion (DRG) neurons at 0 mV. (A) Representative current recordings of the total outward K^+ (left), ScTx-insensitive (right) and ScTx-sensitive (bottom) currents in DRG neurons obtained from 1 week (gray) and 4 weeks (black) old mice elicited by a 500 msec depolarizing pulse to 0 mV from a holding potential of -70 mV. The ScTx-sensitive current was obtained by subtracting the current after application of 300 nmol/L ScTx (i.e., ScTx-insensitive current) from the total outward K^+ current. The scale bar applies to all current recordings. (B) Current densities of the ScTx-sensitive component in the different age groups. The ScTx-sensitive current density did not change during postnatal development. (C) Fraction of the ScTx-sensitive current at the different developmental stages obtained by normalizing the current density of the ScTx-sensitive current to the current density of the total outward K^+ current at the end of the 500 msec pulse at 0 mV. The fraction of the ScTx-sensitive current relative to I_K in DRG neurons from 1 and 2 weeks old mice was significantly larger compared to the same fraction at 4 weeks ($*P < 0.05$). The numbers above each bar indicate the number of cells analyzed.

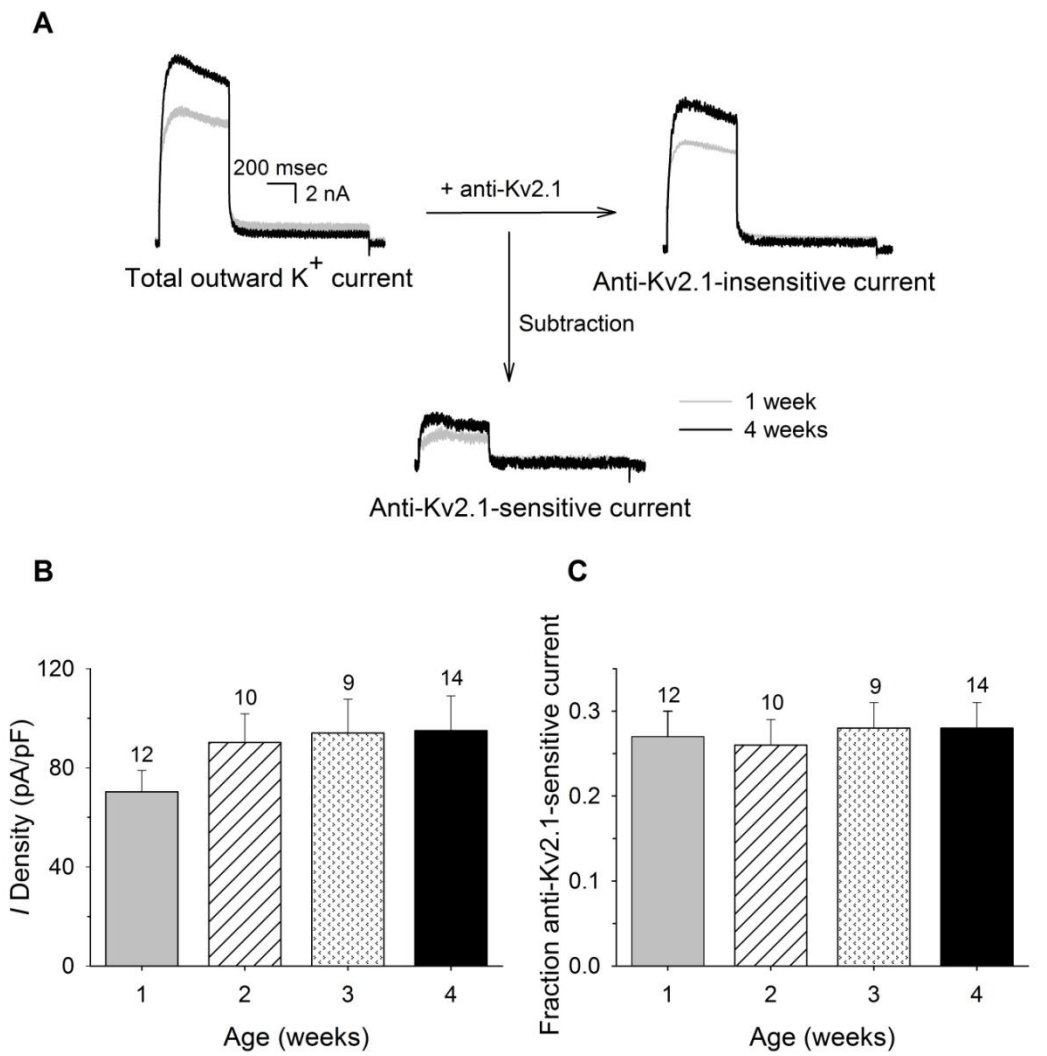

Figure 3: Postnatal development of anti-Kv2.1-sensitive current in dorsal root ganglion (DRG) neurons at 0 mV. (A) Representative current recordings of the total outward K^+ (left), anti-Kv2.1-insensitive (right), and anti-Kv2.1-sensitive (bottom) currents in DRG neurons obtained from 1 week (gray) and 4 weeks (black) old mice elicited by a 500 msec depolarizing pulse to 0 mV from a holding potential of -70 mV. The anti-Kv2.1-sensitive current was obtained by subtracting the current after intracellular diffusion of Kv2.1 antibodies (i.e., anti-Kv2.1-insensitive current) from the total outward K^+ current. The scale bar applies to all current recordings. (B) Current densities of the anti-Kv2.1-sensitive component in the different age groups. The anti-Kv2.1-sensitive current density rose gradually, although not significantly, during postnatal development. (C) The fraction of the anti-Kv2.1-sensitive current relative to I_K at the different developmental stages obtained as described in the Results section remained unchanged. The numbers above each bar indicate the number of cells analyzed.

Since only a fraction of the Kv2.1 and Kv2.2 channels are already in an open state at 0 mV, the above results could be due to an age-dependent depolarizing shift in the voltage dependence of activation of the Kv2-containing currents. Therefore, we determined the fraction of ScTx-sensitive and Kv2.1 antibody-sensitive current at higher depolarizing potentials (+20 and +40mV) (Fig. 4). The fraction of the anti-Kv2.1-sensitive current remained similar at the different postnatal ages, both at +20 mV (Fig. 4A) and +40 mV (Fig. 4B), whereas the ScTx-sensitive fraction of I_K reduced with age at both potentials. At +20 mV, the fractional contribution of the ScTx-sensitive current relative to I_K decreased significantly (regression coefficient = -0.036 ± 0.013 FC_{ScTx}/week, $P < 0.05$): ScTx inhibited 47 ± 5% at 1 week which is significantly different ($P < 0.05$) from the inhibition at 4 weeks (34 ± 3%) (Fig. 4A). At +40 mV, the fractional contribution relative to I_K decreased gradually (regression coefficient = -0.035 ± 0.019 FC_{ScTx}/week, $P = 0.075$), but not significantly, from 41 ± 3% at 1 week to 31 ± 3% at 4 weeks (Fig. 4B). Although the fractional contribution of the ScTx-sensitive current relative to I_K at +20 and +40 mV is lower compared to the fractional contribution at 0 mV due to the incomplete inhibition of the Kv2-containing currents by ScTx at higher potentials (11), a comparable decrease with postnatal age could be observed at all analyzed potentials. These results suggested that the observed developmental changes are not due to age-dependent shifts in the voltage dependence of the Kv2.1- and/or Kv2.2-containing current.

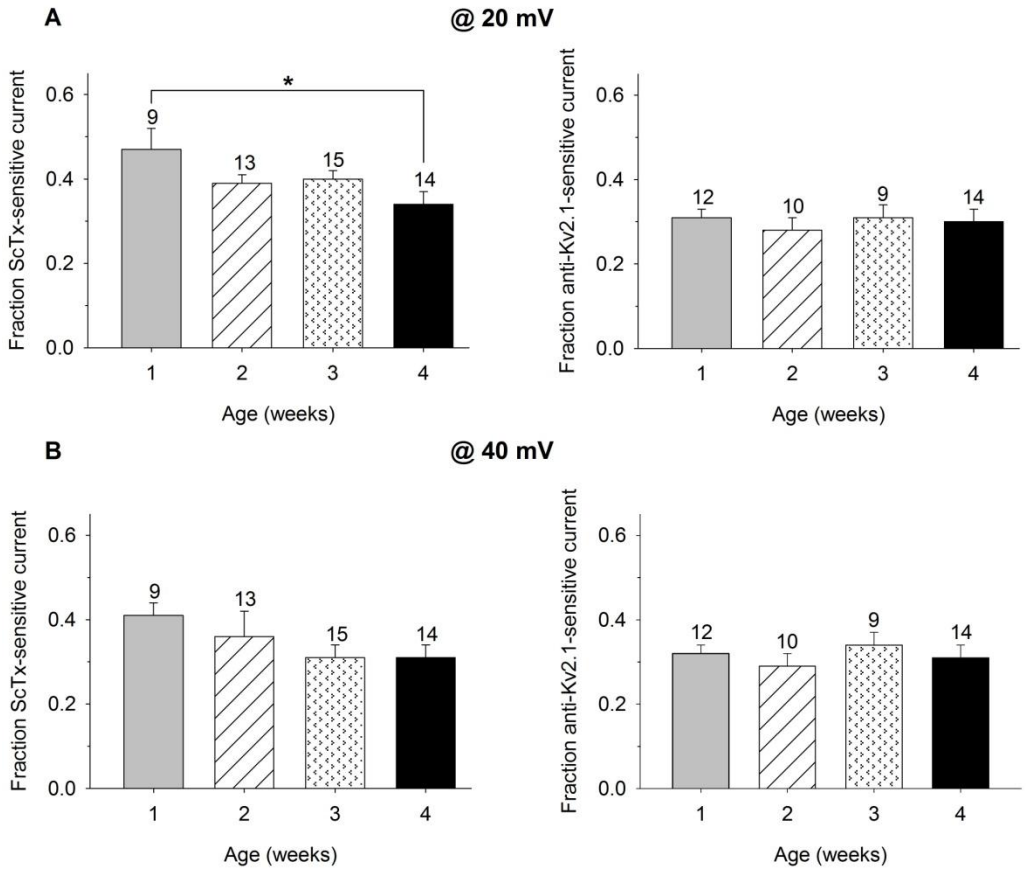

Figure 4: Postnatal development of the ScTx- and anti-Kv2.1-sensitive current at +20 and +40 mV. The fraction of ScTx-sensitive current (left) and anti-Kv2.1-sensitive current (right) relative to I_K of the different postnatal age groups at the end of a 500 msec depolarizing pulse at +20 mV (A) and +40 mV (B). (A) At +20 mV, the fraction of ScTx-sensitive current in dorsal root ganglion neurons from 1 week old mice was significantly larger compared to that from 4 week old mice (*P < 0.05), whereas the fraction of the anti-Kv2.1-sensitive current remained unchanged at the different developmental stages. (B) The fraction of ScTx-sensitive current reduced gradually (although not significantly) with postnatal age at +40 mV, while the fraction of anti-Kv2.1-sensitive current at the same potential remained constant during the same period. The numbers above each bar plot indicate the number of cells analyzed.

The Kv2.2 mRNA level decreases during postnatal development while the Kv2.1 mRNA level remains similar.

To investigate whether the observed ScTx-sensitive and anti-Kv2.1-sensitive current densities can be attributed to developmental changes in Kv2.1 and/or Kv2.2 expression, we examined the Kv2.1 and Kv2.2 mRNA levels in our DRG cultures obtained at the different developmental stages using semiquantitative RT-PCR analysis, as described in Material and Methods. After 35 amplification cycles, the intensity of the Kv signal was normalized to the intensity of the G3PDH signal and plotted as RDV. This semiquantitative RT-PCR approach revealed that the level of Kv2.2 mRNA decreased gradually (regression coefficient = -0.082 ± 0.022 RDV/week, $P < 0.05$) with age, reaching significance ($P < 0.05$) after 3 weeks: the RDV value declined from 0.57 ± 0.03 at 1 week to 0.32 ± 0.06 and 0.35 ± 0.05 at 3 and 4 weeks, respectively (Fig. 5). On the other hand, the Kv2.1 mRNA level remained similar: the lowest RDV value was detected at 1 week (RDV = 0.70 ± 0.05), while the highest RDV value was detected at 4 weeks (RDV = 0.77 ± 0.11) (Fig. 5). These data indicated that the age-dependent decrease of the Kv2.2-mediated current was a result of a developmental decrease of Kv2.2 expression.

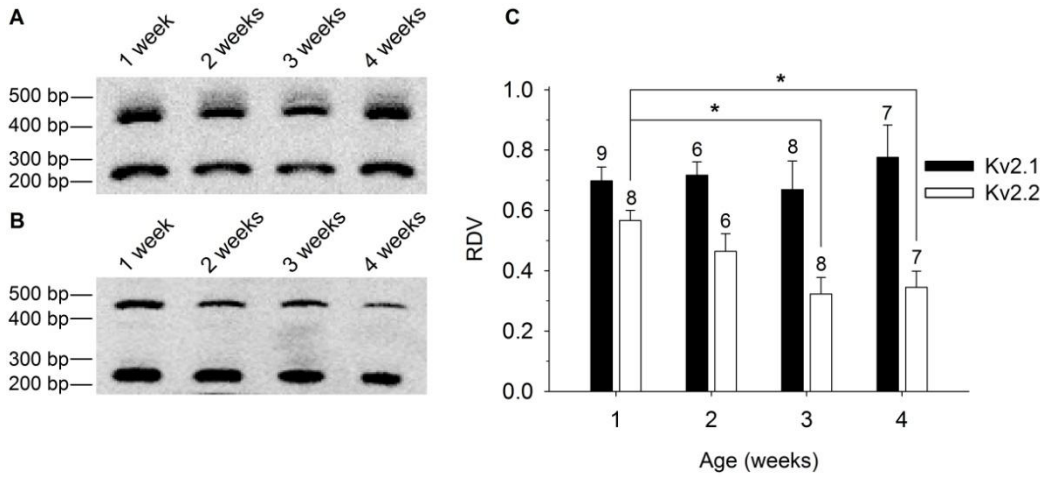

Figure 5: Postnatal development of the Kv2.1 and Kv2.2 mRNA levels in dorsal root ganglion (DRG) cultures. Electrophoretic analysis of the RT-PCR products obtained from cultured DRG neurons of 1, 2, 3, and 4 weeks old mice. The relative densitometric values (RDVs) (presented in panel C) were determined by normalizing the densitometric value of the 450 bp fragment, which corresponds to Kv2.1 (A) and Kv2.2 (B), to the densitometric value of G3PDH, which corresponds to the 250 bp fragment in both panels. (C) The RDV of Kv2.2 (white) decreased significantly determined in DRG cultures from 3 and 4 weeks old mice compared to the RDV determined in DRG cultures from 1 week old mice (*$P < 0.05$). The RDV of Kv2.1 (black) remained unaltered in the different age groups. The numbers above every bar plot indicate the number of samples analyzed.

Developmental changes in KvS mRNA levels

It has been demonstrated that different KvS (i.e., Kv5, Kv6, Kv8, and Kv9) subunits are expressed in small mouse cultured DRG neurons (5), and both Kv2.1 and Kv2.2 subunits assemble with those KvS subunits into heterotetrameric channels that possess unique biophysical properties (for review see (6)). Furthermore, at least heterotetrameric Kv2.1/Kv9.3 and Kv2.1/Kv6.3 channels have been shown to be inhibited by ScTx (11; 30). In addition, we have demonstrated that Kv2.1/Kv9.3 currents are also blocked by Kv2.1 antibodies (5). Therefore, it would be interesting to examine whether the observed developmental changes in the ScTx- and anti-Kv2.1-sensitive currents during the postnatal development of DRG neurons are at least partially due to changes in KvS-mediated currents. However, no compounds are known yet that can discriminate between Kv2/KvS heterotetramers and Kv2 homotetramers or between different Kv2/KvS channels making it difficult to analyze the up- or

downregulation of one of the KvS-containing currents using an electrophysiological approach. Therefore, we used the same semiquantitative approach as described above to investigate the mRNA levels of the different KvS subunits in the different age groups in order to gain a better insight in potential changes that may contribute to the observed developmental changes of the ScTx- and anti-Kv2.1-sensitive currents.

Similar to our previous study (5), the expression of Kv8.1, Kv9.1, and Kv9.3 could readily be observed in our DRG preparations. Furthermore, our semiquantitative approach revealed some age-dependent variations in the mRNA levels of these KvS subunits which were only significant in the case of Kv9.1 (Fig. 6A-C). The mRNA levels of Kv9.1 displayed an overall increase (regression coefficient = 0.069 ± 0.020 RDV/week, $P < 0.05$), with both 1 week (RDV = 0.23 ± 0.02) and 3 weeks (RDV = 0.29 ± 0.03) being significantly different compared to 4 weeks (RDV = 0.49 ± 0.06).

For Kv8.1, the highest mRNA level was detected at 2 weeks (RDV = 0.56 ± 0.04) and the lowest mRNA level at 1 week (RDV = 0.42 ± 0.02), but these differences did not reach statistical significance. The mRNA levels of Kv9.3 decreased from 1 week (RDV = 0.47 ± 0.06) to 4 weeks (RDV = 0.34 ± 0.04), yielding a regression coefficient of -0.048 ± 0.025 RDV/week ($P = 0.06$). We could also detect Kv6.3 mRNA in our DRG preparations with the highest value at 1 week (RDV = 0.26 ± 0.03) and the lowest at 3 weeks (RDV = 0.18 ± 0.03) (Fig. 6D).

Furthermore, Kv5.1 mRNA appeared to be present in our DRG preparations of every age (Fig. S1A). However, sequence analysis revealed a large nonspecific amplification in these reactions and therefore the relative expression level of the Kv5.1 mRNA could not be determined. The mRNA levels of the other KvS subunits (i.e., Kv6.1, Kv6.2, Kv6.4, Kv8.2, and Kv9.2) could not be detected at any postnatal developmental stage (Fig. S1B-F).

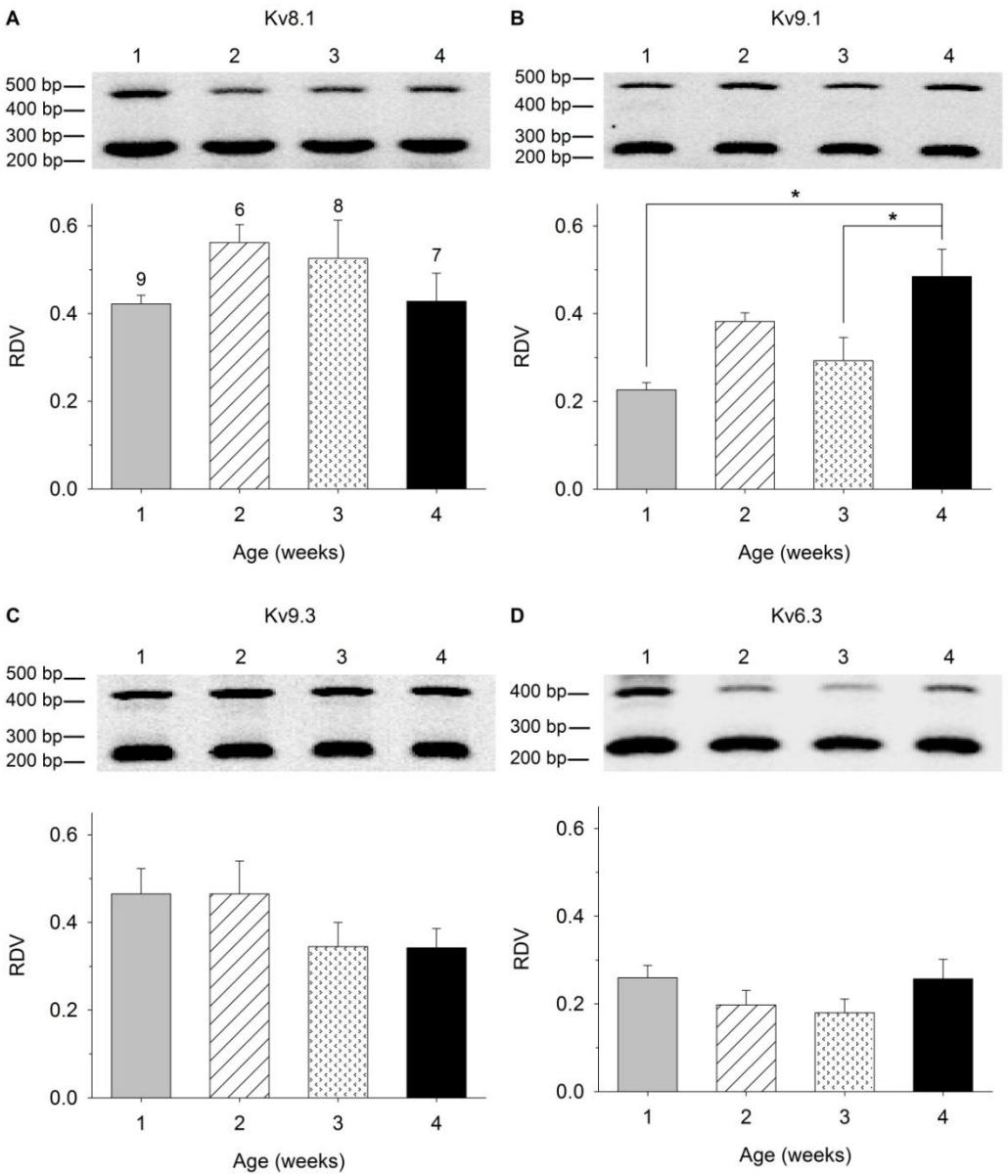

Figure 6: Postnatal development of KvS mRNA levels in dorsal root ganglion (DRG) cultures. Electrophoretic analysis of the RT-PCR products obtained from cultured DRG neurons of 1, 2, 3, and 4 weeks old mice. The number above each lane corresponds to the age of the mouse represented in weeks. The relative densitometric values (RDVs) of Kv8.1 (A), Kv9.1 (B), Kv9.3 (C), and Kv6.3 (D) were determined by normalizing the densitometric value of the largest fragment, which corresponds to the amplified KvS cDNA, to the densitometric value of the smallest fragment, which corresponds to the amplified G3PDH cDNA. The RDV of Kv9.1 (B) determined in DRG cultures from 4 weeks old mice was significantly higher compared to the RDV determined in DRG cultures from 1 and 3 weeks old mice (*$P < 0.05$). The numbers above every bar plot in panel A indicate the number of samples analyzed for each age group and are applicable to the other panels.

Discussion

Maturation of different neuronal cell types involves developmental changes in different Kv currents. For example, during the embryonic development of mouse spinal cord neurons, the delayed rectifier K^+ current appears before the transient outward K^+ current (25). In addition, a developmental increase of the whole-cell delayed rectifier K^+ density has been observed in several neuronal cell types (8; 12; 16; 20; 28; 42; 43). These developmental variations in the I_{DR} density depend heavily on the spatial and temporal expression of a wide variety of Kv subunits. This is illustrated by changes in the Kv2 expression that have been observed during development of neocortical pyramidal, hippocampal, and spinal neurons (2; 16; 18; 27; 40). For example, in cultured hippocampal neurons, clustered Kv2.2 expression at the axon initial segment appeared after 10 days *in vitro* and increased progressively during *in vitro* maturation, although diffuse expression in the soma and dendrites was detected at all time points (40). The expression of Kv2.1 and Kv2.2 subunits and their contribution to I_{DR} has also been demonstrated in DRG neurons (5; 23; 24; 45). However, it was not known whether the expression of these Kv2 subunits also varies during the postnatal maturation of DRG neurons. In this study, we demonstrated that in DRG neurons, the fraction of ScTx-sensitive current that represents both Kv2.1- and Kv2.2-mediated currents (11), decreased with postnatal age while the fraction of anti-Kv2.1-sensitive current that only represents Kv2.1-mediated currents (5; 17; 31), remained similar (Figs. 2 and 3). These results suggested that the fractional contribution of Kv2.2-mediated currents relative to I_K decreased during the postnatal development of DRG neurons which may be caused by a developmental decrease of Kv2.2 expression. Indeed, we detected that the Kv2.2 mRNA level decreased significantly between weeks 1 and 4 (Fig. 5). Since we analyzed current recordings and RNA samples 72 h after isolation, some changes compared to acute isolation might occur. However, Maletic-Savatic et al. (27) observed – in hippocampal neurons – a close spatiotemporal correlation between expression of Kv subunits *in situ* and during 22 days *in vitro* culture.

Furthermore, the observation that the total outward K^+ current increases with age in DRG neurons, is consistent with an earlier report (13). Therefore, we consider it unlikely that major dedifferentiation occurred during the 72 h culture duration, which was the same for each age group.

Although the fractional contribution of the Kv2.1-mediated current relative to I_K remained similar with postnatal age, the absolute current density of the Kv2.1-mediated current increased gradually, but this trend did not reach statistical significance (Fig. 3B). Interestingly, most of the change occurred between weeks 1 and 2. Since there was no increase in Kv2.1 mRNA levels, this may suggest that other factors may modulate the Kv2.1 current density, including post-translational modifications, association with auxiliary β-subunits and a stimulated translation of the existing mRNA. Various studies have shown a clear correlation between I_K density and mRNA levels in neurons (18; 32; 47; 51), suggesting that this developmental increase in the current density is not likely due to a stimulated translation of mRNA. Changes in post-translational modifications, including phosphorylation and SUMOylation (29; 36), and association with the auxiliary β-subunit AMIGO (34), are known to influence the Kv2.1 current density by shifting the voltage dependence of activation of this channel. However, comparison of the fractional contribution of the anti-Kv2.1-sensitive current relative to I_K at higher potentials (> 0 mV) indicated that there are no age-dependent shifts in the voltage dependence of activation of this component (Fig. 4). On the other hand, association of Kv2.1 with other auxiliary β-subunits, including KChAP and KCNE1-5 (10; 48), influences the current density of Kv2.1 without affecting the voltage dependence of activation. Consequently, the up- or downregulation of β-subunits during postnatal development may contribute to our observed changes in Kv2.1 current density.

The biophysical properties and current density of homotetrameric Kv2 channels are also modulated by the formation of heterotetrameric channels with members of the KvS subfamilies (i.e., Kv5, Kv6, Kv8, and Kv9) (for review see (6)). Similarly to the Kv2 subunits, the expression of several KvS subunits (and their potential contribution to I_K) in DRG neurons has been demonstrated; we

previously detected the expression of Kv6.1, Kv8.1, Kv9.1, Kv9.2, and Kv9.3 in cultured small mouse DRG neurons (5) while Tsantoulas et al. (44) demonstrated the expression of Kv9.1 in myelinated DRG neurons. Here, we confirmed the expression of Kv8.1, Kv9.1, and Kv9.3 subunits in DRG neurons at all postnatal ages (Fig. 6). Interestingly, Kv9.1 expression increased significantly suggesting that Kv9.1 may play an important role in the neonatal maturation of DRG neurons. In contrast, no expression of Kv6.1 and Kv9.2 could be detected at any postnatal stage. This discrepancy could be explained by the difference in RT-PCR conditions; in our previous study, the expression of these two subunits could only be detected after 44 cycles of cDNA amplification (5) while now only 35 amplification cycles were used to avoid potential problems of nonspecific amplifications and to ensure that the amplification of the target gene and G3PDH were both within the exponential phase of the PCR reaction. In addition, we demonstrated the presence of Kv6.3 in the DRG neurons obtained at all postnatal ages while we could not detect any Kv6.3 expression in our previous study. However, in that study, RNA was isolated from dorsal root ganglia of embryonic mice (E12-E14) (5), which suggests that Kv6.3 is not expressed in DRG neurons until the late embryonic and/or neonatal stages.

The total outward K^+ current density recorded after 500 msec increased during the first month of postnatal development (Fig. 1), while the Kv2-mediated current density did not change (Fig. 2). This suggests that the density of other delayed rectifier currents such as Kv3-mediated currents (7) and/or M-currents (13; 33) increases during the postnatal maturation of DRG neurons. Interestingly, in rat DRG neurons, it has been demonstrated that during the first two weeks of neonatal life, the current density of I_{DR} decreased, while the current density of I_M increased (13). These data together may suggest that I_{DR} declines during postnatal development due to a decrease in Kv2.2-mediated currents, while the total outward K^+ current density increases due to a rise in I_M density.

Tsantoulas et al. (45) demonstrated that inhibiting Kv2-containing channels in DRG neurons using ScTx resulted in a shortening of the action potential afterhyperpolarization leading to an increased action potential firing rate.

However, an induced downregulation of Kv2 in these neurons did not change the duration of afterhyperpolarization which the authors attributed to an altered expression of other ion channels. This indicates that, at least in DRG neurons, a decrease in the Kv2-containing current either by a decreased Kv2 expression or by blocking the Kv2-containing current using ScTx does not affect the neuronal properties in the same way. Furthermore, Kv2.1 and Kv2.2 homotetramers produce currents that display similar biophysical properties in heterologous expression systems (4; 14; 22). In addition, both Kv2.1 and Kv2.2 subunits can heterotetramerize with members of the KvS subfamilies resulting in Kv2/KvS heterotetramers that display distinct properties and that may be affected differently by the use of Kv2-blocking compounds and/or by changes in Kv2 expression. Taken together, it is difficult to predict the impact of our observed changes on the electrophysiological properties of our DRG neurons. However, the balance between Kv2.1 and Kv2.2 expression changed with postnatal age, suggesting that both subunits predominate (and exert their function) in other stages of the neonatal maturation of DRG neurons.

In conclusion, we propose that the fractional contribution of Kv2.2-mediated currents relative to I_K decreases during the postnatal maturation of DRG neurons while the fractional contribution of Kv2.1-mediated currents remains the same. In addition, the contribution of several KvS-containing channels fluctuates during the development of DRG neurons. This supports an important role of both Kv2 and KvS subunits in DRG neurons during different developmental stages.

Acknowledgements

We thank Abbi Van Tilborg for the excellent technical assistance. This work was supported by the section cardiovascular research of the Sheid-van Bogaert foundation, the postdoctoral fellowships FWO−1291913N and FWO-1291916N to EB and the grants G.0449.11N & G.0443.12N to DJS from the Research Foundation – Flanders (FWO).

References

1. **Akasu T and Tokimasa T**. Cellular metabolism regulating H and M currents in bullfrog sympathetic ganglia. Can J Physiol Pharmacol 70 Suppl: S51-S55, 1992.
2. **Antonucci DE, Lim ST, Vassanelli S, and Trimmer JS**. Dynamic localization and clustering of dendritic Kv2.1 voltage-dependent potassium channels in developing hippocampal neurons. Neurosci 108: 69-81, 2001.
3. **Beekwilder JP, O'Leary ME, van den Broek LP, van Kempen GT, Ypey DL, and Van den Berg RJ**. Kv1.1 channels of dorsal root ganglion neurons are inhibited by n-butyl-p-aminobenzoate, a promising anesthetic for the treatment of chronic pain. J Pharmacol Exp Ther 304: 531-538, 2003.
4. **Blaine JT and Ribera AB**. Heteromultimeric potassium channels formed by members of the Kv2 subfamily. J Neurosci 18: 9585-9593, 1998.
5. **Bocksteins E, Raes AL, Van de Vijver G, Bruyns T, Van Bogaert PP, and Snyders DJ**. Kv2.1 and silent Kv subunits underlie the delayed rectifier K^+ current in cultured small mouse DRG neurons. Am J Physiol Cell Physiol 296: C1271-C1278, 2009.
6. **Bocksteins E and Snyders DJ**. Electrically silent Kv subunits: their molecular and functional characteristics. Physiology (Bethesda) 27: 73-84, 2012.
7. **Bocksteins E, Van de Vijver G, Van Bogaert PP, and Snyders DJ**. Kv3 channels contribute to the delayed rectifier current in small cultured mouse dorsal root ganglion neurons. Am J Physiol Cell Physiol 303: C406-C415, 2012.
8. **Bortone DS, Mitchell K, and Manis PB**. Developmental time course of potassium channel expression in the rat cochlear nucleus. Hear Res 211: 114-125, 2006.
9. **Chien LY, Cheng JK, Chu D, Cheng CF, and Tsaur ML**. Reduced expression of A-type potassium channels in primary sensory neurons induces mechanical hypersensitivity. J Neurosci 27: 9855-9865, 2007.

10. **David JP, Stas JI, Schmitt N, and Bocksteins E**. Auxiliary KCNE subunits modulate both homotetrameric Kv2.1 and heterotetrameric Kv2.1/Kv6.4 channels. Sci Rep 5: 12813, 2015.
11. **Escoubas P, Diochot S, Celerier ML, Nakajima T, and Lazdunski M**. Novel tarantula toxins for subtypes of voltage-dependent potassium channels in the Kv2 and Kv4 subfamilies. Mol Pharmacol 62: 48-57, 2002.
12. **Falk T, Kilani RK, Strazdas LA, Borders RS, Steidl JV, Yool AJ, and Sherman SJ**. Developmental regulation of the A-type potassium-channel current in hippocampal neurons: role of the Kvbeta 1.1 subunit. Neurosci 120: 387-404, 2003.
13. **Fedulova SA, Vasilyev DV, and Veselovsky NS**. Voltage-operated potassium currents in the somatic membrane of rat dorsal root ganglion neurons: ontogenetic aspects. Neurosci 85: 497-508, 1998.
14. **Frech GC, VanDongen AM, Schuster G, Brown AM, and Joho RH**. A novel potassium channel with delayed rectifier properties isolated from rat brain by expression cloning. Nature 340: 642-645, 1989.
15. **Gold MS, Shuster MJ, and Levine JD**. Characterization of six voltage-gated K^+ currents in adult rat sensory neurons. J Neurophysiol 75: 2629-2646, 1996.
16. **Guan D, Horton LR, Armstrong WE, and Foehring RC**. Postnatal development of A-type and Kv1- and Kv2-mediated potassium channel currents in neocortical pyramidal neurons. J Neurophysiol 105: 2976-2988, 2011.
17. **Guan D, Tkatch T, Surmeier DJ, Armstrong WE, and Foehring RC**. Kv2 subunits underlie slowly inactivating potassium current in rat neocortical pyramidal neurons. J Physiol 581: 941-960, 2007.
18. **Gurantz D, Ribera AB, and Spitzer NC**. Temporal regulation of *Shaker*- and *Shab*-like potassium channel gene expression in single embryonic spinal neurons during K^+ current development. J Neurosci 16: 3287-3295, 1996.

19. **Gutman GA, Chandy KG, Grissmer S, Lazdunski M, McKinnon D, Pardo LA, Robertson GA, Rudy B, Sanguinetti MC, Stuhmer W, and Wang X**. International Union of Pharmacology. LIII. Nomenclature and molecular relationships of voltage-gated potassium channels. Pharmacol Rev 57: 473-508, 2005.
20. **Harris GL, Henderson LP, and Spitzer NC**. Changes in densities and kinetics of delayed rectifier potassium channels during neuronal differentiation. Neuron 1: 739-750, 1988.
21. **Hille B**. Ion channels of excitable membranes. Sunderland, Mass: Sinauer, 2001.
22. **Hwang PM, Glatt CE, Bredt DS, Yellen G, and Snyder SH**. A novel K^+ channel with unique localizations in mammalian brain: molecular cloning and characterization. Neuron 8: 473-481, 1992.
23. **Ishikawa K, Tanaka M, Black JA, and Waxman SG**. Changes in expression of voltage-gated potassium channels in dorsal root ganglion neurons following axotomy. Muscle Nerve 22: 502-507, 1999.
24. **Kim DS, Choi JO, Rim HD, and Cho HJ**. Downregulation of voltage-gated potassium channel alpha gene expression in dorsal root ganglia following chronic constriction injury of the rat sciatic nerve. Brain Res Mol Brain Res 105: 146-152, 2002.
25. **Krieger C and Sears TA**. The development of voltage-dependent ionic conductances in murine spinal cord neurones in culture. Can J Physiol Pharmacol 66: 1328-1336, 1988.
26. **Long SB, Campbell EB, and MacKinnon R**. Crystal structure of a mammalian voltage-dependent *Shaker* family K^+ channel. Science 309: 897-903, 2005.
27. **Maletic-Savatic M, Lenn NJ, and Trimmer JS**. Differential spatiotemporal expression of K^+ channel polypeptides in rat hippocampal neurons developing *in situ* and *in vitro*. J Neurosci 15: 3840-3851, 1995.

28. **Martin-Caraballo M and Greer JJ**. Development of potassium conductances in perinatal rat phrenic motoneurons. J Neurophysiol 83: 3497-3508, 2000.
29. **Misonou H, Mohapatra DP, Park EW, Leung V, Zhen D, Misonou K, Anderson AE, and Trimmer JS**. Regulation of ion channel localization and phosphorylation by neuronal activity. Nat Neurosci 7: 711-718, 2004.
30. **Moreno-Dominguez A, Cidad P, Miguel-Velado E, Lopez-Lopez JR, and Perez-Garcia MT**. *De novo* expression of Kv6.3 contributes to changes in vascular smooth muscle cell excitability in a hypertensive mice strain. J Physiol 587: 625-640, 2009.
31. **Murakoshi H and Trimmer JS**. Identification of the Kv2.1 K^+ channel as a major component of the delayed rectifier K^+ current in rat hippocampal neurons. J Neurosci 19: 1728-1735, 1999.
32. **Namba H, Takei N, and Nawa H**. Transforming growth factor-alpha changes firing properties of developing neocortical GABAergic neurons by down-regulation of voltage-gated potassium currents. Neurosci 122: 637-646, 2003.
33. **Passmore GM, Selyanko AA, Mistry M, Al Qatari M, Marsh SJ, Matthews EA, Dickenson AH, Brown TA, Burbidge SA, Main M, and Brown DA**. KCNQ/M currents in sensory neurons: significance for pain therapy. J Neurosci 23: 7227-7236, 2003.
34. **Peltola MA, Kuja-Panula J, Lauri SE, Taira T, and Rauvala H**. AMIGO is an auxiliary subunit of the Kv2.1 potassium channel. EMBO Rep 12: 1293-1299, 2011.
35. **Phuket TR and Covarrubias M**. Kv4 Channels Underlie the Subthreshold-Operating A-type K^+-current in Nociceptive Dorsal Root Ganglion Neurons. Front Mol Neurosci 2: 3, 2009.
36. **Plant LD, Dowdell EJ, Dementieva IS, Marks JD, and Goldstein SA**. SUMO modification of cell surface Kv2.1 potassium channels regulates the activity of rat hippocampal neurons. J Gen Physiol 137: 441-454, 2011.

37. **Rasband MN, Park EW, Vanderah TW, Lai J, Porreca F, and Trimmer JS**. Distinct potassium channels on pain-sensing neurons. Proc Natl Acad Sci U S A 98: 13373-13378, 2001.
38. **Rhodes KJ, Keilbaugh SA, Barrezueta NX, Lopez KL, and Trimmer JS**. Association and colocalization of K^+ channel alpha- and beta-subunit polypeptides in rat brain. J Neurosci 15: 5360-5371, 1995.
39. **Ribera AB and Spitzer NC**. Developmental regulation of potassium channels and the impact on neuronal differentiation. Ion Channels 3: 1-38, 1992.
40. **Sanchez-Ponce D, DeFelipe J, Garrido JJ, and Munoz A**. Developmental expression of Kv potassium channels at the axon initial segment of cultured hippocampal neurons. PLoS ONE 7: e48557, 2012.
41. **Schnizler K, Shutov LP, Van Kanegan MJ, Merrill MA, Nichols B, McKnight GS, Strack S, Hell JW, and Usachev YM**. Protein kinase A anchoring via AKAP150 is essential for TRPV1 modulation by forskolin and prostaglandin E2 in mouse sensory neurons. J Neurosci 28: 4904-4917, 2008.
42. **Spigelman I, Zhang L, and Carlen PL**. Patch-clamp study of postnatal development of CA1 neurons in rat hippocampal slices: membrane excitability and K^+ currents. J Neurophysiol 68: 55-69, 1992.
43. **Surmeier DJ, Stefani A, Foehring RC, and Kitai ST**. Developmental regulation of a slowly-inactivating potassium conductance in rat neostriatal neurons. Neurosci Lett 122: 41-46, 1991.
44. **Tsantoulas C, Zhu L, Shaifta Y, Grist J, Ward JP, Raouf R, Michael GJ, and McMahon SB**. Sensory neuron downregulation of the Kv9.1 potassium channel subunit mediates neuropathic pain following nerve injury. J Neurosci 32: 17502-17513, 2012.
45. **Tsantoulas C, Zhu L, Yip P, Grist J, Michael GJ, and McMahon SB**. Kv2 dysfunction after peripheral axotomy enhances sensory neuron responsiveness to sustained input. Exp Neurol 251: 115-126, 2014.

46. **Utsunomiya I, Yoshihashi E, Tanabe S, Nakatani Y, Ikejima H, Miyatake T, Hoshi K, and Taguchi K**. Expression and localization of Kv1 potassium channels in rat dorsal and ventral spinal roots. Exp Neurol 210: 51-58, 2008.
47. **Veys K, Labro AJ, De Schutter E, and Snyders DJ**. Quantitative single-cell ion-channel gene expression profiling through an improved qRT-PCR technique combined with whole cell patch clamp. J Neurosci Methods 209: 227-234, 2012.
48. **Wible BA, Yang Q, Kuryshev YA, Accili EA, and Brown AM**. Cloning and expression of a novel K^+ channel regulatory protein, KChAP. J Biol Chem 273: 11745-11751, 1998.
49. **Winkelman DL, Beck CL, Ypey DL, and O'Leary ME**. Inhibition of the A-type K^+ channels of dorsal root ganglion neurons by the long-duration anesthetic butamben. J Pharmacol Exp Ther 314: 1177-1186, 2005.
50. **Xu J, Yu W, Jan YN, Jan LY, and Li M**. Assembly of voltage-gated potassium channels. J Biol Chem 270: 24761-24768, 1995.
51. **Zhong CB, Pan YP, Tong XY, Xu XH, and Wang XL**. Delayed rectifier potassium currents and Kv2.1 mRNA increase in hippocampal neurons of scopolamine-induced memory-deficient rats. Neurosci Lett 373: 99-104, 2005.

Electronic Supplementary Material

to

The contribution of Kv2.2-mediated currents decreases during the postnatal development of mouse dorsal root ganglion neurons.

Glenn Regnier[1], Elke Bocksteins[1], Gerda Van de Vijver[2], Dirk J. Snyders[1], Pierre-Paul van Bogaert[2]

Physiol Rep. 2016 March; 4(3):e12731

[1]Laboratory for Molecular Biophysics, Physiology and Pharmacology, Department of Biomedical Sciences, University of Antwerp, CDE, Universiteitsplein 1, 2610 Antwerpen, Belgium
[2]Laboratory for Cardiovascular Research, Institute Born-Bunge, University of Antwerp, CDE, Universitetitsplein 1, 2610 Antwerpen, Belgium

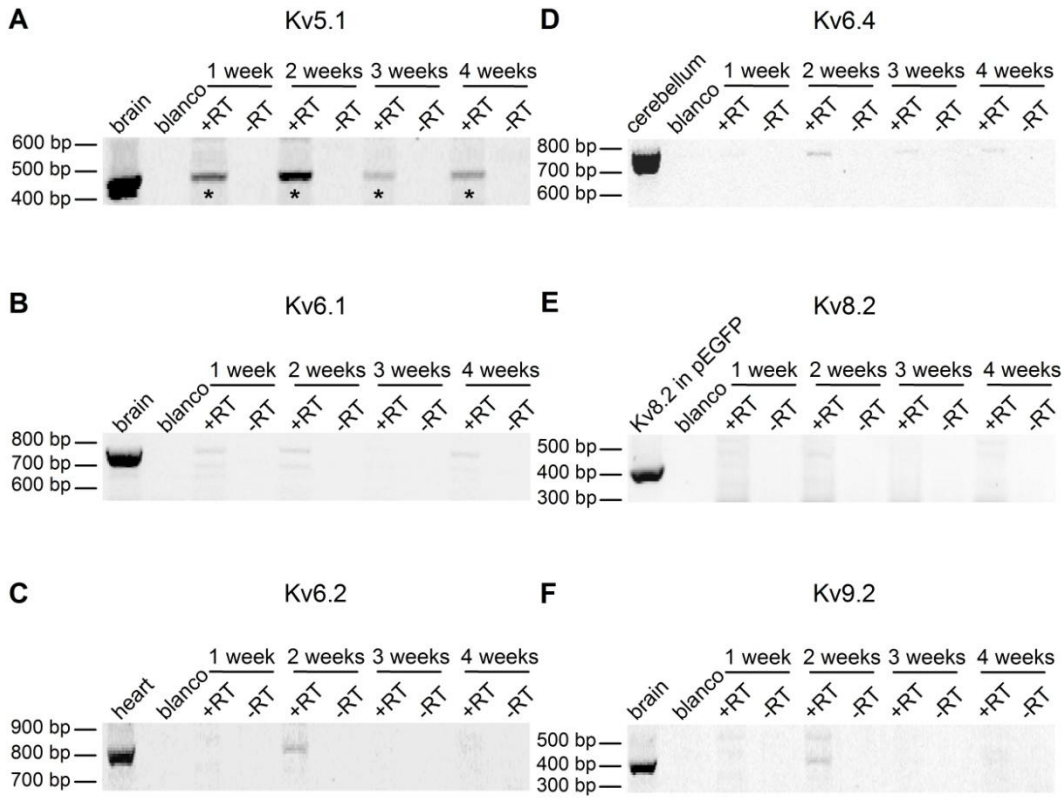

Figure S1: Expression of KvS subunits in adult mouse DRG neurons. RT-PCR analyses of the Kv5.1 (A), Kv6.1 (B), Kv6.2 (C), Kv6.4 (D), Kv8.2 (E), and Kv9.2 (F) subunits in cultured DRG neurons obtained from 1, 2, 3, and 4 weeks old mice. In each panel, the first lane represents the positive control sample in which the target cDNA was certainly expressed. The second lane represents the first negative control sample in which H_2O was used instead of cDNA. For each age group both +RT and –RT samples were tested. The –RT sample represents a negative control whereby the RT reaction was performed without the Reverse Transcriptase enzyme. The +RT sample was used to test the actual expression of the different KvS subunits. No specific amplification of Kv6.1 (B), Kv6.2 (C), Kv6.4 (D), Kv8.2 (E), and Kv9.2 (F) was detected in the DRG samples, whereas the amplification which was detected for Kv5.1 (A) contained a large nonspecific amplification (indicated with an asterisk).

Chapter 4

Targeted deletion of the Kv6.4 subunit causes male sterility due to disturbed spermiogenesis

Glenn Regnier[1], Elke Bocksteins[1], Waleed F. Marei[2,3], Isabel Pintelon[4], Jean-Pierre Timmermans[4], Jo L.M.R. Leroy[2], Dirk J. Snyders[1]

Reprod Fertil Dev. (accepted)

[1]Laboratory of Molecular Biophysics, Physiology and Pharmacology, Department of Biomedical Sciences, University of Antwerp, CDE, Universiteitsplein 1, 2610 Antwerpen, Belgium
[2]Laboratory of Veterinary Physiology and Biochemistry, Department of Veterinary Sciences, University of Antwerp, CDE, Universiteitsplein 1, 2610 Antwerpen, Belgium
[3]Department of Theriogenology, Faculty of Veterinary Medicine, Cairo University, 12211 Giza, Egypt
[4]Laboratory of Cell Biology and Histology, Department of Veterinary Sciences, University of Antwerp, CGB, Groenenborgerlaan 171, 2020 Antwerpen, Belgium.

Abstract

Electrically silent voltage-gated potassium (KvS) channel subunits (i.e., Kv5-Kv6 and Kv8-Kv9) do not form functional homotetrameric Kv channels, but co-assemble with Kv2 subunits, generating functional heterotetrameric Kv2/KvS channel complexes in which the KvS subunits modulate the Kv2 channel properties. Several KvS subunits are expressed in testis tissue but knowledge about their contribution to testis physiology is lacking. Here, we report that the targeted deletion of Kv6.4 in a transgenic mouse model (*Kcng4*$^{-/-}$) causes male sterility as offspring from homozygous females were only obtained after mating with wild-type (WT) or heterozygous males. Semen quality analysis revealed that the sterility of the homozygous males was caused by a severe reduction in total sperm-cell count and the absence of motile spermatozoa in the semen. Furthermore, spermatozoa of homozygous mice showed an abnormal morphology characterized by a smaller head and a shorter tail compared to that of WT spermatozoa. Comparison of WT and *Kcng4*$^{-/-}$ testicular tissue indicated that this inability to produce (normal) spermatozoa was due to disturbed spermiogenesis. These results suggest that Kv6.4 subunits are involved in the regulation of the late stages of spermatogenesis, which makes them a potentially interesting pharmacological target for the development of non-hormonal male contraceptives.

Introduction

Spermatogenesis is a tightly regulated physiological process that takes place in the epithelium of seminiferous tubules. Throughout this complex process, developing spermatogenic cells migrate from the basal membrane to the luminal side of these epithelia, in which diploid spermatogonia proliferate and differentiate into haploid spermatozoa through several well-defined consecutive stages. Type A spermatogonia at the basal membrane divide by mitosis and some of these proliferated cells differentiate into Type B spermatogonia, which, in turn,

differentiate further into primary spermatocytes. These cells migrate through tight junctions, which form the blood-testis barrier, into the adluminal compartment where they develop into secondary spermatocytes and round spermatids by two consecutive meiotic divisions. The round spermatids undergo drastic morphological changes, forming elongated spermatids and eventually spermatozoa by a process called spermiogenesis (for review see (39)). During all these stages, the developing sperm cells are in close proximity to the Sertoli cells. A wide variety of functions that support spermatogenesis have been attributed to these cells including tubular fluid secretion, nourishing of the germ cells, phagocytosis of residual cytoplasm during spermiogenesis, and the secretion of biological co-factors involved in the regulation of the spermatogenic cycle (for reviews see (18; 31)).

Proliferation and differentiation of several cell types, including lymphocytes (6; 9), smooth muscle cells (23), and tumor cells (19; 30), involve voltage-gated K^+ (Kv) channels which trigger changes in membrane potential and regulate cell volume (for review see (29)). In spermatogenic cells, the expression of Kv1.1, Kv1.2, Kv1.3, Kv3.1, and Kv7.1 channel subunits has been demonstrated (11; 15; 33), creating the possibility that Kv channels are also involved in the proliferation and differentiation of these cells. Kv channels are tetramers of α-subunits that enclose a K^+-selective aqueous pore. Based on sequence homology, Kv α-subunits are subdivided into different subfamilies (16). The Kv6.4 subunit (gene name, *KCNG4*) belongs to a subgroup of Kv subfamilies that are designated silent Kv (KvS) subunits (i.e., members of the Kv5, Kv6, Kv8, and Kv9 subfamilies) since they do not produce functional homotetrameric channels (for review see (5)). However, they form functional heterotetrameric channels with members of the Kv2 subfamily. Within these heterotetrameric Kv2/KvS channels, the KvS subunits modulate the Kv2 channel properties and are therefore considered as modulatory α-subunits of the Kv2 subfamily. The most profound modulating effects include a hyperpolarized shift in the voltage dependence of inactivation, slowing of activation and deactivation kinetics, and a reduction of the current density.

The functional diversity within the ubiquitously expressed Kv2 subfamily is rather limited since it consists only of two members, Kv2.1 and Kv2.2, which produce currents with similar biophysical properties (2; 13; 20). Because the members of the KvS subfamilies display a more confined expression pattern, it is assumed that the KvS subunits increase the functional diversity of the Kv2 currents to fulfill more tissue-specific functions. This is illustrated by the increasing number of scientific publications that demonstrate involvement of several KvS subunits in different physiological processes and pathologies (for review see (4)). In case of Kv6.4 subunits, it has been demonstrated that they contribute to the delayed rectifier current in fast motor neurons (24), while a missense mutation in this subunit has been linked to migraine (21).

Since Kv6.4 is expressed in several tissues and given its profound modulating effect on the Kv2 current, it is expected that this subunit is also involved in other physiological processes. To investigate this we created a transgenic mouse model with a targeted deletion of the Kv6.4 subunit. Unexpectedly, *Kcng4*-null male mice appeared to be sterile. By examining and comparing the semen quality and testicular morphology of wild-type (WT) and *Kcng4*-null male mice we found that deletion of the Kv6.4 subunit causes oligoasthenoteratozoospermia, which indicates that this subunit is probably involved in the regulation of spermiogenesis.

Material and methods

Animals

Kcng4-null mice (*Kcng4*$^{tm1(KOMP)Vlcg}$) were generated in a C57BL/6N background by the Knock-Out Mice Program (KOMP) at the University of California (Project ID# VG11043). Heterozygous founder mice were obtained from KOMP and used to obtain wild-type, heterozygous, and homozygous descendants. The mice were housed in an environmentally controlled animal facility of the University of Antwerp on a 12:12 h light:dark cycle. Food and water were available to the mice *ad libitum*. Animal care and experiments were in

agreement with the European Communities Council Directive on the protection of animals used for experimental and other scientific purposes (2010/63/EU). For sperm analysis and histological experiments, three male mice per genotype with an age of 12-16 weeks were used; they were anaesthetized with isoflurane before they were sacrificed by decapitation. For mating experiments one male (10-14 weeks old) and one female (15-23 weeks old) were housed in the same cage during the whole course of the experiment (3 months).

Animal genotyping was performed with the Terra PCR direct Polymerase mix (Clontech Laboratories Inc., Mountain View, CA, USA) according to the manufacturers' guidelines using tail or ear DNA. Primers used for polymerase chain reaction (PCR) were: 5'–GCC TTT ACT ACA GCA GGG C-3' (P1F), 5'-CTC CAG CTT CTT CAG CAG C-3' (P1R), 5'-GTC TGT CCT AGC TTC CTC ACT G-3' (LaclnZRev) and 5'-GCA GAA CCT CCT TAG TGT AG-3' (SU). The primer pair P1F and P1R flanked the amplicon of the WT allele whereas the primer pair LacInZRev and SU flanked the amplicon of the expression-selection cassette that was inserted by the targeting vector and that replaced the coding sequence of the WT allele when this mouse strain was created (Fig. S1). For further details considering the creation of the transgenic mouse model, visit the KOMP Repository website: www.komp.org.

Reverse transcription PCR (RT-PCR)

RNA was precipitated from different mouse tissues using the TriZol reagent (ThermoFisher Scientific, Waltham, MA, USA). To exclude genomic DNA contamination, the RNA samples were treated with deoxyribonuclease I (ThermoFisher Scientific) before the RT-PCR was performed. Total RNA (1 µg) was reverse transcribed using random hexamer primers with the Superscript III RT-PCR system (ThermoFisher Scientific) according to the manufacturer's guidelines. Amplification of the Kv6.4 cDNA was performed for 36 cycles, using primers that spanned intron boundaries. The following primer pair was used: 5'-GCC AGG AGT TCT TCT TCG AC-3' (sense) and 5'-CAT CAG GAG ACC AAA CTC TC-3' (antisense). For each PCR analysis, two negative controls (reaction

without cDNA or without reverse transcriptase) and a positive control (reaction containing the cloned mouse Kv6.4 cDNA) were performed. Amplified fragments were sequenced to confirm the identity of the PCR product. Each RT-PCR analysis was performed in duplicate on two different RNA isolations.

Sperm analysis

Caudae epididymides were isolated in HEPES-buffered *in vitro* fertilization medium Tyrode's albumin lactate pyruvate (IVF-TALP) and subsequently transferred and sliced in 4-well plates (Nunc®, Langenselbold, Germany) containing 500 µL per well IVF-TALP medium composed of: 114 mmol/L NaCl, 3.1 mmol/L KCl, 0.3 mmol/L Na_2HPO_4, 2.1 mmol/L $CaCl_2 \bullet 2H_2O$, 0.4 mmol/L $MgCl_2 \bullet 6H_2O$, 25 mmol/L $NaHCO_3$, 1 mmol/L sodium pyruvate, 36 mmol/L sodium lactate, 10 µg/mL phenol red, 6 mg/mL bovine serum albumin (BSA), and 50 µg/mL gentamycin (1). Caudal epididymal spermatozoa were released by incubation of the sliced caudae epididymides at 37°C in a humidified atmosphere of 6% CO_2 for 15 minutes. Sperm motility was evaluated immediately under a light microscope with an attached heat stage at 37°C (Olympus, Tokyo, Japan) and scored by two independent observers on a subjective scale of 0-100% to the nearest 5% by examining several microscopic fields. Total sperm count was determined with a Burker counting chamber. For analyses of sperm morphology and viability, the samples were stained with eosin-nigrosin (7) and subsequently smeared and dried on glass slides. Sperm morphology and viability were scored by two independent observers blinded to the genotype. A total of 200 sperm cells per animal were evaluated and each scored characteristic was represented as a percentage of the total sperm population.

Histology

Isolated testes and epididymides were fixed in 4% paraformaldehyde for 4-8 hours, washed in 70% ethanol, and processed for paraffin embedding. Tissue sections of 5 µm were prepared and stained with haematoxylin and eosin (H&E) or by the periodic acid-Shiff (PAS) reaction. Six stained sections per animal were

examined in which the distance between sections was at least 50 µm. Histological examination was performed under a light microscope (Zeiss Axiophot, Carl Zeiss, Jena, Germany) by observers blinded to the genotype.

Data analysis

All digital images were taken with a DP70 digital camera and Cell P software (Olympus, Hamburg, Germany) and all measurements on the digital images were executed with the ImageJ software (National Institute of Health, USA). All values are represented as mean ± SEM.

Statistical analysis was done with the unpaired Student's t-test or the Mann-Whitney U test in case unequal variances were present between the data sets. *P*-values < 0.05 were considered to be significant.

Results

Male *Kcng4*$^{-/-}$ mice are sterile

First, we analyzed the expression pattern of Kv6.4 in mice using RT-PCR, which revealed that Kv6.4 is expressed in tissues of the central nervous system, in muscle tissues, and in tissues of the male reproductive system, including testis (Fig. 1). To gain better insight into the physiological function of Kv6.4 we created a transgenic mouse model in which the coding sequence of the *Kcng4* gene was replaced by a LacZ/neomycin-resistant gene (Fig. S1A). This yielded homozygous *Kcng4*-null (*Kcng4*$^{-/-}$) mice (Fig. S1A) which we confirmed with genotyping (Fig. S1B) and RT-PCR analysis of testis tissue (Fig. 1A). *Kcng4*$^{-/-}$ mice of both sexes were viable and were normal in appearance and behavior. However, despite displaying normal mating behavior and ejaculation with normal vaginal plug formation, homozygous *Kcng4*$^{-/-}$ males seemed to be sterile: homozygous females produced offspring when mated with both wild-type (WT) and heterozygous (*Kcng4*$^{+/-}$) males but not with homozygous males.

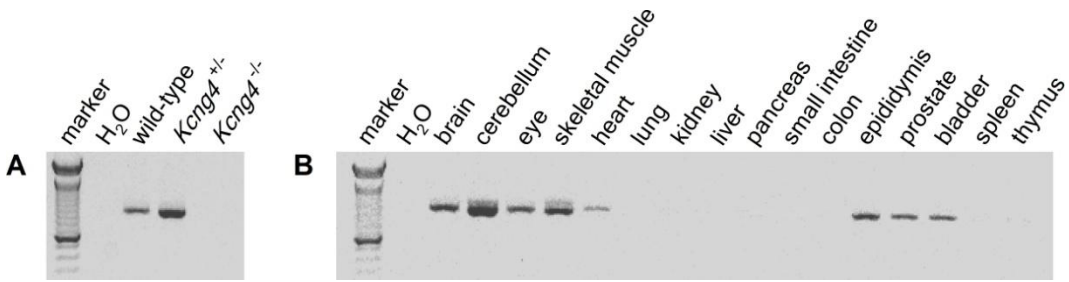

Figure 1: Expression of Kv6.4 in C57BL/6N mice. (A) RT-PCR analysis of Kv6.4 in the testis of WT, *Kcng4*$^{+/-}$, and *Kcng4*$^{-/-}$ mice. Kv6.4 is expressed in WT and *Kcng4*$^{+/-}$ mice, but not in *Kcng4*$^{-/-}$ mice confirming the lack of Kv6.4 expression in the *Kcng4*$^{-/-}$ mouse model. (B) RT-PCR analysis of Kv6.4 expression in various organs.

To confirm this observation we evaluated the reproductive performances of WT, *Kcng4*$^{+/-}$, and *Kcng4*$^{-/-}$ males during a 3-month period. For this purpose, we co-housed one WT (n = 3), *Kcng4*$^{+/-}$ (n = 4), or *Kcng4*$^{+/-}$ (n = 4) male with one homozygous *Kcng4*$^{-/-}$ female and determined the number of litters and pups we obtained during this period (Table 1). Breeding homozygous females with WT and *Kcng4*$^{+/-}$ males yielded several litters with an average size of 8.2 ± 0.4 and 8.3 ± 1.2 pups per litter, respectively, whereas *Kcng4*$^{-/-}$ males produced no offspring, confirming that male *Kcng4*$^{-/-}$ mice are sterile. These results suggest that Kv6.4 has a particularly important function in the testis and therefore we focused in this study on investigating the cause of the *Kcng4*$^{-/-}$ male sterility. Because the reproductive performances of WT and *Kcng4*$^{+/-}$ males were comparable, we only compared WT and *Kcng4*$^{-/-}$ mice in further experiments.

Table 1: *Kcng4*$^{-/-}$ males demonstrate sterility.

Genotype ♂	No. of litters	No. of pups	Average litter size (pups per litter)	*n*
WT	5	41	8.2 ± 0.4	3
Kcng4$^{+/-}$	6	50	8.3 ± 1.2	4
Kcng4$^{-/-}$	0	0	0	4

The parameters presented in this table were determined during a 3-month period, in which one male was co-housed with one homozygous female. Numbers indicate the number of males used for each male genotype.

The semen of homozygous males displays very low sperm count and motility

To determine the cause of sterility of male *Kcng4*$^{-/-}$ mice we analyzed their semen and compared it with that of WT males (Fig. 2A-C). The number of spermatozoa isolated from the caudae epididymides was significantly lower (P = 0.008) in *Kcng4*$^{-/-}$ mice (0.9 ± 0.3 x 10^6, n = 3) compared to the number of sperm cells obtained from WT mice (17.7 ± 3.3 x 10^6, n = 3) (Fig. 2A). This could also be observed on H&E stained sections of epididymal tissues: in WT epididymides, the lumen of the ductules were filled with maturing spermatozoa whereas the lumen of the ductules in *Kcng4*$^{-/-}$ mice contained only a few cells of which a large fraction were round degenerated cells (Fig. 2D). In addition, from this reduced number of spermatozoa in the *Kcng4*$^{-/-}$ semen only a few were motile: the progressive motility was only 5% which was significantly less (P < 0.001) than that of WT mice (73 ± 7%) (Fig. 2B). Furthermore, eosin-nigrosin staining of the spermatozoa revealed that the fraction of dead spermatozoa in the semen of homozygous males (61 ± 5%) was significantly higher (P = 0.003) than that of WT males (28 ± 2%) (Fig. 2C).

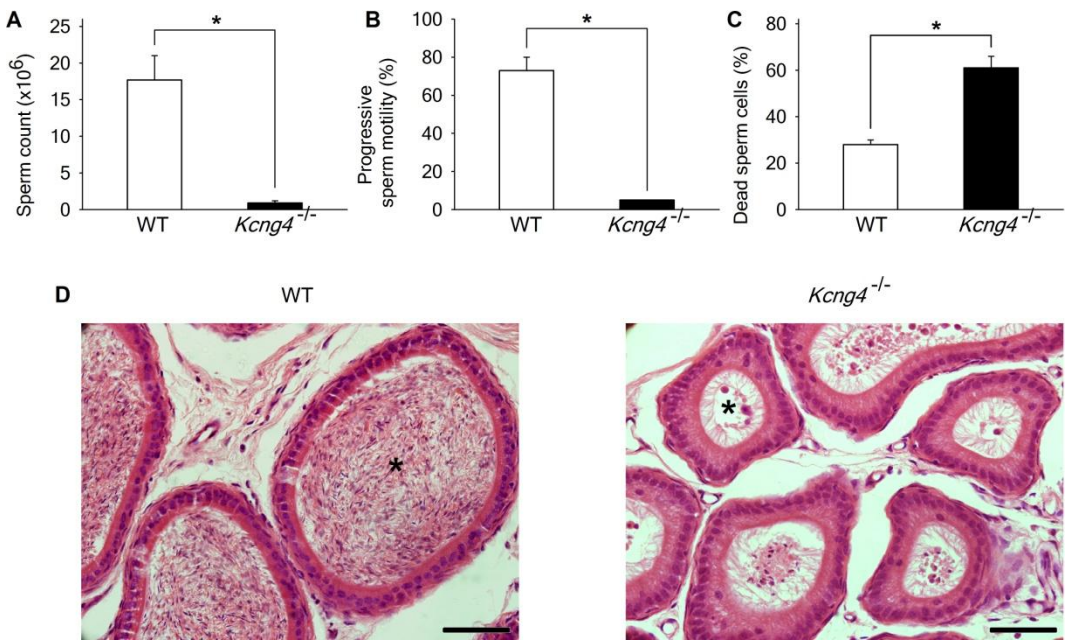

Figure 2: Comparison of cauda epididymal spermatozoa from WT and *Kcng4*$^{-/-}$ mice. Number of spermatozoa (A), the progressive sperm motility (B), and the number of dead spermatozoa (C) detected in the semen isolated from the caudae epididymides of WT and *Kcng4*$^{-/-}$ mice (n = 3). The number of spermatozoa and progressive sperm motility in homozygous males were significantly decreased, whereas the number of dead sperm cells was significantly increased compared to WT (*, $P \leq 0.008$). (D) Representative haematoxylin and eosin-stained sections of the caudae epididymides from WT (left) and *Kcng4*$^{-/-}$ (right) mice. The number of spermatozoa in the lumen of the epididymal tubules from *Kcng4*$^{-/-}$ males was heavily reduced compared to that of WT mice. The lumen of the tubules is indicated with an asterisk. Scale bars, 50 µm.

Spermatozoa of *Kcng4*$^{-/-}$ mice display an aberrant morphology

To further characterize the few spermatozoa that are produced by *Kcng4*$^{-/-}$ males, we compared the morphology of WT (Fig. 3A) and *Kcng4*$^{-/-}$ spermatozoa (Fig. 3B). Several parameters were scored including the presence of protoplasmic droplets and morphological abnormalities (Fig. 3C-H, Table 2). Protoplasmic droplets are remnants of the cytoplasm that is shed off during spermiogenesis and they migrate from the head (proximal droplet (Fig. 3D)) towards the end of the midpiece (distal droplet (Fig. 3C)) during transit of the sperm cells through the epididymis (8). Significantly fewer ($P < 0.001$) distal droplets were observed on *Kcng4*$^{-/-}$ spermatozoa (Table 2), suggesting that the epididymal maturation of *Kcng4*$^{-/-}$ spermatozoa is affected. Observed morphological abnormalities were categorized into head (Fig. 3D-H), midpiece (Fig. 3E), and tail (Fig. 3F) abnormalities. Although the presence of midpiece abnormalities was significantly higher in *Kcng4*$^{-/-}$ semen than in WT semen ($P < 0.001$) (Table 2), the most consistent difference between WT and *Kcng4*$^{-/-}$ spermatozoa was the morphology of the head: in WT mice 92.8 ± 0.5% of the spermatozoa had a normal falciform head (Fig. 3A, C), whereas almost no spermatozoa with a normal head shape were observed from *Kcng4*$^{-/-}$ mice (0.5 ± 0.3%) ($P < 0.001$) (Table 2). Although the specific shape of the head from *Kcng4*$^{-/-}$ spermatozoa differed between individual cells (Fig 3D-H), they all appeared smaller compared to the heads of WT spermatozoa. Indeed, the head area decreased significantly ($P < 0.001$) from 23.7 ± 0.2 μm^2 in WT (n = 60) to 16.4 ± 0.5 μm^2 in *Kcng4*$^{-/-}$ spermatozoa (n = 58) (Fig. 3I). In addition, the sperm tail length of *Kcng4*$^{-/-}$ spermatozoa (101.5 ± 2.0 μm, n = 58) was significantly smaller ($P < 0.001$) than that of WT spermatozoa (115.2 ± 0.3 μm, n = 60) (Fig. 3J). These results indicated that *Kcng4*$^{-/-}$ males are unable to produce normal mature spermatozoa, suggesting that spermatogenesis proceeds abnormally.

Table 2: Morphological characteristics of WT and *Kcng4*$^{-/-}$ spermatozoa.

Genotype	Protoplasmic droplets		Morphological abnormalities		
	Proximal	Distal	Head	Midpiece	Tail
WT	0.8 ± 0.3	14.4 ± 0.8	7.2 ± 0.5	9.3 ± 1.0	3.3 ± 0.8
Kcng4$^{-/-}$	0.8 ± 0.2	2.8 ± 0.6*	99.5 ± 0.3*	25.0 ± 0.9*	5 ± 0.6

The characteristics presented in this table were determined by scoring 200 sperm cells per mouse and are presented as a percentage of the total sperm population (n = 3 for each genotype). Statistical significance is indicated with an asterisk ($P < 0.001$).

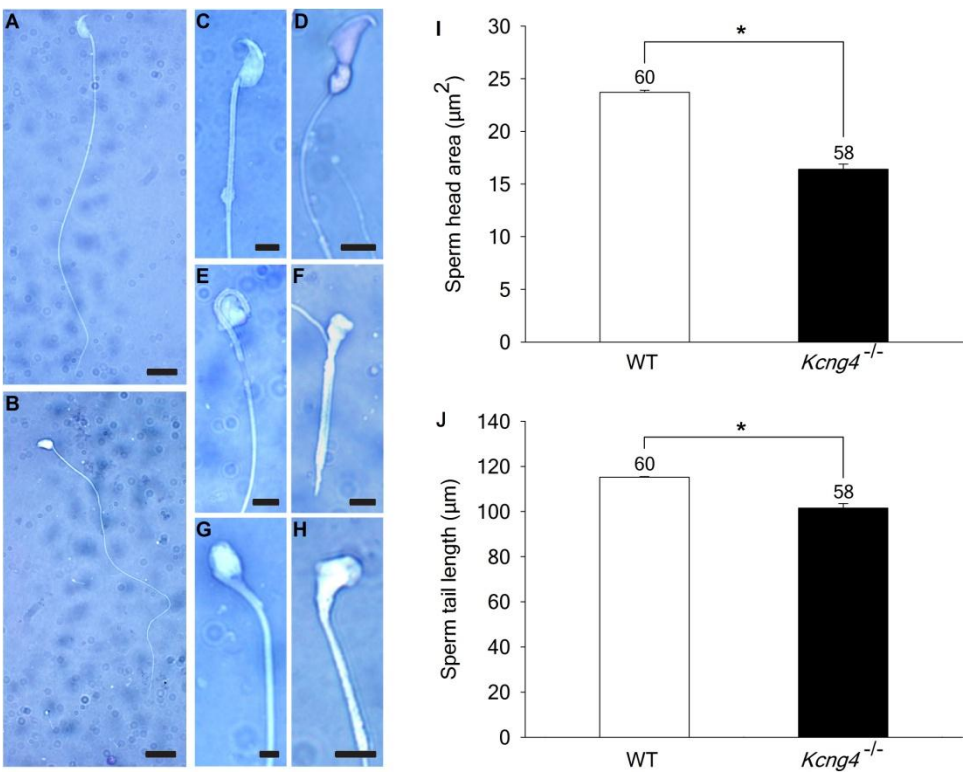

Figure 3: Morphological comparison of WT and *Kcng4*$^{-/-}$ spermatozoa. Representative images of a WT (A) and a *Kcng4*$^{-/-}$ (B) spermatozoon stained with eosin-nigrosin (scale bars, 5 µm) as well as enlarged pictures of a WT sperm cell with (C) a normal head and a distal protoplasmic droplet, and of *Kcng4*$^{-/-}$ sperm cells with (D) an abnormal head and a distal protoplasmic droplet, (E) an abnormal head and an abnormal midpiece, (F) an abnormal head and an abnormal tail, (G, H) an abnormal head (scale bars, 2 µm). Note that all *Kcng4*$^{-/-}$ spermatozoa have an abnormal shaped sperm head. The sperm head area (I) and sperm tail length (J) were significantly decreased in *Kcng4*$^{-/-}$ spermatozoa compared to WT spermatozoa (*, $P < 0.001$). The numbers above every bar plot indicate the number of cells analyzed.

The deletion of *Kcng4* causes abnormalities in the post-meiotic stages of spermatogenesis

To gain better insights into the origin of the reduced number of *Kcng4*$^{-/-}$ spermatozoa and morphological abnormalities, we compared H&E- and PAS-stained sections of WT and *Kcng4*$^{-/-}$ testicular tissue. The first stages of spermatogenesis appeared to proceed normally in *Kcng4*$^{-/-}$ testes; we observed that spermatogonia, spermatocytes, round spermatids, and Sertoli cells were equally present in WT (Fig. 4A-D) and *Kcng4*$^{-/-}$ testes (Fig. 4E-H), and that the morphology of these cell types was similar in both genotypes. In contrast, the differentiation of round spermatids into elongated spermatids appeared to be affected; a severe reduction of elongated spermatids could be observed in a large fraction of the seminiferous tubules from *Kcng4*$^{-/-}$ testes (Fig. 4E-H) compared to those from WT testes (Fig. 4A-D). Furthermore, the morphology of *Kcng4*$^{-/-}$ elongated spermatids (Fig. 4F, H) was abnormal compared to that in WT mice (Fig. 3B,D). These observations suggested that the targeted deletion of Kv6.4 affects the post-meiotic stages of spermatogenesis, resulting in a very low sperm concentration and morphologically abnormal spermatozoa.

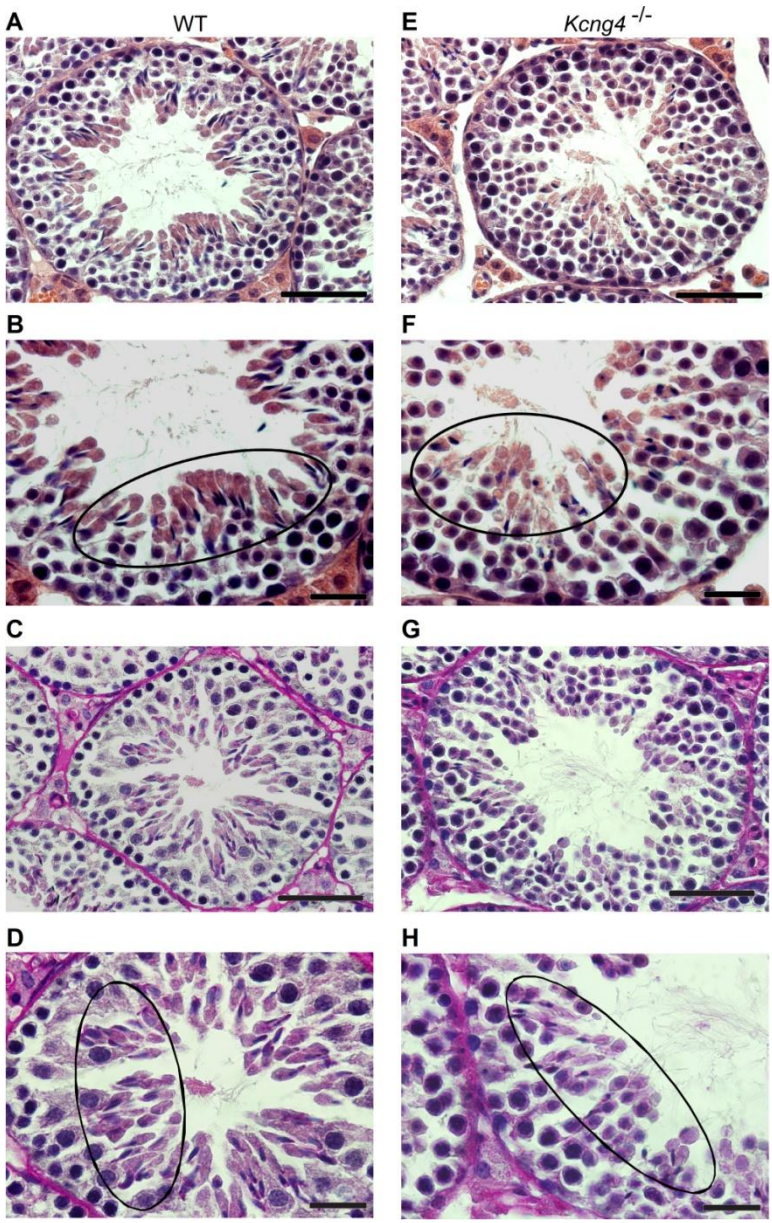

Fig. 4: Spermiogenesis proceeds abnormally in *Kcng4*$^{-/-}$ mice. Representative haematoxylin and eosin-stained (A, B, E, F) and PAS-stained (C, D, G, H) sections of testicular tissue from WT (A-D) and *Kcng4*$^{-/-}$ (E-H) mice. Spermatogonia, spermatocytes, round spermatids, and Sertoli cells were equally present and morphologically similar in WT and *Kcng4*$^{-/-}$ tubules, whereas a severe reduction of elongated spermatids could be observed (E, G) in *Kcng4*$^{-/-}$ males compared to WT males (A, C). In addition, the morphology of the elongated spermatids, of which a representative fraction is highlighted by the circular area, was abnormal in *Kcng4*$^{-/-}$ males (F, H) compared to that of WT males (B, D). Images from panels (B), (D), (F), and (H) are magnifications of the images from panel (A), (C), (E), and panel (G), respectively. Scale bars (A, C, E, G), 50 µm. Scale bars (B, D, F, H), 20 µm.

Discussion

Since the first detection of Kv currents in spermatogenic cells, it has been postulated that Kv channels contribute to the regulation of spermatogenesis (17). Although several studies have identified the expression of different Kv subunits including Kv1.1, Kv1.2, Kv1.3, Kv3.1, and Kv7.1 subunits in the seminiferous tubules of rodents (11; 15; 33), their specific contribution to spermatogenesis regulation remains largely unknown. In this study, we demonstrated the expression of the Kv6.4 subunit in testis (Fig. 1A) where its presence is needed for normal testicular function since the targeted deletion of Kv6.4 in a mouse model causes male sterility.

Kcng4$^{-/-}$ males were sterile due to reduced sperm concentration (oligozoospermia) (Fig. 2A), absence of motile spermatozoa (asthenozoospermia) (Fig. 2B), and altered sperm morphology (teratozoospermia) (Fig. 3A-J). This phenotype is designated as oligoasthenoteratozoospermia (OAT), which has been shown to be accompanied by defects in spermiogenesis and by enhanced spermatogenic cell apoptosis (14; 35; 36). H&E and PAS examination of *Kcng4*$^{-/-}$ testicular tissue (Fig. 4A-H) supported that OAT in our mouse model is caused by similar defects; the first stages of spermatogenesis in WT and *Kcng4*$^{-/-}$ testes were similar whereas in the post-meiotic stages of *Kcng4*$^{-/-}$ testes a severe reduction of elongated spermatids could be observed (Fig. 4A-H). This suggests that the proliferation of spermatogonia and subsequent meiosis were not impaired and, therefore, the oligozoospermia of *Kcng4*$^{-/-}$ mice was probably not due to decreased proliferation of spermatogenic cells, but rather due to enhanced apoptosis of post-meiotic spermatogenic cells. Moreover, elongated spermatids from *Kcng4*$^{-/-}$ mice had an abnormal morphology (Fig. 4A-H), which indicates that the aberrant morphology of *Kcng4*$^{-/-}$ spermatozoa was due to defects in spermiogenesis.

During spermiogenesis, spermatids differentiate into spermatozoa through drastic morphological changes, including formation of the acrosome and flagellum, rearrangement of the mitochondria, nuclear condensation, and loss of

cytoplasm from the sperm head (for review see (26; 40)). Since the morphological abnormalities of *Kcng4*$^{-/-}$ spermatozoa were mainly characterized by a decreased head size (Fig. 3I) and a shortened tail (Fig. 3J), one of the possible causes of these abnormalities may be excessive cytoplasm loss during spermiogenesis. Kv channels have been shown to be involved in osmotic cell volume regulation and particularly in the regulation of cell volume decrease ((3; 10; 22; 25; 37; 41). Therefore, Kv6.4 may be involved in regulating cytoplasm loss during the differentiation of the spermatids into spermatozoa. Interestingly, Gong et al. (2002) showed an increase in Kv current during the course of spermatogenesis. Furthermore, the threshold for activation of this Kv current was approximately -40 mV, which is consistent with the threshold for activation of Kv2.1/Kv6.4 heterotetramers (27). Taken together this may suggest that Kv6.4 subunits play an important role in the regulation of spermiogenesis.

Sertoli cells are known to secrete a K^+-rich fluid into the lumen of the seminiferous tubules, thus creating a microenvironment in which spermiogenesis takes place (12; 34). Because the regulation of cell volume decrease depends heavily on the osmolarities of both the intra- and extracellular solutions (for review see (38)), our results could also be attributed to changes in the luminal fluid composition. Interestingly, it has been demonstrated that maintaining this ionic composition in the lumen is indeed crucial for male fecundity. For example, deficiency of the *Slc12a2* gene, which encodes for an ion transporter (Na^+-K^+-Cl^- co-transporter isoform 1 (NKCC1)) involved in controlling this ionic environment, causes male infertility in mice (28). However, since NKCC1 only transports K^+ from the interstitial fluid into the Sertoli cell, a role for unknown apical K^+ channels has been postulated in maintaining the luminar fluid composition (28). This supports a potential role for Kv6.4 during K^+-secretion into the lumen of the seminiferous tubules, although other K^+ channels and transporters could be involved.

In conclusion, we propose that the targeted deletion of the Kv6.4 subunit in a transgenic mouse model causes oligoasthenoteratozoospermia, which supports an important role for the Kv6.4 subunit in the regulation of

spermiogenesis. Furthermore, it has been demonstrated that drugs can modulate Kv2.1/Kv6.4 heterotetramers differently compared to Kv2.1 homotetramers and other Kv2.1/KvS heterotetramers (32). Therefore the role of Kv6.4 in the regulation of spermiogenesis makes Kv2.1/Kv6.4 channels a potentially interesting pharmacological target for the development of non-hormonal male contraceptives.

Acknowledgements

We thank Abbi Van Tilborg of the Laboratory for Molecular Biophysics, Physiology and Pharmacology, Silke Andries of the Laboratory of Veterinary Physiology and Biochemistry, and Sofie Thys of the Laboratory of Cell Biology and Histology for their excellent technical assistance and also Sara Valckx of the Laboratory of Veterinary Physiology and Biochemistry for her excellent guidance in sperm analysis.

This work was supported by the section cardiovascular research of the Sheid-van Bogaert foundation, the postdoctoral fellowships FWO−1291913N and FWO-1291916N to EB, and the grants G.0449.11N & G.0443.12N to DJS from the Research Foundation – Flanders (FWO).

References

1. **Bavister BD, Leibfried ML and Lieberman G**. Development of preimplantation embryos of the golden hamster in a defined culture medium. Biol Reprod 28: 235-247, 1983.
2. **Blaine JT and Ribera AB**. Heteromultimeric potassium channels formed by members of the Kv2 subfamily. J Neurosci 18: 9585-9593, 1998.
3. **Bobak N, Bittner S, Andronic J, Hartmann S, Muhlpfordt F, Schneider-Hohendorf T, Wolf K, Schmelter C, Gobel K, Meuth P, Zimmermann H, Doring F, Wischmeyer E, Budde T, Wiendl H, Meuth SG and Sukhorukov VL**. Volume regulation of murine T lymphocytes relies on voltage-dependent and two-pore domain potassium channels. Biochim Biophys Acta 1808: 2036-2044, 2011.
4. **Bocksteins E**. Kv5, Kv6, Kv8, and Kv9 subunits: No simple silent bystanders. J Gen Physiol 147(2): 105-125, 2016.
5. **Bocksteins E and Snyders DJ**. Electrically silent Kv subunits: their molecular and functional characteristics. Physiology (Bethesda) 27: 73-84, 2012.
6. **Chandy KG, DeCoursey TE, Cahalan MD, McLaughlin C and Gupta S**. Voltage-gated potassium channels are required for human T lymphocyte activation. J Exp Med 160: 369-385, 1984.
7. **Chen Y, Xu J, Li Y and Han X**. Decline of sperm quality and testicular function in male mice during chronic low-dose exposure to microcystin-LR. Reprod Toxicol 31: 551-557, 2011.
8. **Cooper T.G.** The epididymis, cytoplasmic droplets and male fertility. Asian J Androl 13: 130-138, 2011.
9. **DeCoursey TE, Chandy KG, Gupta S and Cahalan MD**. Voltage-gated K^+ channels in human T lymphocytes: a role in mitogenesis? Nature 307: 465-468, 1984.

10. **Felipe A, Snyders DJ, Deal KK and Tamkun MM**. Influence of cloned voltage-gated K^+ channel expression on alanine transport, Rb^+ uptake, and cell volume. Am J Physiol 265: C1230-C1238, 1993.
11. **Felix R, Serrano CJ, Trevino CL, Munoz-Garay C, Bravo A, Navarro A, Pacheco J, Tsutsumi V and Darszon A**. Identification of distinct K^+ channels in mouse spermatogenic cells and sperm. Zygote 10: 183-188, 2002.
12. **Fisher D**. New light shed on fluid formation in the seminiferous tubules of the rat. J Physiol 542: 445-452, 2002.
13. **Frech GC, VanDongen AM, Schuster G, Brown AM and Joho RH**. A novel potassium channel with delayed rectifier properties isolated from rat brain by expression cloning. Nature 340: 642-645, 1989.
14. **Fujita E, Tanabe Y, Hirose T, Aurrand-Lions M, Kasahara T, Imhof BA, Ohno S and Momoi T**. Loss of partitioning-defective-3/isotype-specific interacting protein (par-3/ASIP) in the elongating spermatid of *RA175* (IGSF4A/SynCAM)-deficient mice. Am J Pathol 171: 1800-1810, 2007.
15. **Gong XD, Li JC, Leung GP, Cheung KH and Wong PY**. A BK(Ca) to K(v) switch during spermatogenesis in the rat seminiferous tubules. Biol Reprod 67: 46-54, 2002.
16. **Gutman GA, Chandy KG, Grissmer S, Lazdunski M, McKinnon D, Pardo LA, Robertson GA, Rudy B, Sanguinetti MC, Stuhmer W and Wang X**. International Union of Pharmacology. LIII. Nomenclature and molecular relationships of voltage-gated potassium channels. Pharmacol Rev 57: 473-508, 2005.
17. **Hagiwara S and Kawa K**. Calcium and potassium currents in spermatogenic cells dissociated from rat seminiferous tubules. J Physiol 356: 135-149, 1984.
18. **Hai Y, Hou J, Liu Y, Liu Y, Yang H, Li Z and He Z**. The roles and regulation of Sertoli cells in fate determinations of spermatogonial stem cells and spermatogenesis. Semin Cell Dev Biol 29: 66-75, 2014.

19. **Hemmerlein B, Weseloh RM, Mello de QF, Knotgen H, Sanchez A, Rubio ME, Martin S, Schliephacke T, Jenke M, Heinz JR, Stuhmer W and Pardo LA**. Overexpression of *Eag1* potassium channels in clinical tumours. Mol Cancer 5: 41, 2006.
20. **Hwang PM, Glatt CE, Bredt DS, Yellen G and Snyder SH**. A novel K^+ channel with unique localizations in mammalian brain: molecular cloning and characterization. Neuron 8: 473-481, 1992.
21. **Lafreniere RG and Rouleau GA**. Identification of novel genes involved in migraine. Headache 52 Suppl 2: 107-110, 2012.
22. **Lock H and Valverde MA**. Contribution of the IsK (MinK) potassium channel subunit to regulatory volume decrease in murine tracheal epithelial cells. J Biol Chem 275: 34849-34852, 2000.
23. **Miguel-Velado E, Perez-Carretero FD, Colinas O, Cidad P, Heras M, Lopez-Lopez JR and Perez-Garcia MT**. Cell cycle-dependent expression of Kv3.4 channels modulates proliferation of human uterine artery smooth muscle cells. Cardiovasc Res 86: 383-391, 2010.
24. **Muller D, Cherukuri P, Henningfeld K, Poh CH, Wittler L, Grote P, Schluter O, Schmidt J, Laborda J, Bauer SR, Brownstone RM and Marquardt T**. Dlk1 promotes a fast motor neuron biophysical signature required for peak force execution. Science 343: 1264-1266, 2014.
25. **Neprasova H, Anderova M, Petrik D, Vargova L, Kubinova S, Chvatal A and Sykova E**. High extracellular K^+ evokes changes in voltage-dependent K^+ and Na^+ currents and volume regulation in astrocytes. Pflugers Arch 453: 839-849, 2007.
26. **O'Donnell L**. Mechanisms of spermiogenesis and spermiation and how they are disturbed. Spermatogenesis 4: e979623, 2014.
27. **Ottschytsch N, Raes A, Van Hoorick D and Snyders DJ**. Obligatory heterotetramerization of three previously uncharacterized Kv channel alpha-subunits identified in the human genome. Proc Natl Acad Sci U S A 99: 7986-7991, 2002.

28. **Pace AJ, Lee E, Athirakul K, Coffman TM, O'Brien DA and Koller BH**. Failure of spermatogenesis in mouse lines deficient in the Na^+-K^+-$2Cl^-$ co-transporter. J Clin Invest 105: 441-450, 2000.
29. **Pardo LA**. Voltage-gated potassium channels in cell proliferation. Physiology (Bethesda) 19: 285-292, 2004.
30. **Pardo LA, del Camino D, Sanchez A, Alves F, Bruggemann A, Beckh S and Stuhmer W**. Oncogenic potential of EAG K^+ channels. EMBO J 18: 5540-5547, 1999.
31. **Rato L, Socorro S, Cavaco JE and Oliveira PF**. Tubular fluid secretion in the seminiferous epithelium: ion transporters and aquaporins in Sertoli cells. J Membr Biol 236: 215-224, 2010.
32. **Stas JI, Bocksteins E, Labro AJ and Snyders DJ**. Modulation of Closed-State Inactivation in Kv2.1/Kv6.4 Heterotetramers as Mechanism for 4-AP Induced Potentiation. PLoS ONE 10: e0141349, 2015.
33. **Tsevi I, Vicente R, Grande M, Lopez-Iglesias C, Figueras A, Capella G, Condom E and Felipe A**. KCNQ1/KCNE1 channels during germ-cell differentiation in the rat: expression associated with testis pathologies. J Cell Physiol 202: 400-410, 2005.
34. **Tuck RR, Waites GM, Young JA and Setchell BP**. Compoition of fluid secreted by the seminiferous tubules of the rat collected by catheterization and micropuncture technics. J Reprod Fertil 21: 367-368, 1970.
35. **Udagawa O, Ito C, Ogonuki N, Sato H, Lee S, Tripvanuntakul P, Ichi I, Uchida Y, Nishimura T, Murakami M, Ogura A, Inoue T, Toshimori K and Arai H**. Oligo-astheno-teratozoospermia in mice lacking ORP4, a sterol-binding protein in the OSBP-related protein family. Genes Cells 19: 13-27, 2014.
36. **van der Weyden L, Arends MJ, Chausiaux OE, Ellis PJ, Lange UC, Surani MA, Affara N, Murakami Y, Adams DJ and Bradley A**. Loss of *TSLC1* causes male infertility due to a defect at the spermatid stage of spermatogenesis. Mol Cell Biol 26: 3595-3609, 2006.

37. **vanTol BL, Missan S, Crack J, Moser S, Baldridge WH, Linsdell P and Cowley EA**. Contribution of KCNQ1 to the regulatory volume decrease in the human mammary epithelial cell line MCF-7. Am J Physiol Cell Physiol 293: C1010-C1019, 2007.
38. **Wehner F**. Cell volume-regulated cation channels. Contrib Nephrol 152: 25-53, 2006.
39. **Xiao X, Mruk DD, Wong CK and Cheng CY**. Germ cell transport across the seminiferous epithelium during spermatogenesis. Physiology (Bethesda) 29: 286-298, 2014.
40. **Yan W**. Male infertility caused by spermiogenic defects: lessons from gene knockouts. Mol Cell Endocrinol 306: 24-32, 2009.
41. **Yeung CH and Cooper TG**. Potassium channels involved in human sperm volume regulation--quantitative studies at the protein and mRNA levels. Mol Reprod Dev 75: 659-668, 2008.

Electronic Supplementary Material

to

Targeted deletion of the Kv6.4 subunit causes male sterility due to disturbed spermiogenesis

Glenn Regnier[1], Elke Bocksteins[1], Waleed F. Marei[2,3], Isabel Pintelon[4], Jean-Pierre Timmermans[4], Jo L.M.R. Leroy[2], Dirk J. Snyders[1]

Reprod Fertil Dev. (accepted)

[1]Laboratory of Molecular Biophysics, Physiology and Pharmacology, Department of Biomedical Sciences, University of Antwerp, CDE, Universiteitsplein 1, 2610 Antwerpen, Belgium

[2]Laboratory of Veterinary Physiology and Biochemistry, Department of Veterinary Sciences, University of Antwerp, CDE, Universiteitsplein 1, 2610 Antwerpen, Belgium

[3]Department of Theriogenology, Faculty of Veterinary Medicine, Cairo University, 12211 Giza, Egypt

[4]Laboratory of Cell Biology and Histology, Department of Veterinary Sciences, University of Antwerp, CGB, Groenenborgerlaan 171, 2020 Antwerpen, Belgium.

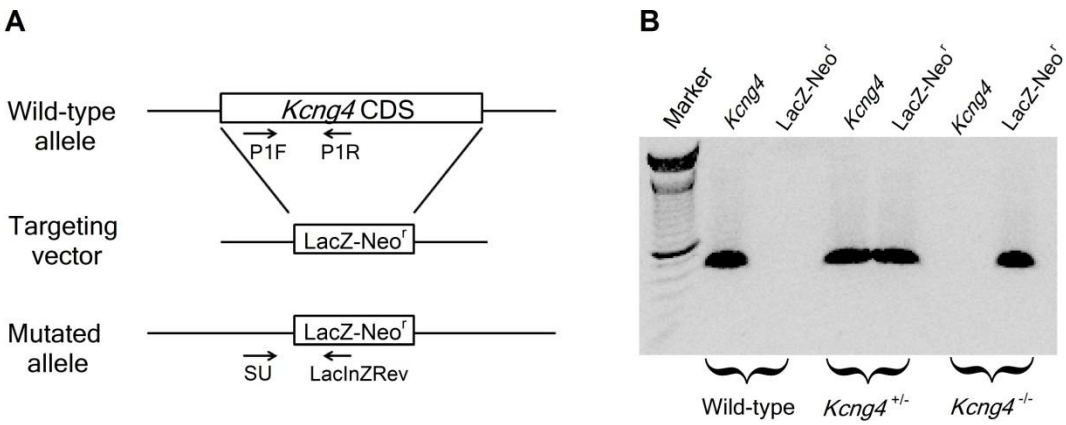

Figure S1: Targeted deletion of *Kcng4*. (A) Schematic overview of the gene targeting strategy. The *Kcng4* coding DNA sequence (CDS) was replaced with the LacZ-Neo^r cassette by homologous recombination between the targeting vector and the WT allele. The presence of the WT allele was examined with genotyping using the P1F and P1R primer pair whereas the presence of the cassette was examined using the SU and LacInZRev primer pair. (B) Genotyping of WT, *Kcng4*$^{+/-}$, and *Kcng4*$^{-/-}$ mice confirmed the replacement of the *Kcng4* CDS with the LacZ-Neo^r cassette.

Chapter 5

General Discussion

The silent Kv subunits form an intriguing and substantial part of the *Shaker*-related Kv gene family. Due to their contribution to a variety of (patho)physiological processes, a promising potential as pharmacological targets has been proposed for these subunits. Nevertheless, many questions about the KvS subunits remain and resolving these would underscore their therapeutic potential. In this study, we elucidated some of these questions by gaining insight into both the stoichiometry of Kv2/KvS heterotetramers and the contribution of these channel complexes to testicular function and neuronal maturation.

Composition of Kv2/KvS heterotetramers

Within the Kv1-Kv4 subfamilies, heterotetramers are supposed to assemble preferentially with a 2:2 stoichiometry (38). It has been suggested that the composition of Kv2/KvS heterotetramers differs from this 2:2 stoichiometry since for Kv2.1/Kv9.3 channels a 3:1 stoichiometry has been proposed (18). However, we demonstrated that – at least in the case of Kv2.1/Kv6.4 channels – Kv2/KvS heterotetramers can be functional in both of these stoichiometric configurations with the restriction that the KvS subunits cannot be positioned side by side in the channel complex (chapter 2). In our experiments, we used concatemers to constrain the stoichiometry of the Kv2.1/Kv6.4 heterotetramers, which raises the question whether these two functional configurations are also formed by the corresponding monomers. Yet, it has been demonstrated that the stoichiometry of several heterotetrameric Kv channels is variable and affected by the expression level of the subunits involved (19; 20; 24; 32; 44), suggesting that Kv2/KvS heterotetramers could indeed assemble with variable stoichiometries. This raises the possibility that cells can regulate the stoichiometry of Kv2/KvS channels by varying the expression level of both the Kv2 and the KvS subunits. Nevertheless, at this point it cannot be completely ruled out that the stoichiometry of Kv2/KvS channels is fixed at one of these two functional configurations.

Despite the fact that both the N-terminal fragments of KvS subunits and their full length proteins are incompatible (8), our results demonstrated that two

silent Kv subunits can exist within the same channel complex without affecting its functionality (chapter 2), which may have a few interesting implications. *In vivo*, several KvS subunits are expressed in the same tissue (6) and it may therefore be possible that Kv2/KvS channel complexes containing two different KvS subunits are formed. Consequently, these tripartite complexes may have specific physiological functions as it can be expected that they would possess unique biophysical and biochemical properties. On the other hand, the above properties may also be affected by the stoichiometric configuration of Kv2/KvS channels containing only one KvS member. Therefore, in order to use Kv2/KvS channels as therapeutic targets, it will be important to unravel the composition and stoichiometry of Kv2/KvS heterotetramers *in vivo* as the pharmacological properties of Kv channels are affected by these two features (1; 2; 23; 31; 44; 45).

Contribution of Kv2 and KvS subunits to the postnatal maturation of DRG neurons

Dorsal root ganglia (DRGs) contain the cell bodies of sensory neurons that are involved in the sensations of touch, pressure, vibration, limb position, heat, cold, and pain. They transmit sensory information to the dorsal horn of the spinal cord, where it is processed and relayed to the brain. Based on their functional, anatomical, and neurochemical properties, DRG neurons are subdivided into several categories. It has been demonstrated that the differential expression of ion channels accounts for this functional diversity (17) and that although the diversification of sensory neuron types already starts during embryonic development, this continues well into the adult life (16). For example, it was demonstrated that in rat, reflexes elicited by mustard oil are not present until P10 due to the lack of expression of the transient receptor potential (TRP) cation channel TRP1A in new-born rats (13; 16).

It is thought that hyperexcitability of DRG neurons is a major issue in pain transmission. Due to their involvement in neuronal excitability, Kv channels are

therefore regarded as key targets in the development of future pain treatments (33; 34). Consequently, it is important to know how Kv channel expression changes during postnatal development in these neurons in order to assess how postnatal age would affect the analgesic action of potential drugs targeting these Kv channels. Kv2.1 and Kv2.2 are amply expressed in DRG neuron cell bodies of all sizes where they contribute to the regulation of the neuronal firing frequency (36). Although Kv2-containing channels form the major component of the delayed rectifier K^+ current in DRG neurons (7), it is not known if they are involved in the postnatal maturation of these neurons. We demonstrated that during the first month of postnatal development, the expression of Kv2.2 decreases in mouse DRG neurons, whereas the expression of Kv2.1 remains similar (chapter 3), suggesting that Kv2.2 plays a role in the maturation of DRG neurons. Since several sensory neuron types only emerge after birth (16), Kv2.2 may therefore directly be involved in the postnatal diversification process of DRG neurons. On the other hand, it is also possible that some of the sensory neuron types that emerge during development, express less Kv2.2 than the neurons they are derived from and thus the Kv2.2 downregulation is rather a consequence of the neonatal maturation of sensory neurons.

Several KvS subunits are expressed in DRG neurons where they form Kv2/KvS heterotetramers that contribute to the delayed rectifier K^+ current (7), but how the expression of these KvS subunits evolves during the postnatal development of these neurons is not known. We demonstrated that during the postnatal development of mouse DRG neurons, the Kv9.1 mRNA levels increase significantly, whereas in the case of the Kv6.3, Kv8.1, and Kv9.1 subunits smaller fluctuations in mRNA levels were observed (chapter 3). It is possible that each sensory neuron type expresses a specific subset of KvS subunits which is well supported by the observation that in rat, Kv9.1 is expressed in myelinated DRG neurons but absent in small unmyelinated DRG neurons (35). Consequently, the observed changes in KvS mRNA levels could be related to the emergence of sensory neuron types during development.

The role of Kv6.4 in testicular function

Although Kv2.1 and several KvS subunits are expressed in human testis, nothing is known about their contribution to the physiology of this tissue (6). We demonstrated that the Kv6.4 subunit plays an important role in testicular function since male *Kcng4*-null mice suffer from oligoasthenoteratozoospermia (OAT) (chapter 4). So how does the absence of Kv6.4 induces this phenotype? In our mouse model, sperm cell morphology was characterized by a severe reduction of the sperm head area and the sperm tail length indicating that spermatids had suffered from excessive loss of cytoplasm during spermiogenesis (chapter 4). This suggests involvement of Kv6.4 in the regulation of the cell volume changes that occur during this process. Therefore, conductive Kv2.1/Kv6.4 heterotetramers are presumably present in the testis since cell volume regulation is accompanied by ion exchange across the membrane mediated by several transporters and ion channels including Kv channels (41). Moreover, this hypothesis can be supported by several reports that demonstrate the involvement of Kv channels in sperm volume regulation (3; 4; 42).

Kv6.4 subunits downregulate the Kv2.1 current density and induce an approximately 40 mV hyperpolarized shift in the voltage dependence of inactivation. Therefore, if Kv2.1/Kv6.4 channels contribute to testicular function in their conductive form, the absence of Kv6.4 subunit would presumably lead to an increased Kv2.1 current density (27). Consequently, several mechanisms may explain the OAT phenotype.

1) In epithelial cells of the inner ear, Kv7.1 channels have a K^+-secreting role crucial for normal inner ear function which is well-illustrated by several known mutations in the Kv7.1 subunit that cause deafness (9; 26). Similarly, Kv2.1/Kv6.4 heterotetramers may be expressed in Sertoli cells where they could contribute to K^+-secretion into the luminal fluid of the seminiferous tubules. This fluid is K^+-rich and hyperosmotic compared to serum and, therefore, provides an extracellular environment for the spermatids that supports cell volume decrease (12; 39). It has been demonstrated that maintaining the osmolarity of the seminal fluid is

important for normal testicular function since increased seminal osmolarity causes asthenozoospermia in human patients (30). Furthermore, the importance of normal fluid secretion has been highlighted by several studies with knock-out mice which showed that targeted deletion of ion channels and transporters involved in seminal fluid secretion, were associated with male sterility (29). Consequently, Kv2.1/Kv6.4 channels may be involved in the K^+-secreting function of Sertoli cells whereby the absence of the Kv6.4 subunit causes changes in the osmolarity of the seminal fluid resulting in male sterility.

2) Kv2.1/Kv6.4 heterotetramers could also be expressed in spermatogenic cells where they may contribute to the regulation of the cell volume decrease of the round spermatids. When placed in a hypo- or hyperosmotic environment, cells respond to volume changes by activating several ion channels and transporters in order to regulate the extent of the cell volume change. It has been demonstrated that several Kv channels are involved in this process (5; 10; 21; 25; 40; 43) indicating that Kv2.1/Kv6.4 heterotetramers could have a similar role in the cell volume regulation of spermatids. Therefore, deletion of the Kv6.4 subunits may disturb this regulatory process resulting in excessive cytoplasm loss from spermatids. On the other hand, Kv2.1/Kv6.4 channels may directly be responsible for inducing the cell volume decrease since a cellular K^+ loss could result in cell shrinkage. Interestingly, cell volume decrease due to cytoplasmic K^+ loss has also been observed during neuronal apoptosis whereby an increased cell surface expression of the Kv2.1 channel results in an enhanced K^+ efflux that initiates apoptosis (28). Therefore, as it could be expected that the absence of Kv6.4 leads to an increased Kv2.1 current density (27), this mechanism may explain both the excessive loss of cytoplasm we observed during spermiogenesis and the severe reduction of sperm cell count in our mouse model.

3) In non-excitable cells, ion channels often influence the membrane potential, thereby regulating the signalling mechanisms involved in various physiological processes. Similarly, Kv2.1/Kv6.4 heterotetramers may influence the signalling mechanisms that regulate spermiogenesis by affecting the

membrane potential, together with several other ion channels that have been detected in spermatogenic cells (11; 14; 15; 37). In this case, deletion of Kv6.4 could disturb the regulation of spermiogenesis which may result in the OAT phenotype.

In addition to the functions of Kv6.4 in testicular physiology suggested above, several other mechanisms may explain the OAT phenotype in the *Kcng4*-null mice. For example, in testis, Kv6.4 subunits may have a nonconductive function that has not yet been described. Therefore, more research will be needed to unravel the exact function of Kv6.4 in testicular tissue. Nevertheless, our results show clearly that Kv6.4 is indispensable for normal testicular function which makes it a potentially interesting pharmacological target for the development of non-hormonal male contraceptives.

Future perspectives

In this study, we demonstrated the variable nature of Kv2/KvS channel stoichiometry and gained insights in the role of KvS subunits in testicular function and neuronal maturation. However, our results raise several new questions that need to be resolved.

Composition of Kv2/KvS heterotetramers

Based on the functionality of Kv2.1/Kv6.4 heterotetramers with a 2:2 stoichiometry, we suggested the existence of Kv2/KvS heterotetramers containing two different KvS subunits which would add to the variety of Kv2 channel complexes *in vivo*. To investigate this intriguing possibility further, we will initially test whether Kv2/KvS channels with a 2:2 stoichiometry are indeed formed when using monomers. Therefore, we will use the single molecule fluorescence technique (22) to determine the most abundant Kv2.1/Kv6.4 stoichiometry by co-expressing GFP-tagged Kv6.4 and unlabelled Kv2.1 subunits and determining the number of photobleaching steps needed to reduce the fluorescent emission to the background signal. Thereafter, we will design new

Kv2/KvS concatemers containing two different KvS subunits and investigate if and how they function.

Contribution of Kv2 and KvS subunits to the postnatal maturation of DRG neurons

In DRG neurons, Kv2-containing channels play an important role in the regulation of the neuronal firing frequency by regulating the duration of action potential hyperpolarization (36). Since our results demonstrate that Kv2.2 is downregulated in DRG neurons during postnatal development, we will investigate the effect of this Kv2.2 downregulation on the neuronal firing pattern and action potential waveform in DRG neurons. Furthermore, since we believe that the observed developmental changes in Kv2 and KvS expression may be correlated to the diversification of sensory neuron types, it would be interesting to compare the expression pattern of the Kv2 and KvS subunits in DRG neurons at different postnatal ages using immunohistochemistry.

The role of Kv6.4 in testicular physiology

Here, we reported that Kv6.4 is indispensable for normal testicular function, but the exact function of Kv6.4 in testis needs to be investigated further. Since we expect that Kv6.4 plays a role in its conductive form, we will need to identify the cell type in which Kv6.4 is expressed and isolate the Kv2-containing current in these cells using ScTx. Thereafter, we will determine how the absence of Kv6.4 influences the Kv2-containing currents in these cells by identifying the differences between the ScTx-sensitive component of wild-type and *Kcng4*-null mice. Furthermore, we will determine the impact of these differences on the membrane potential and electrophysiological response of the Kv6.4 expressing cells in order to gain more insight in the mechanism by which the deletion of Kv6.4 causes male sterility.

References

1. **Al-Sabi A, Kaza SK, Dolly JO and Wang J**. Pharmacological characteristics of Kv1.1- and Kv1.2-containing channels are influenced by the stoichiometry and positioning of their alpha-subunits. Biochem J 454: 101-108, 2013.
2. **Al-Sabi A, Shamotienko O, Dhochartaigh SN, Muniyappa N, Le BM, Shaban H, Wang J, Sack JT and Dolly JO**. Arrangement of Kv1 alpha-subunits dictates sensitivity to tetraethylammonium. J Gen Physiol 136: 273-282, 2010.
3. **Barfield JP, Yeung CH and Cooper TG**. Characterization of potassium channels involved in volume regulation of human spermatozoa. Mol Hum Reprod 11: 891-897, 2005.
4. **Barfield JP, Yeung CH and Cooper TG**. The effects of putative K^+ channel blockers on volume regulation of murine spermatozoa. Biol Reprod 72: 1275-1281, 2005.
5. **Bobak N, Bittner S, Andronic J, Hartmann S, Muhlpfordt F, Schneider-Hohendorf T, Wolf K, Schmelter C, Gobel K, Meuth P, Zimmermann H, Doring F, Wischmeyer E, Budde T, Wiendl H, Meuth SG and Sukhorukov VL**. Volume regulation of murine T lymphocytes relies on voltage-dependent and two-pore domain potassium channels. Biochim Biophys Acta 1808: 2036-2044, 2011.
6. **Bocksteins E**. Kv5, Kv6, Kv8, and Kv9 subunits: No simple silent bystanders. J Gen Physiol 147(2): 105-125, 2016.
7. **Bocksteins E, Raes AL, Van de Vijver G, Bruyns T, Van Bogaert PP and Snyders DJ**. Kv2.1 and silent Kv subunits underlie the delayed rectifier K^+ current in cultured small mouse DRG neurons. Am J Physiol Cell Physiol 296: C1271-C1278, 2009.
8. **Bocksteins E and Snyders DJ**. Electrically silent Kv subunits: their molecular and functional characteristics. Physiology (Bethesda) 27: 73-84, 2012.

9. **Casimiro MC, Knollmann BC, Ebert SN, Vary JC, Jr., Greene AE, Franz MR, Grinberg A, Huang SP and Pfeifer K**. Targeted disruption of the *Kcnq1* gene produces a mouse model of Jervell and Lange-Nielsen Syndrome. Proc Natl Acad Sci U S A 98: 2526-2531, 2001.
10. **Felipe A, Snyders DJ, Deal KK and Tamkun MM**. Influence of cloned voltage-gated K^+ channel expression on alanine transport, Rb^+ uptake, and cell volume. Am J Physiol 265: C1230-C1238, 1993.
11. **Felix R, Serrano CJ, Trevino CL, Munoz-Garay C, Bravo A, Navarro A, Pacheco J, Tsutsumi V and Darszon A**. Identification of distinct K^+ channels in mouse spermatogenic cells and sperm. Zygote 10: 183-188, 2002.
12. **Fisher D**. New light shed on fluid formation in the seminiferous tubules of the rat. J Physiol 542: 445-452, 2002.
13. **Fitzgerald M and Gibson S**. The postnatal physiological and neurochemical development of peripheral sensory C fibres. Neurosci 13: 933-944, 1984.
14. **Gong XD, Li JC, Leung GP, Cheung KH and Wong PY**. A BK(Ca) to K(v) switch during spermatogenesis in the rat seminiferous tubules. Biol Reprod 67: 46-54, 2002.
15. **Hagiwara S and Kawa K**. Calcium and potassium currents in spermatogenic cells dissociated from rat seminiferous tubules. J Physiol 356: 135-149, 1984.
16. **Hjerling-Leffler J, Alqatari M, Ernfors P and Koltzenburg M**. Emergence of functional sensory subtypes as defined by transient receptor potential channel expression. J Neurosci 27: 2435-2443, 2007.
17. **Julius D and Basbaum AI**. Molecular mechanisms of nociception. Nature 413: 203-210, 2001.
18. **Kerschensteiner D, Soto F and Stocker M**. Fluorescence measurements reveal stoichiometry of K^+ channels formed by modulatory and delayed rectifier alpha-subunits. Proc Natl Acad Sci U S A 102: 6160-6165, 2005.

19. **Kitazawa M, Kubo Y and Nakajo K**. The Stoichiometry and Biophysical Properties of the Kv4 Potassium Channel Complex with K^+ Channel-interacting Protein (KChIP) Subunits Are Variable, Depending on the Relative Expression Level. J Biol Chem 289: 17597-17609, 2014.
20. **Kitazawa M, Kubo Y and Nakajo K**. Kv4.2 and Accessory Dipeptidyl Peptidase-like Protein 10 (DPP10) Subunit Preferentially Form a 4:2 (Kv4.2:DPP10) Channel Complex. J Biol Chem 290: 22724-22733, 2015.
21. **Lock H and Valverde MA**. Contribution of the IsK (MinK) potassium channel subunit to regulatory volume decrease in murine tracheal epithelial cells. J Biol Chem 275: 34849-34852, 2000.
22. **McGuire H, Aurousseau MR, Bowie D and Blunck R**. Automating single subunit counting of membrane proteins in mammalian cells. J Biol Chem 287: 35912-35921, 2012.
23. **Moreno-Dominguez A, Cidad P, Miguel-Velado E, Lopez-Lopez JR and Perez-Garcia MT**. *De novo* expression of Kv6.3 contributes to changes in vascular smooth muscle cell excitability in a hypertensive mice strain. J Physiol 587: 625-640, 2009.
24. **Nakajo K, Ulbrich MH, Kubo Y and Isacoff EY**. Stoichiometry of the KCNQ1-KCNE1 ion channel complex. Proc Natl Acad Sci U S A 107: 18862-18867, 2010.
25. **Neprasova H, Anderova M, Petrik D, Vargova L, Kubinova S, Chvatal A and Sykova E**. High extracellular K^+ evokes changes in voltage-dependent K^+ and Na^+ currents and volume regulation in astrocytes. Pflugers Arch 453: 839-849, 2007.
26. **Neyroud N, Tesson F, Denjoy I, Leibovici M, Donger C, Barhanin J, Faure S, Gary F, Coumel P, Petit C, Schwartz K and Guicheney P**. A novel mutation in the potassium channel gene KvLQT1 causes the Jervell and Lange-Nielsen cardioauditory syndrome. Nat Genet 15: 186-189, 1997.

27. **Ottschytsch N, Raes A, Van Hoorick D and Snyders DJ**. Obligatory heterotetramerization of three previously uncharacterized Kv channel alpha-subunits identified in the human genome. Proc Natl Acad Sci U S A 99: 7986-7991, 2002.
28. **Pal S, Hartnett KA, Nerbonne JM, Levitan ES and Aizenman E**. Mediation of neuronal apoptosis by Kv2.1-encoded potassium channels. J Neurosci 23: 4798-4802, 2003.
29. **Rato L, Socorro S, Cavaco JE and Oliveira PF**. Tubular fluid secretion in the seminiferous epithelium: ion transporters and aquaporins in Sertoli cells. J Membr Biol 236: 215-224, 2010.
30. **Rossato M, Balercia G, Lucarelli G, Foresta C and Mantero F**. Role of seminal osmolarity in the reduction of human sperm motility. Int J Androl 25: 230-235, 2002.
31. **Stas JI, Bocksteins E, Labro AJ and Snyders DJ**. Modulation of Closed-State Inactivation in Kv2.1/Kv6.4 Heterotetramers as Mechanism for 4-AP Induced Potentiation. PLoS ONE 10: e0141349, 2015.
32. **Stewart AP, Gomez-Posada JC, McGeorge J, Rouhani MJ, Villarroel A, Murrell-Lagnado RD and Edwardson JM**. The Kv7.2/Kv7.3 heterotetramer assembles with a random subunit arrangement. J Biol Chem 287: 11870-11877, 2012.
33. **Tsantoulas C**. Emerging potassium channel targets for the treatment of pain. Curr Opin Support Palliat Care 9: 147-154, 2015.
34. **Tsantoulas C and McMahon SB**. Opening paths to novel analgesics: the role of potassium channels in chronic pain. Trends Neurosci 37: 146-158, 2014.
35. **Tsantoulas C, Zhu L, Shaifta Y, Grist J, Ward JP, Raouf R, Michael GJ and McMahon SB**. Sensory neuron downregulation of the Kv9.1 potassium channel subunit mediates neuropathic pain following nerve injury. J Neurosci 32: 17502-17513, 2012.

36. **Tsantoulas C, Zhu L, Yip P, Grist J, Michael GJ and McMahon SB**. Kv2 dysfunction after peripheral axotomy enhances sensory neuron responsiveness to sustained input. Exp Neurol 251: 115-126, 2014.
37. **Tsevi I, Vicente R, Grande M, Lopez-Iglesias C, Figueras A, Capella G, Condom E and Felipe A**. KCNQ1/KCNE1 channels during germ-cell differentiation in the rat: expression associated with testis pathologies. J Cell Physiol 202: 400-410, 2005.
38. **Tu L and Deutsch C**. Evidence for dimerization of dimers in K^+ channel assembly. Biophys J 76: 2004-2017, 1999.
39. **Tuck RR, Waites GM, Young JA and Setchell BP**. Composition of fluid secreted by the seminiferous tubules of the rat collected by catheterization and micropuncture technics. J Reprod Fertil 21: 367-368, 1970.
40. **vanTol BL, Missan S, Crack J, Moser S, Baldridge WH, Linsdell P and Cowley EA**. Contribution of KCNQ1 to the regulatory volume decrease in the human mammary epithelial cell line MCF-7. Am J Physiol Cell Physiol 293: C1010-C1019, 2007.
41. **Wehner F**. Cell volume-regulated cation channels. Contrib Nephrol 152: 25-53, 2006.
42. **Yeung CH, Barfield JP and Cooper TG**. Physiological volume regulation by spermatozoa. Mol Cell Endocrinol 250: 98-105, 2006.
43. **Yeung CH and Cooper TG**. Potassium channels involved in human sperm volume regulation--quantitative studies at the protein and mRNA levels. Mol Reprod Dev 75: 659-668, 2008.
44. **Yu H, Lin Z, Mattmann ME, Zou B, Terrenoire C, Zhang H, Wu M, McManus OB, Kass RS, Lindsley CW, Hopkins CR and Li M**. Dynamic subunit stoichiometry confers a progressive continuum of pharmacological sensitivity by KCNQ potassium channels. Proc Natl Acad Sci U S A 110: 8732-8737, 2013.
45. **Zhu XR, Netzer R, Bohlke K, Liu Q and Pongs O**. Structural and functional characterization of Kv6.2 a new gamma-subunit of voltage-gated potassium channel. Receptors and Channels 6: 337-350, 1999.

Nederlandstalige samenvatting

Spanningsgevoelige K^+ (Kv) kanalen komen abundant voor in zowel exciteerbare als niet-exciteerbare cellen, waar ze betrokken zijn in tal van fysiologische processen. Deze transmembraan eiwitten staan vooral in voor het reguleren van de membraanpotentiaal door gecontroleerd het transport van K^+ ionen over de membraan toe te laten. Kv kanalen zijn opgebouwd uit vier α-subeenheden, die met een viervoudige symmetrie een hydrofiele ion selectieve porie omsluiten. Iedere subeenheid bestaat uit zes transmembranaire segmenten (S1-S6), een porie lus P die tussen S5 en S6 gelegen is, en een cytoplasmatische N- en C-terminus. De vier S5-P-S6 segmenten vormen de centrale porie waarin de selectiviteitsfilter gelegen is. Deze wordt gevormd door de sterk geconserveerde aminozuren TVGYGD en is verantwoordelijk voor de kalium selectiviteit van het Kv kanaal. De S1-S4 segmenten vormen het spanningsgevoelige domein waarin het positief geladen S4 segment als spanningssensor fungeert. Door de viervoudige symmetrie bevat elk kanaal vier van deze spanningssensoren, die elk door het maken van een elektromechanische koppeling met de S4-S5 linker bijdragen aan het openen en sluiten van de cytoplasmatische kanaalpoort. De cytoplasmatische N-terminus, ten slotte, bevat het T1 domein die een belangrijke rol speelt bij de tetramerisatie van de individuele subeenheden. Het bevordert namelijk de tetramerisatie van compatibele Kv subeenheden, terwijl het de associatie van incompatibele Kv subeenheden verhindert.

Leden van *Shaker*-gerelateerde Kv kanalen vormen een zeer diverse groep en kunnen op basis van sequentiehomologie onderverdeeld worden in acht subfamilies: Kv1-Kv6 en Kv8-Kv9. Binnen elk van de Kv1-Kv4 subfamilies kunnen de leden functionele kanalen vormen in zowel homo- als heterotetramere configuratie. Leden van de Kv5, Kv6, Kv8 en Kv9 subfamilies zijn echter niet in staat om te tetrameriseren tot een functioneel kanaal ondanks ze de typische topologie van een Kv subeenheid bezitten en worden dan ook gecategoriseerd als stille Kv (KvS) subeenheden. Het niet-functionele karakter van de KvS subeenheden wordt veroorzaakt doordat ze in het endoplasmatisch reticulum (ER) weerhouden worden. Deze ER retentie wordt echter opgeheven wanneer ze

associëren met leden van de Kv2 subfamilie. Hierbij worden er heterotetramere Kv2/KvS kanaal complexen gevormd die, vergeleken met homotetramere Kv2 kanalen, unieke biofysische en farmacologische eigenschappen bezitten waardoor KvS subeenheden dan ook beschouwd worden als modulatoren van de Kv2 kanalen. Meer specifiek leidt de aanwezigheid van een KvS subeenheid in het kanaal complex tot een daling van de stroomamplitude, een verschuiving in de spanningsafhankelijkheid van kanaal (in)activering en een vertraging in de kinetica van kanaal (de)activering.

Kv2.1 subeenheden komen voor in alle weefseltypes, terwijl de verschillende KvS subeenheden een selectiever expressiepatroon vertonen. Hierdoor wordt er aangenomen dat de KvS subeenheden *in vivo* de Kv2 kanaal eigenschappen moduleren naar de noden van het weefsel. Deze hypothese heeft aan kracht gewonnen doordat de betrokkenheid van verschillende KvS subeenheden in specifieke fysiologische en pathofysiologische processen werd aangetoond. Hierdoor hebben KvS subeenheden een enorm potentieel als moleculair doelwit bij de ontwikkeling van nieuwe medicijnen. Er zijn echter nog vele onbeantwoorde vragen over hoe deze KvS subeenheden functioneren *in vivo*. Het doel van deze thesis was om antwoorden te vinden op enkele van deze vragen en zo het therapeutisch potentieel van deze KvS subeenheden kracht bij te zetten.

De farmacologische eigenschappen van heterotetramere Kv kanalen worden beïnvloed door zowel de stoichiometrie als de positie van de betrokken subeenheden in het kanaal complex. Hierdoor is het belangrijk om de samenstelling van heterotetramere Kv kanalen te ontrafelen indien ze bij de ontwikkeling van nieuwe medicatie als potentieel doelwit gebruikt worden. Hoewel de Kv1-Kv4 subfamilies vermoedelijk heterotetrameren vormen met een 2:2 stoichiometrie, werd er in het geval van Kv2.1/Kv9.3 heterotetrameren een 3:1 stoichiometrie afgeleid. Er werd echter aangetoond dat de stoichiometrie van heterotetramere Kv kanalen variabel kan zijn afhankelijk van hoe de expressieniveaus van de betrokken subeenheden zich tot elkaar verhouden. Dit heeft als gevolg dat ook Kv2/KvS heterotetrameren functioneel kunnen zijn in

meerdere stoichiometrische configuraties. Deze hypothese werd in het eerste deel van deze studie nagegaan waarbij de Kv2.1/Kv6.4 heterotetrameer als model werd gebuikt. Hiervoor werd de functionaliteit onderzocht van verschillende concatemere constructen die verschillende stoichiometrische configuraties representeerden. Kv2.1/Kv6.4 dimeren brachten functionele kanalen voort die de typische biofysische eigenschappen van Kv2.1/Kv6.4 kanalen bezaten. Dit toonde aan dat Kv2.1/Kv6.4 heterotetrameren inderdaad functioneel kunnen zijn in een 2:2 stoichiometrie. Deze stoichiometrie werd bovendien bevestigd gebruik makende van tetramere constructen. Experimenten met tetramere constructen toonden echter wel aan dat bij deze stoichiometrische configuratie, de Kv2.1/Kv6.4 kanalen enkel functioneel zijn wanneer de Kv6.4 subeenheden niet naast elkaar gepositioneerd waren. Dit duidde eveneens aan dat er niet meer dan twee Kv6.4 subeenheden in functionele Kv2.1/Kv6.4 kanalen aanwezig kunnen zijn. Verder werd gebruik makende van een ander tetrameer construct, de functionaliteit van Kv2.1/Kv6.4 kanalen met een 3:1 stoichiometrie bevestigd. Onze data suggereren dan ook dat Kv2.1/Kv6.4 functioneel zijn in twee verschillende stoichiometrische configuraties.

'Dorsal root ganglion' (DRG) neuronen maken deel uit van het perifeer zenuwstelsel. Hier zijn ze betrokken bij de geleiding van sensorische prikkels naar het centraal zenuwstelsel waardoor ze een belangrijke rol spelen bij pijnperceptie. Er is reeds aangetoond dat hyperexcitatie van deze neuronen kan leiden tot chronische pijn, waardoor ze dan ook aanzien worden als een belangrijk therapeutisch doelwit bij de bestrijding van neuropathische pijn. Er zijn verschillende types DRG neuronen en hoewel sommige van deze types reeds ontstaan tijdens de embryonale ontwikkeling, loopt deze neuronale diversificatie verder door na de geboorte. Aangezien zowel homotetramere Kv2 als heterotetramere Kv2/KvS kanalen in DRG neuronen een belangrijke component van de delayed rectifier stroom (I_{DR}) vormen, werd er in een tweede luik van deze studie nagegaan of de Kv2 en KvS subeenheden een rol spelen tijdens deze postnatale maturatie van DRG neuronen. Dit werd in eerste instantie onderzocht door de stromatoxine (ScTx)-gevoelige en anti-Kv2.1-gevoelige component van

I_{DR} te bepalen in DRG neuronen van 1 tot 4 weken oude muizen. Aangezien ScTx zowel Kv2.1(/KvS) als Kv2.2(/KvS) kanalen inhibeert terwijl anti-Kv2.1 enkel Kv2.1(/KvS) kanalen inhibeert, werd de grootte van zowel de Kv2.2 als de Kv2.1 stroom bepaald door beide componenten met elkaar te vergelijken. Hierbij werd er aangetoond dat de expressie van Kv2.2 significant afnam tijdens de eerste 4 weken van de postnatale ontwikkeling, terwijl de Kv2.1 expressie tijdens deze periode stabiel bleef. Dit werd bevestigd doordat semikwantitatieve RT-PCR experimenten aantoonden dat ook de Kv2.1 en Kv2.2 mRNA expressie respectievelijk stabiel bleef en afnam tijdens de eerste 4 weken van de postnatale ontwikkeling. Semikwantitatieve RT-PCR experimenten toonden verder aan dat de expressie van Kv9.1 significant toenam tijdens deze periode, terwijl voor de Kv6.3, Kv8.1 en Kv9.3 subeenheden enkel kleine schommelingen in het mRNA peil werden waargenomen. Deze resultaten duiden op een belangrijke rol van zowel Kv2 als KvS subeenheden tijdens de postnatale maturatie van DRG neuronen.

De laatste doelstelling was om de fysiologische rol van Kv6.4 te onderzoeken. Hiervoor werd er een transgeen muismodel ontwikkeld waarin het gen dat codeert voor Kv6.4 werd verwijderd. Fenotypische karakterisering van dit muismodel toonde aan dat Kv6.4 een belangrijke rol speelt bij de fysiologische processen die plaatsvinden in de testis, aangezien homozygote vrouwtjes geen nakomelingen produceerden met homozygote mannetjes, maar wel met heterozygote mannetjes. Om de rol van Kv6.4 in de mannelijke fertiliteit te ontrafelen, werd in eerste instantie de spermakwaliteit van wild type (WT) en homozygote (*Kcng4*$^{-/-}$) muizen vergeleken. Dit toonde aan dat de steriliteit van de *Kcng4*$^{-/-}$ mannetjes veroorzaakt werd door een sterke afname van de spermakwaliteit. De spermaconcentratie was namelijk sterk gedaald en bovendien waren de zaadcellen van *Kcng4*$^{-/-}$ muizen niet motiel. Verder werd er waargenomen dat de spermacellen van *Kcng4*$^{-/-}$ muizen een abnormale morfologie hadden die gekarakteriseerd werd door een gereduceerde kopoppervlakte en een verkorte staart. Analyse van testikelweefsel coupes aangekleurd met hematoxyline en eosine toonde aan dat de abnormale

spermamorfologie een gevolg was van een verstoorde spermiogenese. Deze resultaten suggereren dat Kv6.4 de omvorming van spermatiden naar spermatozoa reguleert en tonen aan dat Kv6.4 een potentieel interessant doelwit is voor de ontwikkeling van niet-hormonale mannelijke anticonceptiemiddelen.

In deze studie hebben we nieuwe inzichten verkregen in de fysiologische rol van KvS subeenheden die het therapeutisch potentieel van deze proteïnen verder onderbouwen. Er werd aangetoond dat de Kv6.4 subeenheid een noodzakelijke rol heeft in de testiculaire functie en dat de expressie van enkele Kv2 en KvS subeenheden verandert tijdens de postnatale maturatie van DRG neuronen wat erop duidt dat deze subeenheden een belangrijke functie hebben in dit proces. Verder werd er gedemonstreerd dat Kv2/KvS kanalen functioneel zijn in meerdere stoichiometrische configuraties. Hierdoor is het mogelijk dat er *in vivo* Kv2/KvS heterotetrameren gevormd worden die twee verschillende KvS subeenheden bevatten wat de moleculaire en functionele diversiteit van deze kanaal complexen nog verder vergroot.

Curriculum Vitae

Personalia

Name:	Glenn Regnier
Day of birth:	13/08/1988
Birth Place:	Borgerhout (Antwerpen)
Nationality:	Belgian
Adress:	Zwijgerstraat 20/31
City:	2000 Antwerpen
E-mail:	glenn.regnier@uantwerpen.be
Tel:	+32 472 56 77 34 (mobile)
Current affilation:	Laboratory for Molecular Biophysics, Physiology and Pharmacology Department of Biomedical Sciences University of Antwerp Universiteitsplein 1, CDE, T5.33 2610 Wilrijk (Antwerpen), BELGIUM +32-3-265-2335 (phone)

Education

2011-now PhD student in Biochemistry
University of Antwerp
Promotors: Prof. Dr. Dirk J. Snyders
Dr. Elke bocksteins

Thesis: *'Heterotetrameric channels of Kv2 and 'silent' Kv subunits: stoichiometry and physiological function'*

2009-2011 Master Biochemistry and Biotechnology
Molecular and Cellular Gene Biotechnology
Option: Research
University of Antwerp
Great Distinction

Masterthesis: *'The role of the N- and C-terminus of Kv2.1 in the subfamily specific Kv2.1/Kv6.4 heterotetramerization'*

2010 Laboratory Animal Science (FELASA cat. C)
University of Antwerp
Distinction

2006-2009 Bachelor Biochemistry and Biotechnology
University of Antwerp
Great Distinction

Bachelorthesis: *'Search for electrostatic interaction partners in the T1 domain of hKv2.1 and their role in channel tetramerization'*

Teaching experience

Tutor on practical sessions (supervised by Prof. Dr. A. Labro) of:

- Cell Physiology (Ba2 Biomedical Sciences, Ba2 Biochemistry & Biotechnology)
- Systems Physiology (Ba2 Biomedical Sciences, Ba3 Biochemistry & Biotechnology)
- Cellular & Molecular Neuroscience (Ma1 Biomedical Sciences)
- Molecular Biophysics (Ma1 Biochemistry & Biotechnology)

Supervision of bachelor thesis:

- Biomedical Research Techniques
- Biomedical Sciences

Workshops

Acute brain slices for *in vitro* electrophysiology - Field potentials in normal and pathological brain, Lohman Research Equipment, Castrop-Rauxel, Germany, May 14th 2012

Skills

Techniques

- Molecular: (RT-) PCR, genotyping, site-directed mutagenesis, cloning, DNA & RNA purification, Western blot, co-IP, ELISA, transfection, cell culture, FRET, (immuno)cytochemistry, (immuno)histochemistry, and cell imaging
- Electrophysiological: Whole cell patch clamp and single- and two-electrode voltage clamp

Software

- Microsoft Office, Reference manager, and Adobe photoshop
- Data analysis: Clampfit, Clampex, Sigmaplot, DNAstar (SeqMan, SeqBuilder, Megalign, Editseq), and ImageJ

Languages

	Verbal communication	*Written communication*
Dutch	Mother tongue	Mother tongue
English	Good	Very good
French	Basic	Basic

Scientific Communications

Peer reviewed articles

Regnier G., Bocksteins E., Van de Vijver G., Snyders D.J., van Bogaert PP. The contribution of Kv2.2-mediated currents decreases during the postnatal development of mouse dorsal root ganglion neurons. Physiol Rep. 2016 March; 4(6): e12731.

Bocksteins E., Mayeur E., Van Tilborg A., **Regnier G.**, Timmermans JP., Snyders D.J. The subfamily-specific interaction between Kv2.1 and Kv6.4 subunits is determined by interactions between the N- and C-termini. PLoS One 2014 Jun; 9(6): e98960.

Regnier G., Bocksteins E., Marei W.F., Pintelon I., Timmermans JP., Leroy J.L.M.R., Snyders D.J. Targeted deletion of the Kv6.4 subunit causes male sterility due to disturbed spermiogenesis. Reprod Fertil Dev. (accepted).

Regnier G., Bocksteins E., Snyders D.J. Kv2.1/Kv6.4 heterotetramers are functional in two stoichiometrical configurations. (Manuscript in preparation).

Published abstracts

Glenn Regnier, Elke Bocksteins, Gerda Van de Vijver, Dirk J. Snyders, Pierre-Paul van Bogaert: 'Postnatal development of Kv currents in cultured small mouse dorsal root ganglion (DRG) neurons.) Biophys J.: 106(2), 541a, 2014

Glenn Regnier, Elke Bocksteins, Dirk J. Snyders: 'Stoichiometric analysis of heterotetrameric Kv2.1/Kv6.4 channels.' Biophys J.: 104(2), 125a-126a, 2013

Oral scientific communications

'Targeted deletion of Kv6.4 disrupts mouse spermatogenesis resulting in male infertility.' Autumn meeting of the Belgian Society of Physiology and Pharmacology, 6th November 2015, Brussels, Belgium

Poster presentations

Regnier G., Bocksteins E., Van de Vijver G., Snyders D.J., van Bogaert PP.: Postnatal development of Kv2-mediated K^+ currents in dorsal root ganglion (DRG) neurons. Autumn meeting of the Belgian Society of Physiology and Pharmacology, 6th November 2015, Brussels, Belgium

Regnier G., Bocksteins E., Van de Vijver G., Snyders D.J., van Bogaert P.P.: Postnatal development of Kv currents in cultured small mouse DRG neurons. Biophysical Society, 58th Annual Meeting, February 2014, San Francisco, California, USA

Regnier G., Bocksteins E., Snyders D.J.: Stoichiometric analysis of heterotetrameric Kv2.1/Kv6.4 channels. Biophysical Society, 57th Annual Meeting, February 2013, Philadelphia, Pennsylvania, USA

Regnier G., Bocksteins E., Mayeur E., Bruyns T. and Snyders D.J: Cytoplasmic N-/C-terminal interactions between Kv2.1 and Kv6.4 subunits are important in the formation of functional heterotetrameric Kv2.1/Kv6.4 complexes. Annual meeting of Inter-University Attraction Poles P6/31, 16 December 2011, Ghent, Belgium

Dankwoord

Aan het einde van mijn PhD thesis dien ik nog de laatste en misschien wel de belangrijkste woorden neer te schrijven. De laatste vijf jaar waren een echt (wetenschappelijk) avontuur gevuld met de nodige frustraties, maar bovenal met een heleboel mooie momenten. Deze momenten waren vooral speciaal omdat ik deze met een heleboel mensen – zowel collega's als familie en vrienden - kon delen. Aangezien ik mijn doctoraat zonder het werk en de opofferingen van deze mensen onmogelijk tot een goed einde had kunnen brengen, zou ik hen in dit gedeelte met een persoonlijk woordje willen bedanken.

Prof. Dr. Dirk Snyders – 7 jaar geleden al kwam ik in uw lab terecht voor een korte stage. Ik was onmiddellijk geïntrigeerd door het onderzoek naar Kv kanalen en was dan ook zeer blij dat ik na mijn master thesis onder uw supervisie kon starten aan mijn doctoraat. Ik heb in al deze jaren enorm veel van u geleerd, maar ik ben u vooral zeer dankbaar voor alle kansen die u me hebt gegeven. Ondanks het mislopen van mijn IWT beurs heeft u steeds vertrouwen in mij blijven hebben en ik besef dan ook dat zonder dit vertrouwen ik mijn doctoraat niet succesvol had kunnen beëindigen. Bedankt voor alles!

Prof. Dr. Pierre-Paul van Bogaert – hoewel ik niet tot uw lab behoor, heb ik enorm veel aan u te danken. Ik heb veel van u opgestoken, vooral dan over de 'old school' elektrofysiologie. Belangrijker is echter dat ik zonder uw financiële steun onmogelijk mijn doctoraat had kunnen verder zetten en dit verdient dan ook mijn eeuwige dank!

Elke – jou kan ik met recht en reden mijn tweede promotor noemen. Van begin tot eind heb je me met volle overgave in zo goed als alles bijgestaan – ondanks dat ik je geduld regelmatig op de proef heb gesteld - en er zijn dan ook geen woorden genoeg om je hiervoor te bedanken. Verder heb ik enorm genoten van onze samenwerking. Het is namelijk niet alleen op wetenschappelijk gebied dat ik zeer veel aan je heb gehad; ook op de vele gezellige momenten - binnen en buiten het lab of op congres – kijk ik met veel plezier op terug!

Gerda – ik herinner me onze eerste ontmoeting nog alsof het gisteren was; met enige argwaan liet je me zien hoe je culturen van DRG neuronen maakt. Hoewel onze samenwerking in het begin soms wat stroef liep – ik moest ook zo nodig met enige regelmaat te laat op het lab aankomen op maandag – heb ik enkel maar goede herinneringen aan onze samenwerking. Ik vind het nog steeds onvoorstelbaar met hoeveel overgave en wilskracht je elke week weer opnieuw achter de opstelling kroop om toch maar zoveel mogelijk data te verzamelen. Enorm bedankt hiervoor! Wat ik echter het meest zal herinneren zijn onze gezellige gesprekken bij de koffie voor we aan onze werkdag begonnen!

Abbi – ondanks dat ik je reeds kende van tijdens mijn master thesis, heb ik je vooral goed leren kennen tijdens de eerste weken dat ik op het lab werkte. Het creëert namelijk wel een band als je twee weken lang om 7 uur 's ochtends met iemand foto's van muizenkonten gaat nemen! Ik moet je dan ook vooral bedanken voor de hulp met alles wat bij de kweek van deze dieren kwam kijken. Uren en dagen hebben we gehangen boven al die kooien ondanks je allergie voor deze beestjes. Gelukkig vonden we altijd wel een onderwerp om een babbeltje over te doen, waardoor de tijd in het animalarium leek voorbij te vliegen. Ook naar alle gesprekken buiten het lab kijk ik met veel plezier op terug. Verder stond je altijd klaar om me bij te staan bij het moleculair werk. Bedankt hiervoor!

Evy – tijdens mijn master thesis heb je me de kneepjes van het vak geleerd. Toen heb ik al kunnen ondervinden – vooral dan wanneer we aan de confocale microscoop zaten – dat praten over koetjes en kalfjes een van je specialiteiten is. En praten over koetjes en kalfjes dat hebben we gedaan! Natuurlijk ben ik ook jou zeer dankbaar voor alle hulp wanneer die nodig was!

Alain – als ik één voorbeeld van een gepassioneerde wetenschapper moet noemen, ben jij dat toch wel! Hoe vaak hebben we niet over wetenschap zitten praten – je kunt het bijna filosoferen noemen – zelfs tussen pot en pint. Ondanks dat je niet echt rechtstreeks betrokken was bij mijn projecten, moet ik je vooral

hiervoor bedanken; als ik het na een hele reeks slechte resultaten even niet meer zag zitten, gaven deze gesprekken genoeg inspiratie om er weer terug voor te gaan. Ook aan de gezellige (soms zatte) gesprekken buiten het werk kijk ik met plezier op terug. Daarbij denk ik vooral aan één specifieke middag die me nog lang zal bij blijven (je zult wel weten welke ik bedoel)!

Jeroen – het heeft eventjes geduurd voor ik je echt goed heb leren kennen, maar sinds we samen een bureau delen heb ik je steeds beter en beter leren kennen en weten waarderen. Als collega PhD student heeft jou werkinzet en doorzettingsvermogen – zonder dat je het misschien zelf weet - me enorm geïnspireerd om zelf beter te willen doen. Bedankt hiervoor! Verder heel veel succes bij het afronden van jouw doctoraat!

Rohit – although you're not officially part of our lab, you have spent a lot of hours in our lab and therefore it seems like you're part of our group. It's always a pleasure to talk to you and I'm very happy you found your way back to Belgium. I wish you all the best for the future, especially with finishing your PhD!

Prof. Dr. Jo Leroy and Waleed - your knowledge and insights about fertility have helped me enormously to successfully publish the male infertility story. You guys were always there to discuss the results and ready to assist with the experiments. Thanks a lot for that!

Sofie en Isabel – ook jullie heb ik te pas en te onpas mogen lastigvallen om de resultaten van de immuno's te bespreken. Natuurlijk had ik deze immuno's zelfs niet kunnen uitvoeren zonder jullie deskundige hulp. Bedankt voor alles!

Evelyn, Tine, Tessa en Ivan – ondanks dat jullie al een tijdje weg zijn uit het labo, hebben ook jullie me in het begin van mijn doctoraat ongetwijfeld bijgestaan waar nodig was. Allemaal bedankt daarvoor!

Verder wil ik de mensen die me het nauwst aan het hart liggen nog ontzettend hard bedanken. Jullie hebben misschien niet wetenschappelijk kunnen bijdragen aan mijn doctoraat, maar zonder jullie steun en liefde had ik dit doctoraat ongetwijfeld niet tot een goed einde kunnen brengen.

Dean, Joeri, Junior, Sam en Wim - alle gezellige avondjes thuis of op café en de vele festivals of reizen die we gedaan hebben, brachten me steeds opnieuw in staat om de zorgen van het werk kwijt te raken, zodat ik zonder al te veel stress terug het labo kon binnen stappen. Ik ben jullie echter vooral dankbaar voor onze hechte vriendschap!

Ellen en Hans – hoewel we elkaar niet elke week zien, lijkt het toch elke keer als we afspreken alsof we elkaar gisteren nog pas zagen. Ook jullie ben ik dankbaar, vooral dan voor de steun die we bij elkaar hebben kunnen vinden!

Steven, bompa, nonkel en tantes – we zijn misschien een kleine familie, maar wel een die op elkaar kan rekenen. Allemaal bedankt om er steeds weer voor me te zijn!

Mama en papa – jullie wil ik bedanken voor de onvoorwaardelijke steun die jullie mij geven. Jullie hebben me niet alleen financieel bijgestaan voor mijn studie, maar jullie hebben steeds weer meegeleefd bij alles wat bij dit doctoraat kwam kijken. Ik kan met wat dan ook steeds bij jullie terecht en kan me dan ook geen betere ouders indenken! Bedankt voor alles!

De laatste persoon die ik wil bedanken is Mattias – door onze hechte vriendschap zijn we zeven jaar geleden in het labo van Prof. Snyders terechtgekomen voor onze bachelorproef. Eerst wist ik niet echt zeker of ik mijn bachelorproef daar wou doen, maar uiteindelijk wist je me toch nog te overtuigen. Op die manier heb ik dit avontuur in feite dus aan jou te danken. Het heeft zelfs niet veel gescheeld of we waren collega’s geweest. Op het laatste nippertje besloot je echter om te gaan doctoreren in Wenen. Als ik zag hoe gelukkig je daar was, was dit zonder twijfel de juiste beslissing voor jou. Spijtig genoeg

hebben we twee jaar geleden afscheid van jou moeten nemen. Toch heb ik voor het behalen van dit doctoraat veel aan jou te danken. In het begin van mijn doctoraat hielden we regelmatig contact, waardoor we beiden onze frustraties over mislukte experimenten aan elkaar kwijt konden en we elkaar wisten te motiveren om verder te werken aan onze projecten. Zeker aan mijn trip naar Wenen heb ik nog veel herinneringen die me nog lang zullen bijblijven. Ondanks dat het heel moeilijk was om jou verlies te verwerken, hebben de herinneringen aan jou als gepassioneerde wetenschapper, eeuwige positivo en levensgenieter me vaak de kracht gegeven om te blijven doorzetten en zo dit doctoraat tot een goed einde te brengen. Ik zou dan ook als laatste eer dit doctoraat aan jou willen opdragen, mijn vriend!

Glenn Regnier,
september 2016